8-2018

In vitro Effect of Graphene Structures as an Osteoinductive Factor in Bone Tissue Engineering: A Systematic Review

Dorsa Mohammadrezaei
University of Tehran

Hossein Golzar
University of Tehran

Maryam Rezai Rad
Shahid Beheshti University of Medical Sciences

Meisam Omidi
Shahid Beheshti University

Hamid Rashedi
University of Tehran

See next page for additional authors

Contents

Abstract 3

INTRODUCTION 3

METHODS AND MATERIALS 4

Eligibility criteria 4

Types of studies 4

Types of participants 4

Types of interventions 4

Types of outcome measures 5

Information source 5

Data collection process 5

DATA items 6

RESULTS 50

Study selection 50

Cell sources 51

Graphene types 51

Chemical composition 51

Characterization 51

DISCUSSION 52

Factors affecting the cellular proliferation and viability 52
Concentration of graphene 53
Types of graphene 54
Size of graphene 54
Dimension 55
Modification of graphene and its derivatives 55
Graphene and metals 55
Graphene and polymers 57
Graphene and minerals 58
Factors affecting the cellular attachment 59
Hydrophilicity, functionalization and roughness 60
Surface area (porosity/pore size) 62
Factors affecting the cellular osteogenic differentiation 62
Graphene and its derivatives' properties affecting osteogenesis 63
Modification of graphene and its derivatives 64
Graphene and metals 65
Graphene and polymers 66
Graphene and minerals 68
LIMITATIONS 69
CONCLUSIONS 69
REFERENCES 70

In vitro Effect of Graphene Structures as an Osteoinductive Factor in Bone Tissue Engineering: A Systematic Review

Dorsa Mohammadrezaei
School of Chemical Engineering, college of Engineering, University of Tehran, Tehran, Iran
Hossein Golzar
School of Chemical Engineering, college of Engineering, University of Tehran, Tehran, Iran
Maryam Rezai Rad

Department of Tissue Engineering, School of Advanced Technologies in Medicine, Shahid Beheshti University of Medical Sciences, Tehran, Iran
Dental Research Center, Research Institute of Dental Sciences, School of Dentistry, Shahid Beheshti University of Medical Sciences, Tehran, Iran
Meisam Omidi
Protein research Center, Shahid Beheshti University, GC, Velenjack, Tehran, Iran
Hamid Rashedi
School of Chemical Engineering, college of Engineering, University of Tehran, Tehran, Iran
Fatemeh Yazdian
Department of Life Science Engineering, Faculty of New Science and Technologies, University of Tehran, Tehran, Iran
Arash Khojasteh
Department of Tissue Engineering, School of Advanced Technologies in Medicine, Shahid Beheshti University of Medical Sciences, Tehran, Iran
Department of Oral and Maxillofacial Surgery, Shahid Beheshti University of Medical Sciences, Tehran, Tehran, Iran
Lobat Tayebi
Biomaterials and Advanced Drug Delivery Laboratory, School of Medicine, Stanford University, Palo Alto, CA
Marquette University School of Dentistry, Milwaukee, WI

Abstract

Graphene and its derivatives have been well-known as influential factors in differentiating stem/progenitor cells toward the osteoblastic lineage. However, there have been many controversies in the literature regarding the parameters effect on bone regeneration, including graphene concentration, size, type, dimension, hydrophilicity, functionalization, and composition. This study attempts to produce a comprehensive review regarding the given parameters and their effects on stimulating cell behaviors such as proliferation, viability, attachment and osteogenic differentiation. In this study, a systematic search of MEDLINE database was conducted for *in vitro* studies on the use of graphene and its derivatives for bone tissue engineering from January 2000 to February 2018, organized according to the PRISMA statement. According to reviewed articles, different graphene derivative, including graphene, graphene oxide (GO) and reduced graphene oxide (RGO) with mass ratio ≤1.5 wt % for all and concentration up to 50 µg/mL for graphene and GO, and 60 µg/mL for RGO, are considered to be safe for most cell types. However, these concentrations highly depend on the types of cells. It was discovered that graphene with lateral size less than 5 µm, along with GO and RGO with lateral dimension less than 1 µm decrease cell viability. In addition, the three-dimensional structure of graphene can promote cell-cell interaction, migration and proliferation. When graphene and its derivatives are incorporated with metals, polymers, and minerals, they frequently show promoted mechanical properties and bioactivity. Last, graphene and its derivatives have been found to increase the surface roughness and porosity, which can highly enhance cell adhesion and differentiation.

INTRODUCTION

Bone tissue engineering (BTE) is a complex and dynamic Strategy that typically requires a bone scaffold for recruitment of stem/progenitor cells, followed by their proliferation, differentiation, matrix formation and remodeling of the bone.[1] Moreover, bone scaffolds are generally made of biomaterials in order to provide proper mechanical support during the stimulation of new bone formation. The desired properties of scaffolds are osteoconductivity, biodegradability, high biocompatibility and mechanical properties and interconnected porosity which are the required properties for fabricating scaffold.[2] For

decades, carbon-based materials such, as carbon nanotubes (CNT), fullerenes and graphene have been introduced as remarkably promising materials, which have been shown to induce cell attachment, proliferation and differentiation, particularly toward the osteoblastic lineage.[3] Graphene is a single atomic layered sheet of conjugated sp^2-carbon atoms, attracting attention among all carbon-based materials due to their specific features. These advantageous features of graphene include large surface area, high mechanical strength, great elasticity modulus, unprecedented electricity properties[4] and potential of providing an interaction site to adsorb various growth factors or other materials that can enhance differentiation.[3, 5-7]

Graphene derivatives include graphene oxide (GO), reduced graphene oxide (RGO) amine-functionalized graphene oxide (AGO), graphene foams (GFs), graphene nanosheets (GNSs) and graphene quantum dots (GQDs). Among all graphene derivatives, GO and RGO have been widely used in BTE.[8] Although GO presents reduced electronic and mechanical properties compared to pristine graphene, it has various benefits from a synthetic chemistry aspect.[9] GO is prepared by oxidation of graphite and has many hydrophilic functional groups, including hydroxyl, carboxyl and epoxy groups, which may cause increased biocompatibility of GO compared to pristine graphene,[10, 11] however, the other parameters such as concentration, size and dimension should be considered as influential factors in evaluating the toxicity of GO.[12–14] RGO, produced by removing the oxygen-containing groups of GO, maintains some of the thermal and mechanical properties observed in pristine graphene.[15] Moreover, RGO has a higher capability in electron transferring which may be effective in accelerating differentiation.[16] The properties of graphene-related materials and their great potential to be easily functionalized and combined with biomolecules and biomaterials present several opportunities to design different bio-composites. Thus, in this article we further provide basic information regarding systematic review on the potential of graphene and its ability to produce polymer-, minerals- and metal-composites with modified mechanical properties and enhanced cell differentiation, mineral deposition and bioactivity. We comprehensively evaluated the effect of graphene and its derivatives on osteogenic differentiation of various stem/progenitor cells. Additionally, we further expand our assessment on compatibility of graphene and its derivatives' effect on cell viability, proliferation and attachment. Indeed, this systematic review aims to clarify the limitations in available studies and contribute to designing future preclinical and clinical studies on the use of graphene family for bone regeneration.

METHODS AND MATERIALS

Eligibility criteria

Types of studies

All *in vitro* studies that used graphene and its derivatives for bone regeneration from January 2000 to February 2018 from MEDLINE were included in this review. Included studies were limited to English-language articles. We excluded the abstracts, reviews, letters and thesis.

Types of participants

Participants were any types of graphene, including GO, RGO, AGO, and GQDs prepared in any shape and composition. Additionally, any type of stem/progenitor cells was considered.

Types of interventions

Studies that conducted an osteogenic induction in presence of graphene and its derivatives were included. Studies that used only osteogenic induction as a part of a multilineage characterization test were excluded.

Types of outcome measures

Cell viability and proliferation was reported in *in vitro* studies using 3-(4,5-dimethylthiazol-2-yl)-2,5-diphenyltetrazolium bromide (MTT), 3-(4,5-dimethylthiazol-2-yl)-5-(3-carboxymethoxyphenyl)-2-(4-sulfophenyl)-2H-tetrazolium (MTS), deoxynucleic acid (DNA) counting, Cell Counting Kit-8 (CCK-8), mitochondrial activity, Alamar Blue, total protein apoptosis, reactive oxygen species (ROS), and quantitative lactate dehydrogenase (LDH) activity assays. Also, various methods of staining were reported, including 4',6-diamidino-2-phenylindole (DAPI), Calcein AM, F-actin, and live and dead assay. Cellular attachment was reported in *in vitro* studies using fluorescence and microscopic images such as fluorescein isothiocyanate (FITC), DAPI, live and dead, fluorescein diacetate, and scanning electron microscope (SEM).

In addition, differentiation toward the osteoblast lineage was reported in *in vitro* studies using alkaline phosphatase (ALP) activity, western blotting, Wnt pathway, flow cytometric analysis, phosphate assay, calcium (Ca) content and calcium phosphate (CaP) measurement, osteocalcin (OCN) content and gene expression analysis. Furthermore, various methods of staining were utilized, including immuno-cytochemical (ICC), immunofluorescent, Alizarin Red-S (ARS), Sirius Red (SR) and Von Kossa.

Information source

Our scientific electronic database was MEDLINE (NCBI PubMed and PMC). Further hand search was performed in the following journals: Carbon, Biomedical Nanotechnology, Nature, Nanoscience and Nanotechnology, Nanoscale, ACS Nano and Nanomedicine. Our search was limited to English-language studies dating from January 2000 to February 2018.

An electronic search was performed to select articles relevant to effect of graphene on stem/progenitor cells using the following terms: graphene AND (BTE OR bone regeneration OR osteogenesis OR osteoblast lineage OR osteogenic lineage OR osteogenic differentiation). A search of the selected articles' bibliographies was also performed manually.

Data collection process

Review and data extraction were performed according to the PRISMA flow diagram shown in Figure 1. Three independent reviewers performed the initial screening of the selected articles, followed by reviewing the full text of the articles and extraction of all data. Disagreements between the three reviewers were resolved by consensus. In case of no agreement, a fourth reviewer decided. Fourth and fifth authors contributed in the discussion section.

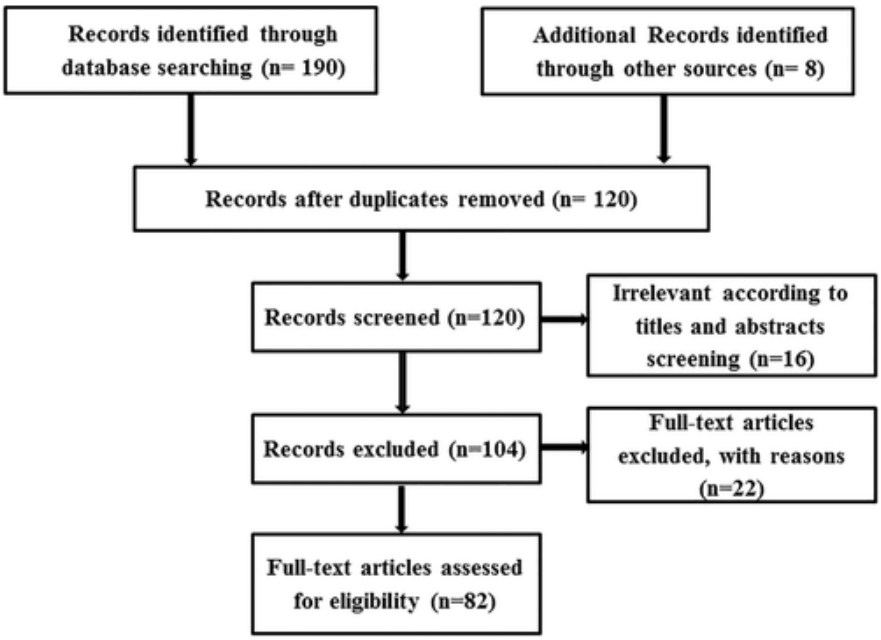

Figure 1 Flow chart of the search strategy.

DATA items

Results and data were extracted from the full text of the articles and tabulated as follows (Table 1): (1) Types of cells used for osteogenesis; (2) chemical composition of graphene and its derivatives used for cell differentiation; (3) types of graphene used in combination with other materials such as metals, metalloids, polymer; (4) size of graphene and its derivatives, including lateral dimension, diameter, and thickness; (5) cultural condition used for cell growth; (6) type of treatment group used for evaluating cell behavior; (7) type of characterization tests conducted for surface characterizing; (8) outcomes of *in vitro* studies, that is, the results of the cell viability, proliferation, attachment and differentiation.

Table 1. Summary of the in Vitro Studies of Graphene-Based Structures in Bone Tissue Engineering

Authors	Cell Source	Chemical Composition and Functionalization	Type of Graphene	Size	Cultural Condition	Treatment Group	Characterization	Outcome
Cicuéndez et al.66	MC3T3-E1	GO-PEG-FITC	GO	Thickness ≈ 10 nm	α-MEM ± 10% FBS ± 50 μg/mL glycerolphosphate ± 10 mM L-AA ± 1 m*M* l-glutamine\pen\strep	-GO-PEG-FITC(40 μg/mL)	-AFM -XPS -ZP -DLS	*Proliferation/viability:* *-PI exclusion and flow cytometry test*: High viability was observed in the presence of GO-PEG-FITC (3 days) *-Proliferation*: Although cells grew and spread well, cell number dramatically decreased on GO-PEG-FITC (3 days)

Authors	Cell Source	Chemical Composition and Functionalization	Type of Graphene	Size	Cultural Condition	Treatment Group	Characterization	Outcome
								-Cell apoptosis assay: Incorporation of GO-PEG-FITC increase cell apoptosis (3 days) *Osteogenic differentiation*: *-ALP activity*: After 3 days of treatment with GO-PEG-FITC, ALP activity decreased *-ARS and ALP*: GO-PEG-FITC ≈ control (12 days of culture in fresh medium)
Qiu et al.[47]	mBMSCs	GO deposited on Ti	GO	Thickness: -Single layer: 1 nm -GO-40: 25 µm -GO-80: 90 µm -GO-120: 136 µm	α-MEM ± 10% FBS ± 1% pen/strep	-Ti-GO-40 (deposition voltage: 40V) -Ti-GO-80 -Ti-GO-120 -Ti	-AFM -SEM -XRD -XPS -Raman spectra -ICP-AES -ZP	*Proliferation/viability*: *-Alamar Blue assay*: Ti > Ti-GO-40 > Ti-GO-80 > Ti-GO-120 (1, 4, 24 days) *Attachment*: *-FITC staining*: Ti > Ti-GO groups (1, 4, 24 h). In addition, it showed: 24 h > 1 h *Osteogenic differentiation:* *-ALP activity, ARS staining: Ti-GO-120 > Ti-GO-80 > Ti-GO-40 > Ti (7, 14 days)* *Collagen secretion*: Ti-GO-120 > Ti-GO-80 > Ti-GO-40 (7, 14 days)
Ren et al.[45]	mBMSCs	GO-DEX-Ti RGO-DEX-Ti	GO RGO	Thickness of GO sheets: 0.83 nm	Cultured in medium containing 10% FBS	-Dex-control -GO-DEX-Ti -RGO-DEX-Ti -GO-Ti -RGO-Ti	-AFM -SEM -FTIR -XPS -Raman spectra	*Proliferation/viability*: *-CCK-8 and F-actin staining*: GO-DEX-Ti > RGO-DEX-Ti > DEX-Control (1, 3, 5 days) *Osteogenic differentiation*: *-ALP activity (7, 14 days), mineralization (21 days), OPN, OCN expression (7, 14 days)*: GO-DEX-Ti > RGO-DEX-Ti > DEX-Control

Authors	Cell Source	Chemical Composition and Functionalization	Type of Graphene	Size	Cultural Condition	Treatment Group	Characterization	Outcome
Ricci et al.[85]	Human osteoblast cells	GONRs	GO	—	DMEM ± 10% FBS ± 100 IU/mL pen ± 100 µg/mL of strep	-GONRs (10, 100, 200, 300 µg/mL)	-SEM -FTIR -XRD	*Proliferation/viability*: *-Cell counting*: Alive cells on control (−) > 10 µg/mL GONRs > 100 µg/mL GONRs > 200 µg/mL GONRs > 300 µg/mL GONRs > Control (+) *Osteogenic differentiation*: *-qRT-PCR (ALP, COL-I, OCN, OPN,Runx-2)*: 200 µg/mL GONRs decrease the gene expression while 100 µg/mL did not affect them significantly
Saravanan et al.[75]	-Rat calvarial osteoprogenitors	GO-Ct-Gn	GO	—	DMEM ± 10%FBS	-Ct-Gn -0.25% GO-Ct-Gn -OM -GM	-SEM -FTIR -XRD -Raman spectra -Porosity measurement -Swelling study -Water absorption -Degradation rate measurement	*Proliferation/viability*: *-MTT assay*: O.D. value: 0.25% GO-Ct-Gn > Ct-Gn No significant cytotoxicity was observed up to 30 mg/mL of scaffolds with rat cells *Osteogenic differentiation*: *-RT-PCR*: ALP, COL-I, and OCN genes increased in mMSCs with 0.25% GO-Ct-Gn in OM (7, 14 days). Runx2 was high only at day 7 with 0.25% GO/Ct/GN *-Western blotting*: Runx2 protein expression increased on 0.25% GO-Ct-Gn in OM (7, 14 days)
Xie et al.[29]	BMSCs	GO-coated TCP GO-coated HAP	GO	—	—	-HAP -GO-HAP -BMP2-GO-HAP -NPs (BMP2-encapsulated BSA-NPs)-GO-HAP -BGO-HAP (mixed	-SEM -ZP	*Proliferation/viability*: *-Live and dead cell staining*: Approximately no dead cells were observed on the pure TCP or HAP and GO groups (7 days) *-CCK-8 assay*: Nos-GO > other groups and no difference between TCP or

Authors	Cell Source	Chemical Composition and Functionalization	Type of Graphene	Size	Cultural Condition	Treatment Group	Characterization	Outcome
						BMP2/GO solution on the GO-HAP) -TCO -GO-TCP -BMP2-GO-TCP -GO-TCP -NPs-GO-TCP -BGO-TCP		HAP and GO groups (7 days) *Osteogenic differentiation*: -*ALP activity*: Nps-GO-HAP > BGO-HAP ≈ BMP2-GO-HAP > GO-HAP > HAP The same trend for TCP (14 days)
Zhang et al.[50]	Rabbit BMSCs	Ag-GO-coated β-TCP With different mass ratio of Ag-GO: -Ag1G1 (Ag:GO = 1: 1) -Ag0.5G1 -Ag2G1	GO	—	DMEM ± 10%FBS ± 1%pen/strep	-β-TCP -β-TCP-GO (β-TCP modified in 0.2 mg/mL GO solution) -β-TCP-3-Ag1G1(β-TCP modified in 3 mL Ag1G1) -β-TCP-4-Ag1G1	-SEM -TEM -EDX	*Proliferation/viability*: *OD*: β-TCP ≥ β-TCP-GO > 3-Ag1G1 > 4-Ag1G1 (1, 3, 7 days) *Osteogenic differentiation*: -*ALP activity*: 3-Ag1G1 > 4-Ag1G1 > β-TCP-GO > β-TCP (14 days) 4-Ag1G1 > 3-Ag1G1 > β-TCP-GO > β-TCP (14 days) -*qRT-PCR*: BSP, OCN and Runx2 expressions: 4-Ag1G1 > 3-Ag1G1 > β-TCP-GO > β-TCP (14 days) OPN expression: 3-Ag1G1 > 4-Ag1G1 > β-TCP-GO > β-TCP
Chen et al.[89]	hMG63	ZnO-GO-COOH	GO	Thickness ≈ 0.84 nm	α-MEM ± 10% FBS ±1% pen/strep	-ZnO-GO-COOH -GO-COOH -Gl (control group)	-AFM -TEM -XRD -XPS -ICP-AES -Raman spectra -Wettability evaluation	*Proliferation/viability*: -*CCK-8 assay*: No significant cytotoxicity for GO-COOH below 50 µg/mL *Osteogenic differentiation*: -*ALP activity*: ZnO-GO-COOH ≫ GO-COOH and control group (7 days), GO-COOH > control group (14 days) -*OCN expression*: ZnO-GO-COOH > GO-COOH > Gl (14 days) -*ARS staining*: ECM mineralization on ZnO-

Authors	Cell Source	Chemical Composition and Functionalization	Type of Graphene	Size	Cultural Condition	Treatment Group	Characterization	Outcome
								GO-COOH ≫ other two groups (7 days) -*RT-qPCR*: ZnO-GO-COOH showed the most increased gene expression of ALP, OCN, and Runx2 (14 das)
Fan et al.[67]	MC3T3-E1	BGs-GNS	GO	—	DMEM ± 4.5 g/L d-glucose ± 10% FBS ± 100 U/mL pen ± 100 U/mL strep	-GO -BG -BG1GO1 (BG/GO [wt/wt] = 1:1) -BG5GO1 -BG10GO1	-SEM -TEM -FTIR spectra -XRD -EDX -Mechanical tests -Nanoindentation measurements	*Proliferation/viability*: -*MTT assay*: BG10GO1 > BG5GO1 > BG1GO1 > BG > GO (2, 4 days) *Osteogenic differentiation*: -*ALP activity*: BG10GO1 > BG5GO1 > BG1GO1 ≈ BG > GO (5 days)
Kumar et al.[37]	BMSCs	GO-PEI	GO	The thickness of GO sheets ≈ 0.8 nm	OM:10 nM Dex ± 20 m*M* β-glycerophosphate ± 50 µ*M* AA	-GO -GO-PEI -PCL -PCL-GO1 (10 mg of GO/g of PCL, 0 mg of GO-PEI/g of PCL) -PCL-GO3 -PCL-GO5 -PCL-GO-PEI1 (0 mg of GO/g of PCL, 10 mg of GO-PEI/g of PCL) -PCL-GO-PEI3 -PCL-GO-PEI5 -GM -OM	-AFM -FTIR -XRD -XPS -TGA -Raman spectra -CA measurement -Mechanical test	*Proliferation/viability*: -*DNA content*: PCL-GO5 and all the PCL-GO-PEI composite ≫ neat PCL (7 days) *Attachment*: -*Fluorescence micrographs*: More cells were seen on PCL-GO-PEI composite films especially on PCL-GO-PEI5 (7 days) -*Live/dead assay*: All cells were viable on all the substrates and the cell area decreased with increase in the content of GO and GO-PEI. *Osteogenic differentiation*: -*ALP activity*: OM > GM (14, 21 days) PCL-GO-PEI5 > PCL-GO5 > PCL (14, 21 days)

Authors	Cell Source	Chemical Composition and Functionalization	Type of Graphene	Size	Cultural Condition	Treatment Group	Characterization	Outcome
								-*ARS staining*: GM < OM PCL-GO-PEI5 > PCL/GO-PEI3 > PCL-GO5 (14 days). In addition, at day 21, mineral deposited was highest -*Adsorption of osteogentic factors*: Adsorbtion of glycerol phosphate and AA: PCL-GO-PEI5 > PCL-GO5 > PCL -Adsorbtion of Dex: PCL-GO5 ≥PCL-GO-PEI5 > PCL
Shao et al.[61]	mMSC	GO-PLGA-tussah (O/C ratio of the GO:0.44)	GO	—	DMEM ± 10% FBS	-Cover slip -PLGA -PLGA-tussah -GO-PLGA-tussah	-SEM -TEM -FTIR -Raman spectra -CA measurement -Porosity measurement -Mechanical tests	*Proliferation/viability*: -*MTT assay*: Cell proliferation was slightly higher in the presence of GO (1, 4, 7 days). Also, the number of cells on GO-PLGA-tussah > PLGA-tussah > PLGA nanofiber *Attachment*: -*DAPI staining*: The highest cell density was observed on GO-PLGA-tussah *Osteogenic differentiation*: -*RT-PCR*: The expression of CD29 and CD44 on GO-doped PLGA-tussah < PLGA-tussah < PLGA ALP and COL-I on GO-doped PLGA-tussah > PLGA-tussah > PLGA > cover slip (10, 14 days) -*OCN expression*: GO-doped PLGA-tussah > PLGA-tussah > PLGA > Cover slip (10, 14 days)

Authors	Cell Source	Chemical Composition and Functionalization	Type of Graphene	Size	Cultural Condition	Treatment Group	Characterization	Outcome
								-*SEM*: Cells on GO-PLGA-tussah were more densely mineralized than those on scaffolds without GO (14 days) -*EDC*: Ca/P ratio: PLGA-tussah > GO-doped PLGA-tussah > PLGA
Silva et al.[90] 2016	MG-63	PDLLA-MWNCTO-GO	GO	—	DMEM ± 10% FBS ± 100mg/mL Strep ± 100 mg/mL Pen	-PDLLA -PDLLA-MWNCTO-GO	-FESEM -TEM -Porosity measurement -Mechanical tests	*Proliferation/viability*: -*MTT assay*: Scaffolds did not show any cytotoxicity effects (7 days) *Osteogenic differentiation*: -*ALP activity*: PDLLA-MWNCTO-GO > PDLLA > control (3 days) -*ARS staining*: Scaffolds were able to induce mineralized realized (14 days)
Xie C et al.[48] 2016	mBMSCs	GO-Ct	GO	—	α-MEM ± 10%FBS ± 1%pen/strep	-GO-Ct-CBB-Ag-OCP -GO-Ct-CBB-OCP -GO-Ct-BMP-Ag-OCP -GO-Ct-OCP -GO-Ct	-SEM -FTIR -XRD -Raman spectra -Porosity measurement -Degradation assay -Adsorption assay	*Proliferation/viability*: The OCP mineralized scaffolds showed significantly higher proliferation than that on the GO/CS scaffolds *Attachment*: -*SEM*: Cells spread very well on the all scaffolds *Osteogenic differentiation*: -*ALP activity*: GO-Ct-CBB-OCP, GO-Ct-CBB-Ag-OCP > GO-Ct-BMP-Ag-OCP > GO-Ct-OCP,GO/Ct (14 days)
Zanca nela DC et al.[13] 2016	Osteoblast	GO	GO	—	OM	-GO (0, 25, 50 µg/mL) -Ti disk -GO (0, 25, 50 µg/mL)	-SEM -EDS -Raman spectra	*Proliferation/viability*: -*MTT assay*: GO-plastic > GO-Ti (7, 14, 21 days) -7, 14 days: GO(0)-plastic > GO(25)-

Authors	Cell Source	Chemical Composition and Functionalization	Type of Graphene	Size	Cultural Condition	Treatment Group	Characterization	Outcome
						-Plastic surface		plastic > GO(50)-plastic > GO(25)-Ti > GO(0)-Ti -21 days: GO(25)-plastic > GO(0)-plastic > GO(50)-plastic > O(25)-Ti > GO(0)-Ti *Osteogenic differentiation*: -*ALP activiy*: GO-Ti disks ≈ GO-plastic surface (7, 14, 21 days). All groups exhibited higher ALP activity at day 14. -*ARS staining*: GO-plastic surface > GO-Ti disk (21 days)
Zhang W et al.[49] 2016	mBMSCs	GO-Cu-Cpc	GO	Thickness ≈ 0.8 nm	DMEM.	-GO (10, 20, 40, 160 µg/mL) -GO-Cu (10, 20, 40, 160 µg/mL) -control (10, 20, 40, 160 µg/mL) -GO-Cpc -GO-Cu-Cpc -Cpc	-AFM -SEM -XRD -UV–Vis -ICP-OES	*Proliferation/viability*: -*Live and dead assay*: The cell viability gradually decreased by increasing GO-Cu concentration from 10 to160 µg/mL. -Concentration of GO and GO-Cu less than 40 µg/mL showed good biocompatibility. *Attachment*: -*IFS*: The amount of the integrin β1: GO-Cpc, GO-Cu-Cpc ≫ Cpc (12 h) *Osteogenic differentiation*: -*OCN*: GO-Cu-Cpc > GO-Cpc > Cpc (7 days). -*ALP activity*: GO and GO-Cu increased ALP expression in a concentration-dependent manner: GO-Cu > GO > control (3 days) -*Western blot*: The phosphorylation of

Authors	Cell Source	Chemical Composition and Functionalization	Type of Graphene	Size	Cultural Condition	Treatment Group	Characterization	Outcome
								Erk1/2, the activation of Hif-1α, the inhibition of VHL facilitated by using GO and GO-Cu. In addition, the expression of VEGF and BMP2 were significantly enhanced by utilizing 40 μg/mL GO or GO-Cu (3 days)
Zhou Q et al.[26] 2016	hPDLSCs	GO-coated Ti	GO	The height of GO sheets on the quartz substrate ≈ 1 nm	DMEM ± 10% FCS ± 2 mM L-glutamine ± 100 mM L-ascorbate-2-phosphate ± 1 mM sodium pyruvate ± 50 U/mL pen G ± 50 mg/mL strep (10–14 days).	-Na-Ti -GO-Ti	-AFM -SEM -Raman spectra	*Proliferation/viability*: -*MTT assay*: The proliferated rate of hPDLSCs on GO-Ti was substantially higher than those on Na-Ti (3, 5, 7, 10 days). *Attachment*: -*CLSM*: cells on GO-Ti substrates were more dense than those on Na-Ti substrates (3 days) *Osteogenic differentiation*: -*ALP Activity*: GO-Ti ≈ Na-Ti (3, 5 days) GO-Ti > Na-Ti (7, 10 days). -*qRT-PCR*: COL-I, Runx2, BSP and ALP expression peaked at day 14 and: GO-Ti > Na-Ti (7, 14, 21 days). BSP expression level was the lowest (21 days) among all genes. -*OCN*: OCN expression level peaked at day 21 and: GO-Ti > Na-Ti (14, 21d). -*Western blot assay*: BSP and Runx2 expression: GO-Ti > Na-Ti (7, 14 days), GO up-regulated the OCN expression (14 days)

Authors	Cell Source	Chemical Composition and Functionalization	Type of Graphene	Size	Cultural Condition	Treatment Group	Characterization	Outcome
Dong W et al.92 2015	hMG63	GO-Titanate	GO	—	DMEM ± 10%FBS ± antibiotics (100 U/mL pen ± 100 mg/mL strep)	-Neat titanate -GO -GO-Titanate -COOH grafted GO-titanate -OH grafted GO-titanate -NH_2 grafted GO-titanate	-SEM -TEM -XRD. -FTIR -Porosity measurement -Mechanical tests	*Proliferation/viability*: -*MTT assay*: OH grafted GO-titanate > NH_2 grated GO-titanate > GO-titanate> COOH grafted GO-titanate> neat titanate (6 days) *Attachment*: -*Fluorescence microscopy*: -OH group terminals presents the highest density of attached cells (2, 4, 6 days) *Osteogenic differentiation*: -*ALP ctivity*: OH grafted GO-titanate> NH_2 grated GO-titanate > COOH grafted GO-titanate > GO > neat titanate (2, 4, 6, 10, 15 days) -*ARS staining*: COOH grafted GO-titanate > NH_2 grated GO-titanate > OH grafted GO-titanate > GO > neat titanate (2, 4 days) -OH grafted GO-titanate > NH_2 grated GO-titanate > COOH grafted GO-titanate > GO > neat titanate (6, 10, 15 days) -*Ca content*: COOH grafted GO-titanate ≫ other scaffolds (2, 4 days). –OH functioned scaffold presents the best Ca deposition afterward
Jung HS et al.69 2015	MC3T3-E1	Dex-RGO-MPCR-TNZ	GO	Size: 0.3–2 µm	OM: α-MEM ± 10 mM of glycerol 2-phosphate and 0.2 mM of AA	-ST-TNZ -STA-TNZ -MPCR-TNZ -RGO-MPCR-TNZ	-AFM -XPS -Raman spectra	*Proliferation/viability*: -*MTT assay*: Cell viability: ST-TNZ < STA-TNZ < MPCR-TNZ < RGO-MPCR-TNZ (3 days)

Authors	Cell Source	Chemical Composition and Functionalization	Type of Graphene	Size	Cultural Condition	Treatment Group	Characterization	Outcome
						-Dex-RGO-MPCR-TNZ -TCPS -OM -GM	-Mechanical test -CA measurement -Drug release test (UV-Vis spectroscopy)	-Cell growth on RGO-MPCRTNZ > MPCR-TNZ (1, 3, 7 days) *Osteogenic differentiation*: *-ARS staining*: Dex-RGO-MPCR-TNZ ≫ RGO-MPCR-TNZ > MPCR-TNZ *-CSLM*: Significant OCN expression was observed in Dex/RGO-MPCR-TNZ *-ALP activity*: The cells on Dex-RGO-MPCR-TNZ > RGO-MPCR-TNZ > MPCR-TNZ (OM > GM) *-RT-qPCR*: Remarkably higher expression levels of Runx2, OPN, Col-1, and OCN was shown on Dex-RGO-MPCR-TNZ than RGO-MPCR-TNZ, MPCR-TNZ and TCPS
Kim TH et al.[18] 2015	hADSCs	Different G patterns on Gl/Au, TCP, PDMS, and PLGA	NGO	Size ≈ 50–100 nm	GM: 0.5% FBS ASC medium OM: 100 nM Dex ± 50 µ*M* AA ± 10 mM β-glycerolphosphate	-NGO 100 (line pattern) -NGO 100 (No pattern) -Bare Au	-AFM -TEM -DLS -XPS -ZP -Raman spectra	*Attachment* -Cell spreading was the highest on NGO line patterns. *Osteogenic differentiation*: *-ALP activity*: NGO 100 (line pattern) > NGO 100 (no pattern) > Bare Au (14 days) *-Immunostaining*: Cells on the NGO line pattern enhanced expression of OCN (21 days). *-ARS staining*: OM ≫GM In OM: NGO 100 (line pattern) > NGO 100 (no pattern) > bare Au (21 days)
kumar S et	hMSCs	PCL-GO/RGO/AGO	-GO -RGO -AGO	The thickness of	DMEM ± 15 vol % MSC-qualified	-PCL -PCL-GO1 (addition of 1	-AFM -SEM -DLS	*Proliferation/viability*: *-DNA content (7 days)*: PCL-AGO3 ≥PCL-AGO1 ≥

Authors	Cell Source	Chemical Composition and Functionalization	Type of Graphene	Size	Cultural Condition	Treatment Group	Characterization	Outcome
al.[36] 2015		(C/O ratio: GO: C/O=2.2 RGO: C/O=4.0 AGO =2.3)		GO sheets ≈2 nm The thickness of RGO sheets ≈1 nm and Lateral size ≈ 500 nm The thickness of AGO ≈3 nm The average size of dispersed GO, RGO and AGO were 823, 529 and 886 nm, respectively.	FBS ± 1%gultamax ± 1% pen–strep	wt % of GO to PCL) -PCL-GO3 -PCL-GO5 -PCL-RGO1 -PCL-RGO3 -PCL-RGO5 -PCL-AGO1 -PCL-AGO3 -PCL-AGO5	-FTIR -XRD -XPS -Raman spectra -CA measurement - Mechanical test	PCL-AGO5 > PCL-GO3 > PCL-GO5 ≥PCL-RGO5 > PCL-GO1 > neat PCL *Attachment*: -*Fluorescence micrographs*: Corporation graphene NPs into polymer minimizes toxicity *Osteogenic differentiation*: -*ARS staining*: PCL-AGO > PCL-GO > PCL-RGO > neat PCL, The mineral content increased with increase in content of GO and AGO
kumar S et al.[14] 2015	MC3T3-E1	GO-PCL (2D, 3D) RGO-PCL (2D,3D)	GO,RGO	Lateral dimension of RGO ≈ 2.4 × 1.5 µm	DMEM ± 10% FBS ± 10 µg/mL Strep ± 10 U/mL Pen	-neat PCL (2D, 3D) -PCL-GO (2D, 3D) -PCL-RGO (2D, 3D)	-AFM -SEM -FTIR -XRD -Physical tests	*Proliferation/viability*: -*DNA content and cellular nuclei staining*: 2D composite >3D composite (7, 14 days). In both 2D and 3D composites:

Authors	Cell Source	Chemical Composition and Functionalization	Type of Graphene	Size	Cultural Condition	Treatment Group	Characterization	Outcome
				Lateral dimension of GO ≈ 5.1 × 3.8 µm Thickness of GO films ≈ 1–3 nm			-Porosity measurement -CA measurements	GO-PCL > neat PCL > RGO-PCL (7, 14 days) *-Proliferation rate*: 3D scaffold: PCL > PCL-GO > PCL-RGO 2D composit: PCL-GO > PCL > PCL-RGO *Attachment*: Initial cell attachment was nearly same for both 2D and 3D (3 days) *Osteogenic differentiation*: *-ALP activity and ARS staining*: ALP expression and mineralized matrix on 3D scaffolds were significantly higher than that of 2D substrates (14, 21 days) Among 3D scaffolds: PCL > PCL-GO > PCL-RGO Among 2D substrate: PCL-GO > PCL > PCL-RGO (14, 21 days)
Luo Y et al.[63] 2015	hMSCs	GO-PLGA	GO	—	DMEM/F12 (50/50) ± 10% FBS ± 100 U/mL Pen ± 100 µg/mL strep	-TCP -15PLGA (PLGA concentrations 15%) -GO-15PLGA -18PLGA -GO-18PLGA -GM (without Dexa) -OM (with Dexa)	-SEM -FTIR -Raman spectra -CA measurement - Mechanical test -Protein absorption	*Proliferation/viability*: *-MTT assay*: The rates of cell proliferation increased dramatically by doping GO (7 days) *Attachment*: *-Cells adhesion*: GO-PLGA > PLGA > TCPC (8 h) *Osteogenic differentiation*: *-qRT-PCR*: With increasing time, the CD44 and CD105 genes on the PLGA and GO-PLGA decreased slightly (14, 28 days). COL I and ALP expression: GO-PLGA > PLGA (14, 28 days).

Authors	Cell Source	Chemical Composition and Functionalization	Type of Graphene	Size	Cultural Condition	Treatment Group	Characterization	Outcome
								-ALP activity, OCN (normalized for the total DNA content): OM: GO-18PLGA > GO-15PLGA > 18PLGA > 15 PLGA. TCP (14, 28 days) GM: GO-PLGA > PLGA (14, 28 days) OM ≫ GM
Nair M et al.[21] 2015	hADSCs	GO-Gn-HAP	GO	The thickness of GO flakes is less than 4 nm The lateral dimension ≈ 1 µm	GM: α-MEM ± 10% FBS ± 1% antibiotic-antimycotic solution OM:α-MEM ± 10% FBS ± antibiotics ± 10 m*M* β-glycerophosphate, 10^{-8}*M* Dex ± 0.05 mg/mL L-AA	-Gn-HAPNM -GO-Gn-HAP1 -GO-Gn-HAP0.5 -Gn-HANM (NM: normal medium) -GO-Gn-HAPNM -Gn-HAPOM (OM: osteogenic medium) -GO-Gn-HAPOM	-AFM -SEM -FTIR -Raman spectra -Porosity measurement -Mechanical tests	*Proliferation/viability*: *-Proliferation*: GO-Gn-HAPOM > GO-Gn-HAPNM > Gn-HAPOM > Gn-HAPNM (14 days). However, the cell proliferation was slightly reduced (21 days) *-Quantitative LDH activity*: The percentage of viable cells from day 7 to 21 was equivalent (7, 14, 21d) *Osteogenic differentiation*: *-ALP activity*: GO reinforced scaffolds > other groups (7, 14d). GO-Gn-HAPOM showed highest ALP activity among all groups (7d). *-Flow cytometric analysis*: OPN expression: GO-Gn-HAPOM>GnHAOM>GO-Gn-HAPNM>Gn-HAPNM (21d)
Zhao C et al.[79] 2015	MC3T3-E1	GO-coated quartz	GO	The thickness of GO sheets ≈ 0.8–1.2 nm Diameter ≈	α-MEM ± 10% FBS ± 100 U/mL pen ± 100 mg/mL strep	-GO coated substrate -GO noncoated substrate -TCP	-AFM -SEM -FESEM -XRD -Raman spectra	*Proliferation/viability*: *-CCK-8 assay*: There were no significant differences in cell proliferation of various groups (1, 2 days) *-Cell apoptosis assay*: GO coatings did not induce any prominent apoptosis or necrosis

Authors	Cell Source	Chemical Composition and Functionalization	Type of Graphene	Size	Cultural Condition	Treatment Group	Characterization	Outcome
				1–5 μm				*Osteogenic differentiation*: -*ALP activity*: GO coated substrate > GO noncoated substrate > TCP (14 days) -*OCN*: The coated substrate significantly increased OCN production (14 days)
Elkhenany H et al.[53] 2014	cBMSCs	GO-coated plates	GO	—	DMEM ± 10% FBS ± 1% pen/strep	-TCP -GO (Different cell densities: -1.0 × 10^3 cells -5.0 × 10^3 -10 × 10^3 -20 × 10^3) -GO+OM -GO+GM	-AFM -SEM -TEM	*Proliferation/viability*: -*MTS assay*: GO with different cell densities ≈ TCP (2, 7, 10 days) -*Calcein-AM staining*: Cells on GO were metabolically active, viable and well-distributed throughout the surface (2, 7, 10 days) *Osteogenic differentiation*: -*ARS staining*: GO+GM ≫ GO+OM (21 days)
Kanayama L et al.[70] 2014	MC3T3-E1	GO-COL RGO-COL	GO RGO	Thickness of GO monolayer ≈1nm Average width ≈ 20 µm	MEM ± 10% FBS ± 1% pen	-GO -RGO -RGO/AA (GO film reduced by AA) -RGO/SH -control	-AFM -SEM -XRD -CA measurements -Porosity measurement -Mechanical test -Electrical measurement	*Proliferation/viability*: -Early cell proliferation on GO and RGO ≪ control (24, 48 h) *Attachment*: -*Measurement of DNA content*: GO ⩽ RGO ≪ control (7, 14 days) *Osteogenic differentiation*: -*ALP activity*: RGO ≫ GO ≳ control (7 day) RGO > control ≫ GO (14 days) -*Ca adsorption*: The RGO film dramatically adsorbed Ca rather than GO film
La WG et al.[39] 2014	hBMSCs	GO-coated Ti	GO	—	DMEM ± 10% FBS ± 1%pen/strep	-No BMP2 -Ti-BMP2 -Ti-GO-BMP2—Daily addition of BMP2	-AFM	*Osteogenic differentiation*: -*ALP activity*: Ti-GO-BMP2 ≈ positive control > Ti-BMP2 group (14 day) -*qRT-PCR*: mRNA expression of ALP and

Authors	Cell Source	Chemical Composition and Functionalization	Type of Graphene	Size	Cultural Condition	Treatment Group	Characterization	Outcome
						(positive control)		Runx2 in positive control > Ti-GO-BMP2 > Ti-BMP2 > No BMP2
liu H et al.[74] 2014a	MC3T3-E1	GO–Gn	GO	—	H-DMEM ± 10% FBS ± 100 U/mL pen ± 100 U/mL strep sulfate	-GO -GO–Gn -Gl	-SEM -XRD -EDX -FTIR	*Proliferation/viability*: -*MTT assay*: No significant differences observed among all scaffolds (1 day) GO > GO-Gn > Gl (3 day) GO-Gn > GO > Gl (7 day). -*LSCM*: Cells are more spread on GO–Gn (3 days) and cells density: GO–Gn ≫ GO, Gl (7 days) *Osteogenic differentiation*: -*ALP activity*: GO, GO-Gn > Gl (3 days) GO-Gn > GO > Gl (7 days) -*SEM*: More complex fibrous organic bundles and embedded CaP on the surface of GO–Gn (14 days) -*ARS staining*: GO-Gn promoted mineral nodular aggregations (14 days)
liu H et al.[73] 2014b	MC3T3-E1	GO-Car	GO	—	H-DMEM ± 10% FBS ± 100 U/mL pen ± 100 U/mL strep sulfate	-Gl -GO -GO-Car	-SEM -FTIR -XRD -EDX -CA measurement	*Proliferation/viability*: -*MTT assay*: The GO-Car films exhibited greater cell growth than that of GO and Gl (1, 3, 7 days) -*LSCM*: There was a higher density of cells on GO-Car than other two (3, 7 days) -*FIN and FIC*: GO-Car ≫ GO, Gl (3, 7 days) *Attachment*: -*Area of cell analyze*: GO-Car, GO > Gl (1 days) GO ≈ GO-Car (3 days) GO-Car > GO, Gl (7 days) *Osteogenic differentiation*: -*ALP activity*: The ALP activity increases

Authors	Cell Source	Chemical Composition and Functionalization	Type of Graphene	Size	Cultural Condition	Treatment Group	Characterization	Outcome
								remarkably with culture time (7 days) GO-Car > GO, Gl (3, 7 days) *-ARS staining*: The Ca deposition of the GO-Car was higher than that of the pure GO and Gl
Subbiah R et al.[76] 2014	Preosteoblast	GO-Fn-Ti	GO	The thickness of the GO matrix on the Ti substrate ~2 *μ*m.	GM*: α*-MEM ± 10% FBS ± 1%pen/strep OM:GM ± 10 m*M* β glycerophosphate ± 0.1 μ*M* Dex ± 50 μg/mL l-ascorbic-2-phosphate ± 50 ng/mL BMP2	-Ti -GO-Ti -GO-Ti-Fn	-SEM -XRD -EDS -Raman spectra -Nanoindentation measurements -CA measurement	*Proliferation/viability*: *-Live and dead cell assay*: There was no great cell viability difference between cells grown on GO-Ti and GO-Ti-Fn (24 h) *-CCK-8 assay*: GO-Ti-Fn > GO-Ti > Ti (1, 3 days) *Attachment*: *-FA assay*: FA quantification: GO-Ti-Fn > GO-Ti > Ti (24 h) *Osteogenic differentiation*: *-ARS and von kossa staining, ALP activity, Ca content*: GO-Ti-Fn > GO-Ti > Ti (7, 14 days)
Tatavarty R et al.[64] 2014	hMSCs	GO-CaP	GO	The size of GO sheets ≈ 0.5–5 μm	OM	-GO 0.5 (μg/mL) -CaP 10 -GO–CaP 10.5	-TEM -ICP-MS -Raman Spectra	*Proliferation/viability*: *-MTT assay*: The greatest viability was 10, 0.5, and 10.5 μg/mL of GO, CaP, and GO-CaP, respectively (3 days) *Osteogenic differentiation*: *-ARS staining*: GO–CaP showed superior osteoinductivity (2, 3 and 4 weeks) GO microflakes increased calcification up to 50% more than the control (3, 4 weeks) Calcification in OM > GM *-Phosphate assay*:

Authors	Cell Source	Chemical Composition and Functionalization	Type of Graphene	Size	Cultural Condition	Treatment Group	Characterization	Outcome
								GO–CaP > CaP ≫ GO > control (2 and 3 weeks) *-ALP activity and OCN expression*: OCN GO–CaP > CaP ≫ GO > control (2 weeks)
kim J et al.[17] 2013	hADSCs	GO-Gl	GO	Lateral size ≈ 1–5 µm thickness of the GO film ≈ 33 nm	DMEM ± 10% FBS ± 1% pen/strep	-Uncoated GO substrate (Gl, TCPS) -GO film (different concentrations: 0, 0.01, 0.1, 1 mg/mL) -with FBS -without FBS	-AFM -FESEM -XRD -XPS -Raman spectra	*Proliferation/viability*: *-MTT assay*: Approximately similar cell viability was shown on GO film compared to the Gl and TCPS, even without FBS -GO concentration of <0.1 mg/mL showed good cells viability *Attachment*: *-Immunofluorescent images*: -Cells on the GO film indicated a larger number of FAs than on the Gl (14 h) *Osteogenic differentiation*: *-ARS staining*: Higher Ca deposits on the GO film were shown than on the control (3 weeks)
La WG et al.[38] 2013	hBMSCs	GO-coated Ti	GO	—	DMEM ± 10% FBS ± 1% pen/strep	-Ti-GO^- (GO-COO^-) -Ti-BMP2 -Ti-GO^--BMP2 -Ti	-AFM -SEM -XPS -EDX -CA measurement -ZP measurement	*Osteogenic differentiation*: *-OCN expression*: Ti-GO-BMP2 > Ti-BMP2 (2, 3 weeks) *-qRT-PCR*: mRNA expressions ALP and OCN on Ti-GO-BMP2 > bare Ti (2, 3 weeks)
kaur T et	MG-63	GNP-PLGA	G	—	DMEM ± 10% FBS ± 100 U/mL Pen/Strep	-GNP-PLGA -CNT-PLGA -AC-PLGA	-FESEM -TEM -FTIR	*Proliferation/viability*: *-MTT assay*: Cell viability:

Authors	Cell Source	Chemical Composition and Functionalization	Type of Graphene	Size	Cultural Condition	Treatment Group	Characterization	Outcome
al.[91] 2017						-PLGA	-XRD -SAED -CA measurements -Degradation assay -Mechanical tests -Protein absorption	GNP-PLGA > CNT-PLGA > AC-PLGA > PLGA > control (2 days) *Attachment*: *Protein adsorption*: GNP-PLGA > CNT-PLGA > AC-PLGA > PLGA *Osteogenic differentiation*: *-ALP activity and ARS staining*: ALP expression and mineralized matrix: GNP-PLGA > CNT-PLGA > AC-PLGA > PLGA > control (7 days).
Li K et al.[28] 2017	bone BMSCs	G-coated Ti_6Al_4V	G	—	DMEM-F12 ± 10%FBS ± 100 U/mL Pen ± 100 mg/mL strep	-G-Ti_6Al_4V -Ti_6Al_4V	-Raman spectra -CA measurement	*Proliferation/viability*: *-CCK-8 assay*: OD:G-$Ti_6Al_4V \gg Ti_6Al_4V$ (1, 3, 5, 7 days) *Attachment*: -ICC: Cell areas on: G-Ti_6Al_4V > Ti_6Al_4V (1 day) Cell areas on: G-$Ti_6Al_4V \approx Ti_6Al_4V$ (3, 5 days). *Osteogenic differentiation*: *ARS staining (21 days), ALP activity (7, 14 days), qRT-PCR (ALP, BMP2, COL-I-α1, and Runx2) (7, 14 days)*: G-Ti_6Al_4V > Ti_6Al_4V
Shie M et al.[60] 2017	hMSCs	G-CS	G	—	DMEM	-G0 (0% graphene content) -G25 (0.25 wt % G) -G50 (0.5 wt % G) -G100 (1.0 wt % G)	-SEM -XRD -XPS -DTS	*Proliferation/viability*: *-Proliferation of cells*: 7 days ⩾3 days ⩾1 day G100 ⩾G50 ⩾G25 ⩾G0 ⩾ control *Attachment*: *-Adsorption of COL-I*: COL-I adsorption was dramatically greater on G50 and G100 than on the pure CS (G0)

Authors	Cell Source	Chemical Composition and Functionalization	Type of Graphene	Size	Cultural Condition	Treatment Group	Characterization	Outcome
								-*Fluorescent images*: The cell density on G50 and G100 were significantly higher than on other two composites (3, 7 days) *Osteogenic differentiation*: -*Western blotting*: ALP, OPN and OCN expression: G100 ⩾G50 ⩾G25 ⩾G0 ⩾ control (7 days) -*ALP activity*: G100 ⩾G50 ⩾G25 ⩾G0 ⩾control (3, 7 days) -*OCN enzyme linked immunosorbent assay kit*: -*OCN expression*: G100 ⩾ G50 ⩾G25 ⩾G0 ⩾control (7, 14 days) -*ARS staining*: G100 ⩾G50 ⩾G25 ⩾G0 (7, 14 days)
Zou Y et al.[87] 2017	iMADs, iMEFs, iCALs,	GL (O/C composition: 0.0864)	G	—	DMEM ± 10% (v/v) FBS ± 100 U/mL pen ± 100 µg/mL strep	-GL scaffold -GL powder -BMP9 -GFP	-SEM -TEM -XPS -TGA -Raman spectra -Porosity measurement	*Proliferation/viability*: -The GL-scaffolds can support long-term proliferation of MSCs -*GLuc activity assay*: The GLuc activity of cells increased at day 5 and slightly dropped at day 7. *Osteogenic differentiation*: -*SEM*: Well-mineralized nodules with many mineral particles were observed on the surface of scaffolds (15 days) -*ALP activity*: Effect of GL powder on iMADs cells: BMP9 > BMP9+GL > GFP, GFP+GL {3, 5, 7 days) Effect of GL powder on iMEFs cells: BMP9+GL > BMP9 > GFP+ GL,GFP (3, 5, 7 days)

Authors	Cell Source	Chemical Composition and Functionalization	Type of Graphene	Size	Cultural Condition	Treatment Group	Characterization	Outcome
								-*ARS staining*: When GL-powder used with Ad-BMP9 matrix mineralization in both iMADs and iMEFs was greatly promoted. -*qRT-PCR*: OPN, OCN, and Runx2 expression were remarkably enhanced by GL-powder
Balikov DA et al.[32] 2016	hMSCs	G (as a cell culture)	G	—	α-MEM ± nucleosides ± 16.7% heat-inactivated FBS ± 1% pen/strep ± 4 μg/mL plasmocin prophylactic agent	-Different stimulation voltages: 0, 0.1, 0.3 V -Gl (unsimulated) -Gl (simulated) -Flat G(unsimulated) -Flat G (simulated) -Grid G (unsimulated) -Grid G (simulated) -Column G (unsimulated) -Column G (simulated) -Voltage	-Raman spectra	*Proliferation/viability*: -*Live/dead assay*: The majority of cells were alive across all voltages on G and Gl (1 Hz, 24 h) *Attachment*: -*Live and dead assay*: Attatchment on Gl > G *Osteogenic differentiation*: -*Immunostaining assay*: The expression of the Runx2 was greatly enhanced by stimulation on all G substrates A noticeable enhancement of OPN was observed when stimulation was coupled with the presence of physical parameters (72 h)
Jakus et al.[35] 2016	hBMSCS	(3D)G-HAP	G		DMEM	-(3D)G -HAP -(3D)-printed HAP-(3D)G -PLGA	-SEM -Porosity measurement -Mechanical test	*Proliferation/viability*: -Cell number on HAP-(3D)G ≈ HAP ≫ (3D)G (day 14) *Osteogenic differentiation*: -*RT-qPCR*: The OCN, OPN, and COL-I expression were upregulated by day 14.

Authors	Cell Source	Chemical Composition and Functionalization	Type of Graphene	Size	Cultural Condition	Treatment Group	Characterization	Outcome
							- Electrical measurements	This expression was Significantly less than that observed on (3D)G and HAP, respectively
Liu Y et al.[19] 2016	hMSCs hADSCs	G-coated Gl G-coated Ti	G	—	GM: DMEM ± 10% (v/v) FBS ± 100 U/mL pen G ± 100 mg/mL strep OM: GM ± 10 n*M* Dex ± 10 m*M*-glycerophosphate and 50 µg/mL l-AA	-G group -G-absent group	-AFM -Raman spectra	*Proliferation/viability*: -*CCK-8 assay*: G group > G-absent group (2, 12, 24 h) -*Cell proliferation*: no significant differences between two groups (2–8 days) *Attachment*: -*FITC staining*: morphology of the adhered cells in G group was extended lamellipodia in G absent group was short pseudopodium extension (12 h) *Osteogenic differentiation*: -*ALP activity (14 day), ARS staining (21 day), mineralization assay (21 day)*: G group > G-absent group
Qiu J et al.[94] 2016	rMSCs	GQDs	GQDs	lateral size ≈ 3.0 ± 0.6 nm	L-DMEM ± 10% FBS ± 1% pen-strep	-GQDs (0–100 µg/mL)	-TEM -PL spectra	*Proliferation/viability*: -*MTT assay*: Up 10 µg/mL GQDs: reached 100% cell viability; 50 µg/mL GQD: viability decreases to 93% (1, 3 days). -*Proliferation*: 14 days > 7 days > 3 days > 1 day -GQDs1 (1 µg/mL) and 10 did not cause negative effect but GQDs50 arrested the growth of MSCs down to 88% (14 days) *Attachment*: -*Fluorescence images*: The GQDs50 distributed

Authors	Cell Source	Chemical Composition and Functionalization	Type of Graphene	Size	Cultural Condition	Treatment Group	Characterization	Outcome
								homogenously thorough the cell body (1, 3 days) *Osteogenic differentiation*: -*ALP activity*: GQDs50 > GQDs10 > GQDs 1 > control (10, 14 days) GQDs50 ≈ GQDs10 ≈ GQDs1 ≈ control (7 days) -*qRT-PCR*: Runx2 expression: GQDs50 > GQDs10 > GQDs 1 > control (7, 10, 14 days) OPN expression also increased up to 10 days exposure, although it was down-regulated at high GQDs doses (14 days) *OCN expression*: GQDs50 > GQDs10 > GQDs 1 > control (10, 14 days) -*IFS*: The OPN and OCN staining strength increases together with increasing the concentration of GQDs (14 days) -*ARS staining*: GQDs10 > GQDs50 > GQDs 1 > control (14 days) -*Microarray analysis of the global gene-expression*: BMP6, TGF-β2, and COLV-α3 were upregulated by GQDs -*Molecule annotation system analysis*: TGF-β signaling, MAPK signaling, Wnt signaling, ECM-receptor interaction, Notch signaling, Ca signaling, and FAs were stimulated by GQDs

Authors	Cell Source	Chemical Composition and Functionalization	Type of Graphene	Size	Cultural Condition	Treatment Group	Characterization	Outcome
Xie H et. al[24] 2016	hDPSC	G-Gl	G	—	DMEM ± 10% FBS ± 1% pen/strep	-Gl (Source)-Gl (Destiny) -Gl(S)-G(D) -G(S)-Gl(D) -G(S)-G(D)	-AFM -Raman Spectra	*Osteogenic differentiation*: -*ARS staining*: G induced higher levels of mineralization as compared to Gl (14, 28 days). -*RT-PCR*: MSX-1, PAX, and DMP genes were down-regulated, though Runx2, COL, and OCN genes were significantly upregulated on G comparing to Gl -*IFS and FACS*: The cells on G showed significantly higher levels of both OPN and OCN as compared to Gl
Yan X et al.93 2016	rMSCs	G-SWCNT	G	—	DMEM/F12 ± 10% FBS ± 1% pen/strep	-G (0, 2.5, 5, 10, 20 µg/mL) -SWCNT (0, 2.5, 5, 10, 20 µg/mL) -G/SWCNT (0, 2.5, 5, 10, 20 µg/mL)	-TEM -Raman spectra	*Proliferation/viability*: -*CCK-8 assay*: G-SWCNT > G > SWCNT In addition, up to 10 µg/mL of G-SWCNT did not inhibit proliferation (1, 3, 7 days) *Osteogenic differentiation*: -*ALP activity*: 14 days > 10 days > 7 days and 5 µg/mL G-SWCNT ≈ 10 µg/mL G-SWCNT ≥ NaF > 2.5 µg/mL G-SWCNT ≈ control (14 days) -*ARS staining*: 14 days ≈ 18 days ≈ 21 days and 10 µg/mL of G-SWCNT at day 14 showed the best result -*Gene expression (OCN, OPN, and Runx-2)*: G-SWCNT at a concentration of 10 µg/mL > other concentrations and NaF -*Western blotting*: The genes related to the MAPK cellular signaling

Authors	Cell Source	Chemical Composition and Functionalization	Type of Graphene	Size	Cultural Condition	Treatment Group	Characterization	Outcome
								pathways were dramatically upregulated
Zhang S et al.[52] 2016	mC3H10T1/2	G-nHAP-PA66	G	The thickness of G ≈ 1.0 nm	DMEM ± 1 g/L glucose, l-glutamine, ± sodium pyruvate ± 10% FBS ± 1% pen/strep OM:10 m*M* β-glycerophosphate ± 10^{-8}*M* Dex ± 0.2 m*M* AA	-G-nHAP-PA66 -nHAP-PA66	-SEM -XRD -Mechanical tests	*Proliferation/viability*: -*CCK-8 assay*: G additives in nHAP-PA66 exhibited higher optical density *Attachment*: -*IFS*: Cells grown with G-nHAP-PA66 illustrated a higher density and a significantly clearer cytoskeleton (4, 24, 72 h) *Osteogenic differentiation*: -*ARS assay*: The G-nHAP-PA66 caused cells to produce more Ca precipitation than the nHAP-PA66 (7, 14 days) -*qRT-PCR*: The ALP and OCN expressions were significantly upregulated by using G-nHAP-PA66 (7, 14 days)
Zhou Z et al.[41] 2016	hBMSCs	(3D)G-VC	G	—	α-MEM ± 15% ES-FBS ± 100 µg/mL strep ± 2 m*M* l-glutamine ± 100 U/mL pen	-H_2O_2 -VC+H_2O_2 -GF+H_2O_2 -GF+H_2O_2+VC	-XPS -Raman spectra -CA measurement	*Proliferation/viability*: -*MTT assay*: Cell viability was restored to normal level by using 25 µg/mL VC, G, and VC+G (5 days) -*ROS*: The H_2O_2-induced ROS increase was attenuated by cotreatment of VC+G (7 days) -*GSH*: It was dramatically rescued by VC+G (7 days) -*SOD*: It was significantly rescued by VC, G, and VC+G (7 days) -*MDA*: It was significantly inhibited by in the VC+G (7 days) *Attachment*:

Authors	Cell Source	Chemical Composition and Functionalization	Type of Graphene	Size	Cultural Condition	Treatment Group	Characterization	Outcome
								-*DAPI*: cell attached and grew well on the GF surface *Osteogenic differentiation*: -*ALP activity*: 0.2 m*M* H_2O_2 decreased the ALP activity (8 days), rescued in the VC, G, and VC+G -*Ca contents*: VC+G rescued the H_2O_2-suppressed differentiation more significantly -*Western blotting*: 0.2 m*M* H_2O_2 inhibited the expression of β-catenin and cyclin D1, restored by VC+G
Li J et al.[57] 2015	MSCs	G-NiTi	G	—	DMEM ± 10%FBS ± 100 U/mL strep ± 100 U/mL pen ± 200 U/mL heparin	-NiTi -G-NiTi-1050°C -G-NiTi-1000°C -G-NiTi-950°C	-SAED -Raman spectra	*Attachment*: G can better promote initial adhesion of cells *Osteogenic differentiation*: -*Gene expression*: levels of OCN, OPN, BMP2, and Runx2 on Gr-NiTi-1050°C > G-NiTi-950°C > NiTi -*Immunofluorescence*: More ALP-positive areas were shown on G, especially on Gr-NiTi-1050°C Compared to NiTi, the G can better promote the expression of integrin β1
Lyu CQ et al.[20] 2015	hADSCs	SGH	G	—	DMEM ± 10% FBS ± 1% Pen/strep	-SGH -G -Carbon fiber -Gl -OM	-SEM -CA measurement. -Mechanical tests -Protein absorption	*Proliferation/viability*: -*Live/dead assay*: ADSCs more strongly proliferate on SGH (1, 3 days) *Attachment*: -*SEM*: Cells attached tightly to the SGH and spread out (3 days), and reached a high cell density (7 days)

Authors	Cell Source	Chemical Composition and Functionalization	Type of Graphene	Size	Cultural Condition	Treatment Group	Characterization	Outcome
								Osteogenic differentiation: -*Flow cytometry*: High level expression of the CD29, CD44, and CD105, and rarely expression of both CD45 and CD34 -*qRT-PCR*: mRNA expression: OM > SGH > G > carbon fiber > control (1, 7, 15 days). Moreover, the expression of BMP2, Runx2, and OCN was significantly higher on the SGH (7, 15 days) -*IFS*: BMP2 and Runx2: SGH > G (15, 21 days) -*ALP activity*: OM > SGH > G > carbon fiber > control (1, 4, 7 days) -*ARS staining*: OM > SGH > G > carbon fiber > control (21 days). In addition, cells displayed an irregular polygonal morphology (21 days)
Wang CH et al.[78] 2015	MC3T3-E1	G-coated PET-ALs	G	The size of G-PET-AL scaffold sheets are 35 mm in diameter	α-MEM ± 10% FBS ± 100 U/mL pen ± 100 U/mL strep	-PET-ALs -G-PET-ALs	-SEM -Raman spectra -CA measurments -Porosity measurments -Mechanical tests	*Proliferation/viability*: -*MTT and live/dead assay*: The OD value and number of live cells: G-PET-ALs ≫ PET-ALs (1, 3, 5, 7 days) *Osteogenic differentiation*: -*ALP*: G-PET-ALs ≫ PET-ALs (7, 14 days) -*ARS staining*: G-PET-ALs ≫ PET-ALs (21, 28 days) -*RT-PCR*: Runx2, OCN, OPN, and COL-IA1 expression on G-PET-ALs were dramatically upregulated compared to PET-ALs (7, 14, 21 days)

Authors	Cell Source	Chemical Composition and Functionalization	Type of Graphene	Size	Cultural Condition	Treatment Group	Characterization	Outcome
Duan S et al.[46] 2014	mBMSCs	PLLA-MWCNTs/G	G	—	BMSC basal culture medium ± 10% FBS ± 100 IU/mL pen ± 100 mg/mL strep	-P0 (pure PLLA) -P1C (containing 1 wt % of MWCNTs) -P3C (containing 3 wt % of MWCNTs) -P1G (containing 1% wt of G) -P3G (containing 3 wt % of G) -TCPS (control group)	-SEM -CA measurement	*Proliferation/viability*: -Cells grown on G > MWCNTs -The cell quantities on PLLA-CNM ≫ pure PLLA *Attachment*: -Incorporation of G resulted in the most cell adhesion rates *Osteogenic differentiation*: *-ALP activity*:. P3G > P3C > P1G > P1C > P0 > TCPS (7, 14 days) P3G ≈ P3C ≈ P1G ≈ P1C ≈ P0 ≫ TCPS (21 days) *-Ca contents*: P3G ⩾P3C ⩾ P1G ⩾P1C ⩾P0 ⩾TCPS (7, 14, 21 days) *-COL-I (ELISA method) and the Ca contents*: P3G > P3C > P1G > P1C > P0 > TCPS (7, 14, 21 days)
Oyefusi A et al.[84] 2014	hFOB 1.19	G-HAP	G	—	1:1 mixture of DMEM and F-12 medium ±10% FBS ± 0.3 mg/mL geneticin ± 1% pen/strep	-Temperature (34, 39°C) -G-HAP200 (200 ng/mL) -G-HAP400 (400 ng/mL)	-SEM -FTIR -XRD -TGA	*Proliferation/viability*: *-Total protein assay*: Cells treated with G-HAP (200, 400 ng/mL) showed increase in total protein with time while peaked at day 9 (at 34°C) *Osteogenic differentiation*: *-Western blot assay*: OCN expression G-HAP400 (39°C) > G-HAP400 (34°C) (9, 12 days) G-HAP200 (34°C) > G-HAP200 (39°C) (9, 12 days)
Talukdar Y et al.[10]	hBMSCs hADSCs	GONRs GNOs GONPs	G&GO	—	StemLife™ MSC medium	-DSPE-PEG (control) -GNOs (0, 5, 10, 50, 100, 300 µg/mL)	-TEM -TGA -ZP -Raman spectra	*Proliferation/viability*: *-Calcein AM staining*: A decrease in viability of both stem cell types with an increasing

Authors	Cell Source	Chemical Composition and Functionalization	Type of Graphene	Size	Cultural Condition	Treatment Group	Characterization	Outcome
9 2014						-GONRs (0, 5, 10, 50, 100, 300 μg/mL) -GONPs (0, 5, 10, 50, 100, 300 μg/mL)		concentration of nanoparticles. CD50 value (for both cell lines): GNOs > GONRs > GONPs (1, 3 days) *Osteogenic differentiation*: -*ARS staining*: More amounts of nanoparticles GONR treated cells. In addition, visible aggregates of varying sizes observed in GONPs treated groups (14 days) *ALP activity and Ca content*: No dramatic difference between groups (14 days)
Xie Y et al.56 2014	hMSCs	G-CS	G	The size of G plates ≈ 0.5–20 μm And thickness ≈ 5–25 nm	GM:α-MEM ± 10% FBS and antibiotics OM:GM ± 50 μ*M* l-AA ± 10*M* glycerophosphate ± 100 n*M* Dex	-G-CS 0.5 (wt % G) -G-CS 1.5 -G-CS 4 -Pure CS -Ti	-SEM -Porosity measurement - Mechanical tests	*Proliferation/viability*: -*MTT assay*: G-CS 1.5 showed a good cytocompatibility and higher proliferation rate (2, 4, 6 days). In addition, the cell number: G-CS 1.5 ≫ CS > Ti (6 days) *Osteogenic differentiation*: -*RT-PCR*: ALP and OPN expression of the cells on the GC 1.5 reached at a peak value (14 days), but OCN expression continued to increase (21 days) GC 1.5 ≈ CS > Ti (4, 14, 21 days)
Crowder SW et al.33 2013	hBMSC	(3D)GF	GF	—	DMEM ± 10% heat-inactivated FBS ± 1% pen/strep	-GF -TCPS (control)	-SEM -EDX -Raman spectra -Porosity measurement	*Attachment*: -Cells attachment on GF ≤ TCPS *Osteogenic differentiation*: -*OCN and OPN secretion*: GF > TCPS

Authors	Cell Source	Chemical Composition and Functionalization	Type of Graphene	Size	Cultural Condition	Treatment Group	Characterization	Outcome
							-Protein adsorption	
Lee WC et al.[59] 2011	MSCs	G&GO sheets	G & GO	—	DMEM ± 10% FBS ± 1% pen/strep	-PDMS -G -GO	-AFM -XPS -Raman spectra -CA measurement -Mechanical test	*Proliferation/viability*: *-Fluorescent images*: Density of cells on G, GO > PDMS (1, 4, 7, 10 days) *Attachment*: *-Fluorescent images*: Attachment of cells on PDMS < G and GO *-Loading capacity*: G and GO adsorbed up to 8% and 25% of the serum proteins, respectively, compared to only <1% adsorption on PDMS (1 day) *Osteogenic differentiation*: *-ARS staining*: G > GO > PDMS (12 days) *-Ultraviolet spectrophotometry*: G adsorbed the most amount of Dex and β-glycerolphosphate and the least amount of AA compared to GO and PDMS (1 day)
Nayak TR et al.[62] 2011	hMSCs	G sheet	G	—	GM: DMEM ± 10% FBS ± 1% pen/strep ± 1% nonessential amino acids ± 1% sodium pyruvate OM: DMEM basal medium ± Dex ± l-glutamine ± AA ± β-glycerophosphate	-Cover slip (control) -Gl slide -Si/SiO_2 -PET -PDMS -G coated Gl slide -G coated Si/SiO_2 -G coated PET	-AFM -Raman spectra	*Proliferation/viability*: *-MTT assay, DAPI (blue), and Calcein AM staining*: No significance difference between uncoated and G coated substrates *Osteogenic differentiation*: *-IFS staining of CD-44 for hMSCs and OCN for osteoblasts and ARS staining*: Without BMP2: GO coating dramatically

Authors	Cell Source	Chemical Composition and Functionalization	Type of Graphene	Size	Cultural Condition	Treatment Group	Characterization	Outcome
						-G coated PDMS -All the groups with BMP2 -All the groups without BMP2		increase differentiation especially on stiffer surface, Gl slide and Si/SiO_2 With BMP2: G further improve the osteogenesis especially on softer surface, PET and PDMS (15 days)
Nie W et al.[4] 2017	mBMSCs	nHAP-RGO	RGO	—	DMEM/F12 ± 15% FBS ± 100 U/mL pen ± 100 mg/mL strep	-RGO -20%, nHAP-RGO -40% nHAP-RGO -80% nHAP-RGO	-SEM -TEM -XRD -EDS -Mechanical test -Porosity measurement	*Proliferation/viability*: -*Live cell staining and cell counting*: 20%, nHAP-RGO > RGO > 40%, nHAP-RGO80%, nHAP-RGO (4, 8 days) *Attachment*: -*Fluorescence signals*: Live cells on 20% nHAP-RGO > RGO ≫ 40% nHAP-RGO > 80% nHAP-RGO (6, 12 h). -*Live cell staining*: Cells number on 20% nHAP-RGO > RGO ≫ 40% nHAP-RGO > 80% nHAP-RGO (4, 8 days). *Osteogenic differentiation*: -*ALP activity*: 20% nHAP-RGO > RGO (3, 7, 14 days) -*mRNA expression*: Runx2 showed an upregulation on the 20% nHAP-RGO scaffold. COL-I A1, OCN, and OPN showed a delayed upregulation -*Von Kossa and ARS staining*: Confirmed the ability of 20% nHAP-RGO to induce the cell mineralization (21 days) -*SEM and EDS*: mineralized nodule was observed as an oval solid

Authors	Cell Source	Chemical Composition and Functionalization	Type of Graphene	Size	Cultural Condition	Treatment Group	Characterization	Outcome
								sphere mostly containing of Ca, P, and O
Tian Z et al.[77] 2017	MC3T3-E1	(3D)RGO films	RGO	Diameter: 0.5–3 μm Thickness: 0.55–1.2 nm	GM: α-MEM ± 10% FBS ± 1% pen/strep OM:GM +10 m*M* β-glycerol phosphate ± 0.2 m*M* AA	-3D-RGO films -RGO -Cover Gl	-AFM -SEM -TEM -XRD -XPS -Raman spectra -CA measurement	*Proliferation/viability*: *-Percentage of live cells*: Cover Gl > 3D-RGO (1, 4 days). Besides, both groups reached to approximate 99% cell viability (7 days) *-CCK-8 assay*: Cover Gl > 3D-RGO (1, 4, 7 days) *Attachment*: *-Live-dead assay*: The number of live cells in both groups gradually increased (1, 7 days) *-DAPI staining*: The number of attached cells on cover glass was greater than that on 3D-RGO (24 h) *Osteogenic differentiation*: *-ALP activity (7, 14 days)*: 3D-rGO film ≈ RGO ≫ cover Gl *-qRT-PCR (ALP, Runx2, OCN, and OPN)*: 3D-RGO film > RGO > cover Gl (14 days)
Feng P et al.[34] 2016	MG-63 hBMSCs	2D GNSs/1D CNTs/HAP–PEEK	2D GNSs	—	GM:DMEM ± 10% FBS ± 1% pen/strep	-S5 (PEEK–10 wt % HAP–0.2 wt % GNSs–0.8 wt % CNTs) -Control	-SEM -XRD -EDS -Raman spectra -Porosity measurement -Mechanical tests	*Proliferation/viability*: *-MTT assay*: Cell proliferation on S5 scaffold > control (1, 3, 5, 7 days) *Attachment*: *-Live/dead assay*: Most of the cells were viable on S5 scaffold (1 3, 5, 7 days) The attachment area on the scaffold surface increased with increasing the culture time *Osteogenic differentiation*:

Authors	Cell Source	Chemical Composition and Functionalization	Type of Graphene	Size	Cultural Condition	Treatment Group	Characterization	Outcome
								-ALP activity: The ALP activity of cells on the S5 on day 7 > day 3
Jia Z et al.[68] 2016	MC3T3-E1	RGO-PDA	RGO	—	α-MEM ± 10% FBS ± 1% pen/strep	-Bulk GO -RGO-PDAx (for x = 1, 2, 5, 10) -TCPS (negative control) -cpTi	-AFM -FTIR -XPS -Raman spectra -CA measurement -Protein adsorption	*Proliferation/viability*: *-Mitochondrial activity*: Cell viability (relative to TCPS) of cells on cpTi > RGO-PDA > GO (2 days). At day 6, all surface showed viability about 100%. *Attachment*: -The number of cells on RGO-PDA ≥ bulk GO ≥ cpTi (4, 8 h) *-Live/dead assay*: around 100% confluence was reached for all groups *Osteogenic differentiation*: *-ALP activity*: Bulk GO > RGO-PDA > TCPS > cpTi (7 days) *-SR staining (collagen content)*: Bulk GO > RGO-PDA ≈ TCPS > cpTi (21 days) *-ARS staining (Ca content)*: Bulk GO ≈ TCPS > RGO-PDA > cpTi (28 days)
Lim KT et al.[25] 2016	hABMSCs	RGO-PEMFs (O/C ratio:0.255)	RGO	Thickness ≈ 1–2 nm	α-MEM ± 10% FBS ± 10 × 10^{-3} ml-AA ± antibiotics ± sodium bicarbonate	-Gl -Gl+PEMFs, -RGO -RGO+PEMFs, (the group cultured on RGO substrates and irradiated by PEMFs)	-AFM -SEM -XRD -XPS -Raman spectra -Elemental analysis experiment -Magnetometry	*Proliferation/viability*: *-WST-1 assay and DNA content*: *Test.*: RGO+PEMFs showed the highest cell viability and DNA concentration ratio *-ICC*: Fn expression: RGO, RGO+PEMFs > Gl, Gl+PEMFs. CaM expression: Gl+PEMFs, RGO+PEMFs > Gl, RGO *Attachment*:

Authors	Cell Source	Chemical Composition and Functionalization	Type of Graphene	Size	Cultural Condition	Treatment Group	Characterization	Outcome
							- Electrical measurement	-*Microscopy images*: Cells on RGO+PEMFs were more numerous than on the other groups (7 days) *Osteogenic differentiation*: -*ALP activity*: ALP was highly secreted on RGO+PEMFs (1 week) -*ICC*: OPN (2 weeks) and NeuN (7 days) were expressed highest on RGO+PEMFs (2 weeks) -*RT-PCR*: RGO+PEMFs promoted the expression of Runx2, OPN, OCN, BSP, SMAD-1, nestin and MAP2. Inversely, the gene expression of ALP decreased (2 weeks) -*ARS and VKS*: RGO+PEMFs exhibited the highest mineralization (2 weeks)
Chen S et al.[65] 2015	MC3T3-E1	RGO – aminosilica hybrid	RGO	—	α-MEM ± 10% FBS ± 100U/mL pen ± 100 µg/mL strep ± GOAP0 (APTES = 0, i.e.,GO) ± GOAP058(APTES = 0.58 mL) at the concentration of 0.00625–0.025 mg/mL	-RGOAP0 (APTES = 0) 0.00625–0.025 mg/mL -RGOAP058(APTES = 0.58 mL) 0.00625–0.025 mg/mL	-SEM -FTIR -XPS -ICP-AES -Raman spectra	*Proliferation/viability*: -*WST assay*: Viability of cells exposed to RGOAP058 ≪ RGOAP0 (1 day) GOAP0 =GOAP058 (3 day) -day 3 > day 1 *Attachment*: -*Live/dead assay*: The most viable cells exposed to both samples (3 day) *Osteogenic differentiation*: -*ALP activity*: RGOAP058 ≫ RGOAP0 (14 days) -*OPN secretion*: RGOAP058> RGOAP0(4 weeks)
Jin L et	hMSCs	RGO NPs	RGO	Lateral sizes ≈ 100–	MSC basal medium ± 50 mL MSC growth	-RGO (at different concentratio	-SEM	*Proliferation/viability*: -*WST-8 assay*: The RGO NPs decreased the cell

Authors	Cell Source	Chemical Composition and Functionalization	Type of Graphene	Size	Cultural Condition	Treatment Group	Characterization	Outcome
al.[58] 2015				1000 nm. Average particle size ≈ 450 nm.	supplement ± 10 mL l-glutamine ± 0.5 mL GA-1000	n: 0, 0.5 1, 2, 4, 8, 16, 31, 63, 125, 250, 500 µg/mL) -Control		viability at about 60 µg/mL. the cell viability increased with time for up to 14 days. -The RGO NPs did not influence cell proliferation. *Osteogenic differentiation*: -*ALP activity*: RGO NPs ⋙ other groups (21 days) -*ARS staining*: Staining was highest in the group with RGO NPs (21 days)
Lee J et al.[72] 2015	MC3T3-E1	RGO-HAP	RGO	—	α-MEM ± 10% FBS ± 1% pen/strep/amphotericin B	-RGO -HAP -RGO-HAP	-FESEM -Raman spectra -XRD	*Proliferation/viability*: -*CCK-8 assay*: HAP, RGO, and RGO/HAP at lower concentrations than 10, and 31.3 µg/mL exhibited no significant cytotoxicity, respectively. -*Proliferation test*: The proliferation patterns of cells did not affected by using HAP, RGO, and RGO/HAP (21 days) *Osteogenic differentiation*: -*ALP activity and ARS staining*: RGO-HAP > RGO > HAP > control (14, 21 days). -*Von Kossa staining*: Corroborated the ability of RGO-HAP to induce the cell mineralization (28 days) -*Western blotting*: OPN and OCN expression: RGO-HAP > RGO > HAP > control (21 days)
Lee J et	hMSCs	RGO-HAP	RGO	Thickness ≈ 1.5 nm	MSC basal medium ± 10% MSC growth ± 2%	-RGO -HAP -RGO-HAP	-AFM -FESEM -XRD	*Proliferation/viability*: -*CCK-8 assay*: HAP, RGO, and RGO/HAP at lower

Authors	Cell Source	Chemical Composition and Functionalization	Type of Graphene	Size	Cultural Condition	Treatment Group	Characterization	Outcome
al.[40] 2015				Lateral size ≈ 438 ± 180 nm	l-glutamine ± 0.1% GA-1000 ± 1%antibiotic antimycotic solution		-Raman spectra -ZP	concentrations than 10, and 62.5 µg/mL exhibited no significant cytotoxicity, respectively *-Proliferation test*: The proliferation patterns of cells did not affected by using HAP, RGO, and RGO/HAP (21 days) *Osteogenic differentiation*: *-ALP activity and ARS staining*: RGO-HAP > RGO > HAP > control (14, 21 days) *-Von Kossa staining*: corroborated the ability of RGO-HAP to induce the cell mineralization (28 days) *-Western blotting and ICC assay*: OPN and OCN expression: RGO-HAP > RGO > HAP > control (21 days)
kumar S et al.[71] 2014	MC3T3-E1	RGO-Sr PCL-RGO-Sr	RGO	Lateral dimension ≈5 µm.	α-MEM ± 10% (v/v) FBS ± 1% (v/v) pen/strep	-Neat PCL -PCL-RGO1 (10 mg of RGO per g of PCL and 0 mg of Sr per g of PCL) -PCL-RGO3 -PCL-RGO5 -PCL-RGO-Sr1 (10 mg of RGO-Sr per g of PCL and 2.2 mg of Sr per g of PCL) -PCL-RGO-Sr3 (30 mg of	-SEM -TEM -XRD -TGA -ICP-OES -Raman spectra -CA measurement -Porosity measurement -Degradation rate	*Proliferation/viability*: *-DNA content and cellular nuclei staining*: All three PCL-RGO-Sr > neat PCL (3, 7 days). DNA content increased with increase in the content of RGO-Sr *Osteogenic differentiation*: *-ARS staining*: PCL-RGO-Sr5 showed the highest mineral deposition (nearly double the mineral content in neat PCL and PCL-RGO5) (14, 21 days)

Authors	Cell Source	Chemical Composition and Functionalization	Type of Graphene	Size	Cultural Condition	Treatment Group	Characterization	Outcome
						RGO-Sr per g of PCL and 6.6 mg of Sr per g of PCL) -PCL-RGO-Sr5 (50 mg of RGO-Sr per g of PCL and 11 mg of Sr per g of PCL) -OM -GM	measurement	
Mehrali M et al.[86] 2014	hFOB 1.19	RGO-CS	RGO	lateral size: GO: 3.88 ± 0.99 μm RGO: 2.37 ± 0.65 μm	DME/F-12 ± 10% FBS ± 100 U/mL pen ± 100 μg/mL strep	-Xonotlite nanowires -CS -CS−0.25 wt % RGO -CS−0.5 wt % RGO -CS−0.75 wt % RGO -CS−1.0 wt % RGO -CS−1.5 wt % RGO	-FESEM -TEM -FTIR -XRD -Raman spectra -Porosity measurement -Mechanical tests	*Proliferation/viability*: *-CLSM*: More cells are attached to the CS/RGO surface than the pure CS surface (3, 5 days) *-MTT assay*: The number of cells increased significantly with increasing RGO concentration (1, 3, 5 days) *Attachment*: *CLSM*: CS/RGO > CS (3, 5 days) *Osteogenic differentiation*: *-ALP activity*: ALP activity increased with increasing RGO content (7 days) *-EDX pattern*: indicated the formation of a Ca phosphate based on the preponderance of Ca and P elements (3 days)
Dubey N et al.[88] 2018	hMG63	G coating on Ti	G	—	DMEM ± 10% FBS ± 1% pen/strep	-G coating on Ti via wet transfer technique (WGp) -G coating on Ti via direct dry transfer	-AFM -XPS -Raman spectra -CA measurement	*Proliferation/viability*: *-MTS assay*: Both WGp and DGp presented significantly higher proliferation compared to CpTi (120 h) *-LDH*: G coating has no effect on cellular

Authors	Cell Source	Chemical Composition and Functionalization	Type of Graphene	Size	Cultural Condition	Treatment Group	Characterization	Outcome
						technique (DGp). -Ti	-Mechanical test	membrane damage (3 days) *Osteogenic differentiation*: *-qRT-PCR (ALP, COL-I, OCN, Runx-2)*: Except for Runx2 at 24 h, both WGp and DGp increased the expression of all osteogenic-related genes (24, 72, 167 h) *-Ca content*: WGp and DGp ≫ Ti
Fu C et al.[81] 2017	MC3T3-E1	GO-PLGA-HAP	GO	—	DMEM ± 10% FBS ± 100 IU/mL pen ± 100 μg/mL of strep	-PLGA -PLGA-HAP -GO-PLGA -GO-PLGA-HAP	-SEM -XRD -CA measurement -Mechanical test -Protein absorption	*Proliferation/viability*: *-MTT assay*: GO-PLGA-HAP > GO-PLGA > PLGA-HAP > PLGA (1, 4, 7 days) *Attachment*: *-FITC & DAPI staining*: GO-PLGA-HAP showed the best cytoskeleton (4d). *Osteogenic differentiation*: *-ALP activity (7, 14 days), ARS staining (14, 21 days)*: GO-PLGA-HAP > GO-PLGA > PLGA-HAP > PLGA *-qRT-PCR (OPN, Runx-2)*: GO-PLGA-HAP > GO-PLGA > PLGA-HAP > PLGA (7 days)
Han I et al.[30] 2018	BMSCs	GO-Ti/BMP2/VAN/GelMS	GO	—	DMEM ± 10% FBS	-Ti -BMP2-Ti -GO-Ti -GO-Ti/GelMS -GO-Ti/BMP2/VAN/GelMS	-SEM -DLS -TEM -FTIR -XRD	*Proliferation/viability*: *-MTT assay*: GO-Ti/BMP2/VAN/GelMS ≈ GO-Ti/GelMS > GO-TI > BMP2-Ti > Ti (3, 7 days) *Osteogenic differentiation*: *-ALP activity*: GO-Ti/BMP2/VAN/GelMS showed the highest ALP activity (14 days)
Sunny C et	ADSCs	GONP-Ti GONR-Ti	GO	GONP: 1–2	ADSC basal media + heat-	-GONP-Ti -GONR-Ti	-AFM -SEM	*Proliferation/viability*:

Authors	Cell Source	Chemical Composition and Functionalization	Type of Graphene	Size	Cultural Condition	Treatment Group	Characterization	Outcome
al.[22] 2018				µm (grain size) GONR: 400–700 nm (in width)	inactivated FBS + ADSC Growth media	-SWCNT-Ti -MWCNT-L-Ti -MWCNT-H-Ti	-Raman spectra -Protein absorption	*-LDH*: SWCNT-Ti ≈ MWCNT-H-Ti > MWCNT-L-Ti ≈ GONP-Ti ≈ GONR-Ti (5 days) *Osteogenic differentiation*: *-ALP activity*: PS > MWCNT-H > SWCNT > MWCNT-L > GONP > GONR > Ti (14 days) GONR > GONP ≈ MWCNT-H ≈ MWCNT-L > SWCNT ≈ PS > Ti (21 days) *-Ca content*: There were no differences at day 14, but at day 21:MWCNT-H > GONP > GONR > Ti > MWCNT-L > SWCNT > PS *-OCN*: MWCNT-H > Ti > SWCNT > MWCNT-L > GONR > GONP (21 days)
Xiong K et al.[44] 2017	mBMSCs	RGO-ZS-CS	RGO	—	DMEM ± 10% FBS	-RGO-ZS-CS-ES (with electrical stimulation) -RGO-ZS-CS-NES (without electrical stimulation)	-FESEM -TEM -XRD -XPS -EDS	*Osteogenic differentiation*: *-ALP activity*: RGO-ZS-CS-ES > RGO-ZS-CS-NES (7 days) *-qRT-PCR (COL-I, OCN, Runx-2)*: RGO-ZS-CS-ES > RGO-ZS-CS-NES (7 days)
Elkhenany H et al.[23] 2017	Goat ADSCs	LOG	G	—	—	-LOG -Polystyrene -G	-SEM -XPS	*Proliferation/viability*: *-MTS assay and live/dead assay*: Cells retained their proliferation and maintained their viability on LOG films (2, 10 days) *Osteogenic differentiation*: *-ARS staining*: Cells underwent osteogenesis (7 days) *-Trilineage differentiation*: Cells retained the expression of CD44

Authors	Cell Source	Chemical Composition and Functionalization	Type of Graphene	Size	Cultural Condition	Treatment Group	Characterization	Outcome
Kim J et al.[51] 2018	C3H10T1/2	GO substrate	GO	—	DMEM ± 10% FBS ± 1% pen/strep -OM -CM -GM	-GO-CM -GO-GM -Gl-GM -Gl-CM	-CA measurement	*Proliferation/viability*: *-Live/dead assay*: GO or CM had no significant cytotoxicity to cells (1 day) *-Alamar Blue assay*: GO-CM > Gl *Attachment*: *-SEM*: The attached cells and the surface area of a single cell were larger compared to that of a glass slide *Osteogenic differentiation*: *-RT-PCR*: OCN, BMPR1A, and RUNX2 secretion: GO-CM > GO-GM ≈ GL-CM > GL-GM (14 days) ALP secretion: GO-CM > GL-CM > GO-GM > GL-GM (14 days) BMP2 secretion: GO-GM > GL-CM ≈ GO-CM > GLGM (14 days) *-ARS staining*: GO-CM showed the greatest calcium deposition rate among all groups (14 days)
Liu M et al.[83] 2018	osteoblast	TP-RGO-Ti	RGO	—	DMEM ± 10% FBS ± 1% pen/strep	-TP-RGO-Ti -Ti	-AFM -SEM -XRD	*Proliferation/viability*: *-CCK-8 assay*: TP-RGO-Ti > Ti (1, 3 days) *Attachment*: *-SEM*: There were fewer cells on Ti surface compared to TP-RGO-Ti (1, 3 days) *Osteogenic differentiation*: *-RT-PCR*: BMP2, BMP4 and OPN secretion: TP-RGO-Ti > Ti (3 days)
Wang Q et	mBMSCs	GO-Ct-HAP-SF	GO	—	DMEM ± 10% FBS	-GO-Ct-HAP (1:4)-SF (wt %	-SEM -TEM -FTIR	*Proliferation/viability*: *-MTT assay*: Cell density was higher on GO-Ct-HAP

Authors	Cell Source	Chemical Composition and Functionalization	Type of Graphene	Size	Cultural Condition	Treatment Group	Characterization	Outcome
al.[43] 2017						GO:wt % HAP) -GO-Ct-HAP (1:2)-SF -HAP-SF -GO-Ct-HAP -SF -Cover slip	-XRD -XPS -Mechanical test -Protein absorption	(1:4)-SF than on SF and HAP-SF (1, 4, 7 days) *Attachment*: -*SEM*: The cells formed a dense and interconnected network *Osteogenic differentiation*: -*ALP activity*: GO-Ct-HAP (1:4)-SF > HAP-SF > SF > cover slip (7, 10, 14 days) -*RT-PCR*: COL-I, OCN, ALP genes: GO-Ct-HAP (1:4)-SF > HAP-SF > SF > cover slip (7, 10, 14 days). CD44 and cD29 genes: GO-Ct-HAP (1:4)-SF > HAP-SF > SF > cover slip (7, 10 days), but at day 14 expression of these genes on GO-Ct-HAP (1:4)-SF was lower
Wei C et al.[31] 2017	BMSCs	GO	GO	—	OM GM:DMEM ± 10% FBS ± 1% pen/strep	-GO/OM (0.01, 0.1, 1, 10 µg/mL) -GO/GM (0.01, 0.1, 1, 10 µg/mL)	-TEM	*Proliferation/viability*: -*CCK-8 assay*: GO/GM at 10 µg/mL inhibited cell growth while GO/GM at 0.1 µg/mL promoted cell proliferation (1, 3, 5, 7 days) *Attachment*: -*CLSM*: Adhesion density of cells was reduced after incubation with 1 and 10 µg/mL of GO/GM (72 h) *Osteogenic differentiation*: -*ALP activity*: GO/DMEM has no effect on ALP activity, while GO/OM (0.1 µg/mL) significantly increased ALP (3, 7 days) -*ARS staining*: GO/OM (0.1 µg/mL) > GO/OM (0.01 µg/mL) (21 days)

Authors	Cell Source	Chemical Composition and Functionalization	Type of Graphene	Size	Cultural Condition	Treatment Group	Characterization	Outcome
								-*RT-PCR*: RUNX2 and β-catenin expression: GO/OM (0.1 μg/mL) > GO/OM (0.01 μg/mL) (14 days)
Yao Q et al.[55] 2017	hMSCs	(3D)GF-PLGA-Ct-BMP2	G	—	α-MEM ± 10% FBS ± 1% pen/strep	-GF -GF-PLGA -GF-PLGA-Ct -GF-PLGA-Ct-BMP2	-SEM -Raman spectra -Mechanical test	*Proliferation/viability*: -*MTS and live/dead staining*: GF-PLGA-Ct-BMP2 > GF (1, 4 days) *Osteogenic differentiation*: -*ALP activity (7 days) and calcium content (21 days)*: GF-PLGA-Ct-BMP2 > GF-PLGA-Ct ≈ GF -*RT-PCR*: BSP, OCN, ALP, RUNX2 expression: GF-PLGA-Ct-BMP2 > GF (7 days)
Zhang L et al.[82] 2018	MC3T3-E1	NT-nGO-PEG-PEI/siRNA (NT-GPP/siRNA)	GO	Hydrodynamic diameters: 561.8 nm	-α-MEM ± 10% FBS ± 100 U/mL pen/strep	-NT -PT -NT-nGO-PEG-PEI (GPP) -NT-nGO-PEG-PEI/siRNA -NT-nGO-PEG-PEI/siCkip-1 -NT-nGO-PEG-PEI/siNC	-AFM -SEM -TEM -DLS -TGA -CA measurement	*Proliferation/viability*: -*CCK-8 assay*: The cell viability on NT was significantly higher than PT and there were no differences among NT, NT-GPP, NT-GPP/siRNA (1, 3, 7 days) *Attachment*: -*SEM*: Cells adhered better on NT and NT-GPP/siRNA compared to PT (24 h) *Osteogenic differentiation*: -*ALP and ARS and collagen secretion*: NT-GPP/siCkip-1 > NT-GPP/siNC = NT-GPP > NT > PT (7 days)
Akhavan o et al.[54] 2013	hMSCs	GONR RGONR	GO RGO	Thickness ~1 nm	-DMEM ± 10% FBS ± 1% pen/strep ± 2 m*M* l-glutamine ± 10 ng/mL basic	-PDMS -RGONR -GONR -GO -RGO -Coverslip	-AFM -SEM -XPS -Raman spectra	*Proliferation/viability*: -*Cell density*: GONR > RGONR > GO > RGO > PDMS (1, 3, 5, 7 days). *Osteogenic differentiation*:

Authors	Cell Source	Chemical Composition and Functionalization	Type of Graphene	Size	Cultural Condition	Treatment Group	Characterization	Outcome
					fibroblast growth factor -OM		-CA measurement	-*ARS staining*: With OM medium: RGONR > RGO > GONR > GO > coverslip > PDMS (7 days) Without OM medium: GONR > RGONR > GO > coverslip > RGO ∼ PDMS (7 days) -*RhP staining*: With OM medium: GONR > RGONR > GO ∼ coverslip > RGO > PDMS (7 days) Without OM medium: GONR > RGONR > GO > RGO > coverslip > PDMS (7 days)
Xie H et al.[27] 2015	hPDLSCs	2DG 3DG	G	—	- GM:DMEM ± 10% FBS ± 1% pen/strep -OM	-Gl/OM -Gl/GM -2DG/OM -3DG/OM -2DG/GM -3DG/GM -PS/OM -PS/GM	-Raman spectra	*Proliferation/viability*: -*MTS assay*: 3DG > 2DG > Gl > PS (5 days) *Attachment*: -*SEM*: Cells efficiently adhered on all experimental substrates (1, 5 days) *Osteogenic differentiation*: -*ARS staining*: 2DG and 3DG under GM presented higher mineralization as compared to Gl and PS with OM -*RT-PCR*: RUNX2 expression (2DG): 2DG/OM > 2DG/GM > Gl/OM (7, 14, 28 days) COL-I and OCN expression: 2DG/OM > GL/OM > 2DG/GM (7, 14, 28 days) RUNX2, COL-I and OCN expression (3DG):

Authors	Cell Source	Chemical Composition and Functionalization	Type of Graphene	Size	Cultural Condition	Treatment Group	Characterization	Outcome
								3DG/OM > 3DG/GM > PS/OM (7, 14, 28 days) MYH10 and MYH10-V2 expression: 2DG/OM was the highest compared to other (28 days). 2DG/GM was higher than Gl/GM (7, 14, 28 days). Gl/OM was similar to 2DG/GM after 7 days but lower after 28 days 3DG presented higher expression regardless the use of OM
Qiu J et al.[42] 2017	mBMSCs	3DRGO-Ti	RGO	Thickness ~1.13 µm	-α-MEM ± 10% FBS ± 100 U/mL pen/strep	-Ti -APS-Ti -GO-Ti -RGO-Ti	-AFM -FESEM -FTIR -XPS -ZP -Raman spectra -CA measurement -Mechanical test -Protein absorption	*Proliferation/viability*: *-Live/dead assay*: all the samples have a good compatibility without cytotoxicity (4 days) *-Alamar Blue assay*: Ti > GO-Ti > RGO-Ti > APS-Ti (1, 4, 7 days) *Attachment*: *-SEM*: Cells adhered well on all substrates (1, 4, 24 h) *Osteogenic differentiation*: *-ALP and ARS and collagen secretion*: RGO-Ti > GO-Ti > APS-Ti > Ti (7, 14 days) *-RT-PCR*: ALP, OPN, OCN and BMP-2 expression: RGO-Ti > GO-Ti > APS-Ti > Ti (7 days)
Jaidev LR et al.[80] 2017	MC3T3-E1	PCL/RGO Cu	RGO	—	—	-PCL/RGO -PCL -PCL/Cu -PCL/RGO_Cu_5 (wt %)	-AFM -SEM -TEM -XRD -EDS -XPS	*Proliferation/viability*: *DNA content (1, 3, 7, 14 days)*: - PCL/RGO > PCL > PCL/Cu > PCL/RGO_Cu_5 (3, 7 days)

Authors	Cell Source	Chemical Composition and Functionalization	Type of Graphene	Size	Cultural Condition	Treatment Group	Characterization	Outcome
								- PCL/RGO = PCL > PCL/RGO_Cu_5 > PCL/Cu (14 days) *Osteogenic differentiation*: *-ARS staining*: PCL/RGO_Cu_5 > PCL/Cu > PCL/RGO > PCL (14 days)

Abbreviations. 1D, one-dimensional; Ad, adenovirus; APTES, 3-aminopropyltriethoxysilane; ASC, adipose stormal cell; Au, gold; BSP, bone sialo-protein; CaM, calmodulin; CBB, Ct-BMP-BSA; CD, circular dichroism; CLSM, confocal laser scanning microscope; DA, hydrochloride; DMEM, Dulbecco's modified eagle medium; FACS, fluorescence-activated cell sorting analysis; FBS, fetal bovine serum; FCS, fetal calf serum; FIC, fluorescent intensity of cytoplasm; FIN, fluorescent intensity of nuclear; GA, entamicin, amphotericin; GC, graphene/calcium silicate; GFP, green fluorescent protein; GLuc, gaussia luciferase; GM, growth medium; GSH, glutathione; hFOB 1.19, human fetal osteoblastic cell line; hMSCs, human mesenchymal stem cells; IFS, immuno-fluorescence staining; MDA, malondialdehyde; mMSCs, mouse mesenchymal stem cells; Na, sodium; NaF, sodium fluoride; PA66, poly-amide66; PDLLA, poly (D, L-lactic acid); PEMFs, pulsed electromagnetic fields; Pen, penicillin; PI, propidium iodide; rMSCs, rat mesenchymal stem cells; RT-PCR, real time polymerase chain reaction; RT-qPCR, real-time quantitative reverse transcription polymerase chain reaction; RUNX2, Runt-related transcription factor 2; SH, sodium hydrosulfite; SOD, superoxide dismutase; strep, Streptomycin; TCPS, tissue culture poly-styrene; α-MEM, alpha-minimum essential medium; VAN, vancomycin; GelMS, gelatin microspheres; MWCNT-L, low diameter multiwalled carbon nanotubes; MWCNT-H, high-diameter multiwalled carbon nanotubes; TCPS, tissue culture polystyrene; ZS, zinc silicate; ES, electrical stimulation; LOG, low oxygen content graphene, CM, chondrocyte-conditioned medium; NT, titania nanotubes; PS, polystyrene scaffold; APS, 3-animopropyl-trimethoxysilane; PT, Ti wet polished with SiC.

RESULTS

Study selection

The process of article selection and data extraction is illustrated in Figure 1. In the primary search, 190 articles were found from the NCBI PMC and PubMed databases, 3 results from other sources and five other articles also found by hand searching. A total of 120 articles were chosen after duplicates were removed. Then, records were screened and irrelevant studies, according to the titles and abstracts were removed with regards to eligibility criteria, and 104 studies remained. In the next step, the full texts of the 104 selected articles were reviewed and 22 more articles were excluded. Four of the studies were excluded as it described a myogenic, neural and chondrogenic differentiation rather than osteogenic differentiation. Five of the studies were excluded because osteogenesis was only a part of the multilineage differentiation characterization tests. Four studies were excluded because it evaluated osteogenesis only through *in vivo* experiments. Nine other studies were excluded due to only the mechanical strength and its influence on cell proliferation and attachment were investigated, and the osteoability of graphene and its derivatives were not evaluated. Ultimately, a total of 82 articles were included in this systematic review.

Cell sources

The most dominant cell types used in the included articles were mesenchymal stem cells (MSCs), including human adipose-derived stem cells (hADSCs),[17-22] Goat ADSCs,[23] human dental pulp stem cells (hDPSCs),[24] human alveolar bone marrow stem cells (hABMSCs),[25] human periodontal ligament stem cells (hPDLSCs),[26, 27] and bone MSCs (BMSCs),[28-31] such as human BMSCs[19, 32-41] (hBMSCs), murine BMSCs (mBMSCs),[4, 42-49] rabbit BMSCs (rBMSCs),[50] murine MSCs cell line C3H10T1/2[51, 52] and Caprine BMSCs (cMBSCs).[53]

The type of the MSCs in fifteen studies[19, 32, 36, 40, 54-64] was not defined. Sixteen studies used preosteoblast cells,[14, 65-79] including mouse osteoblastic cells[14, 65-74, 77-82] (MC3T3-E1) and rat calvarial osteoprogenitors,[75] while the type of the preosteoblast cells in one study[76] was not defined. Five articles[13, 83-86] used osteoblasts. Immortalized mouse embryonic fibroblasts (iMEFs), immortalized mouse adipose-derived cells (iMADs), immortalized mouse calvarial cells (iCALs)[87] and human osteosarcoma cell line hMG63[34, 88-92] were other types of the cells used.

Graphene types

Different types of graphene used in the included studies were pristine graphene,[19, 20, 23, 24, 27, 28, 32, 35, 41, 46, 52 55-57, 59, 60, 62, 78, 84, 87, 88, 91, 93 GO,13, 14, 17, 21, 22, 26, 29-31, 36-39, 43, 45 47-51, 53-55, 59, 61, 63, 64, 66-70, 73-76, 79, 82, 85, 89, 90, 92 RGO,[4, 14, 25, 36, 42, 44 45, 54, 58, 65, 70-72, 77, 80, 83, 86 AGO,[36] GFs,[33] GNSs,[34] GQDs,[94] and nanosized graphene[18] (NGO).

Chemical composition

Different functional groups and materials were used in order to improve the bioactivity of graphene and its derivatives for fabrication of bone regenerative compositions. The materials were metals or metalloids, polymers and mineral substrates. The metal or metalloid category consists of silicon (Si),[65] zinc oxide (ZnO),[89] titanate,[92] strontium (Sr),[71] copper (Cu),[49, 80] silver (Ag),[50] titanium (Ti),[19, 22, 26, 30 38, 39, 42, 45, 47, 69, 76, 83, 88] Ti alloy (Ti_6Al_4V)[28] and nitinol (NiTi).[57] Polymers include poly(L-lactide) (PLLA),[46] poly(dopamine) (PDA),[68] poly(ε-caprolactone) (PCL),[14, 36, 203] poly(ethylenimine) (PEI),[37, 82] poly(lactic-coglycolic acid) (PLGA)-tussah,[61] silk fibroin (SF),[43] polyethylene terephthalate-based artificial ligament group (PET-ALs),[78] PLGA,[55, 63, 81, 91] carrageenan (Car),[73] collagen (COL),[70] chitosan (Ct)/gelatin (Gn),[21, 74, 75 Ct,43, 48, 55] poly-ether-ether-ketone (PEEK),[34] tea polyphenol (TP),[83] poly(ethylene glycolamine) (PEG)/FITC[66] and PEG.[82] The mineral substrates were hydroxyapatite (HAP),[4, 21, 29, 35, 40, 43, 72, 81, 84] glass (Gl),[17, 24, 67] calcium silicate (CS),[56, 60, 86] CaP,[64] quarts[79] and vitamin C (VC).[41]

Characterization

Synthesized graphene, graphene derivatives and their compositions were chemically characterized using Fourier-transform infrared (FTIR)[14, 21, 30, 36, 37, 42, 43, 45, 48, 61, 63, 65, 66, 68, 73 74, 75, 84-86, 91, 92] and raman spectroscopy.[13, 17-19, 21, 22, 24-28 32-34, 36, 37, 40-42, 45, 47, 48, 54, 55, 57, 59, 61-65, 68, 69, 71, 72, 75-78, 86-89, 93] Also, morphology and topography of the samples were characterized by SEM,[4, 13, 20-23, 25, 26, 29, 33-36, 38, 43, 45-56, 58, 60, 61, 63, 65, 66, 70, 71 73-85, 87, 91, 92] field emission scanning electron microscope (FESEM),[17, 40, 42, 44, 72, 79, 86, 90, 91] transmission electron microscopy (TEM),[4, 18, 30, 31, 43, 44, 50, 53, 61, 64, 66, 71, 77, 80, 82, 86, 87, 89-94] and atomic force microscope (AFM).[14, 17-19, 21, 24-26, 36-40, 42, 45, 47, 49, 53, 54, 59, 62 69, 70, 77, 79, 80, 82, 89] Surface hydrophobicity of the composites and their chemical environments were evaluated by contact angle (CA) measurements[14, 20, 28, 36-38, 41, 42, 46, 51, 54, 59, 61, 63, 68-71, 73, 76, 77 78, 80-82, 88, 91] and X-ray photoelectron spectroscopy (XPS).[17, 18, 23 25, 36-38, 41-45, 54, 59, 60, 65, 66, 68, 69, 80, 87-89] Moreover, mineral phase on compositions were investigated by X-ray diffraction (XRD).[4, 14, 17, 25, 34, 36, 37, 40, 43, 44, 47-49, 52, 60, 67, 70-77, 79-86, 89, 91, 92] Mechanical tests[4, 14, 20, 21, 34-37, 42, 43, 52, 55, 56, 59, 61, 63, 67, 69, 70,

[78, 81, 86, 88, 91, 92] were employed in the various studies to evaluate mechanical strength. Inductively coupled plasma atomic emission spectrometry (ICP-AES)[47, 65, 89] and inductively coupled plasma-optical emission spectroscopy (ICP-OES)[49, 71] were employed to measure the release rate of ions, and inductively coupled plasma-mass spectroscopy (ICP-MS)[64] was utilized to assess the Ca/P ratio. Additional assays and measures used for sample characterization include thermal gravimetric analysis (TGA),[37, 71, 82, 84, 87] energy dispersive X-ray spectroscopy (EDX),[33, 38, 50, 67, 73, 74] energy dispersive spectrometer (EDS),[4, 13, 34, 44, 76, 80] porosity measurement,[4, 35, 61, 75, 78] electrical tests,[25, 35, 70] protein adsorption test,[20, 22, 42, 43, 48, 63, 68, 75, 81, 91] ultraviolet–visible (UV-Vis) spectroscopy,[49, 69] calcium absorption test,[70] dynamic light scattering (DLS),[18, 30, 36, 66, 82] zeta potential (ZP) measurement,[18, 29, 38, 40, 42, 47, 66] degradation rate measurement,[48, 71, 75, 91] water absorption,[75] swelling study,[75] weight loss measurement,[60] diametral tensile strength (DTS),[60] nanoindentation measurements,[67, 76] photoluminescence (PL) spectra,[94] elemental analysis experiment,[25] magnetometry,[25] selected-area electron diffraction (SAED),[57, 91] wettability evaluation,[89] roughness evaluation[14, 28, 89] and PL spectrum.[94]

DISCUSSION

Various biomaterials, including ceramic phosphates and synthetic or natural polymers, have been widely used in BTE;[2, 95, 96] however, the challenge of these materials matching chemical and material properties of natural bone still remains.[97] Graphene and its derivatives have specific mechanical, physical, and chemical properties and were shown to facilitate attachment and growth of cells and enhance osteogenic differentiation.[10] In the current review, we conducted the comprehensive review on potential of graphene and its derivatives in promoting cell activities.

Factors affecting the cellular proliferation and viability

Various factors influence the cellular interactions of graphene families, which include graphene concentration, size, type, dimension and composition or functional groups (Fig. 2), as discussed below.[98]

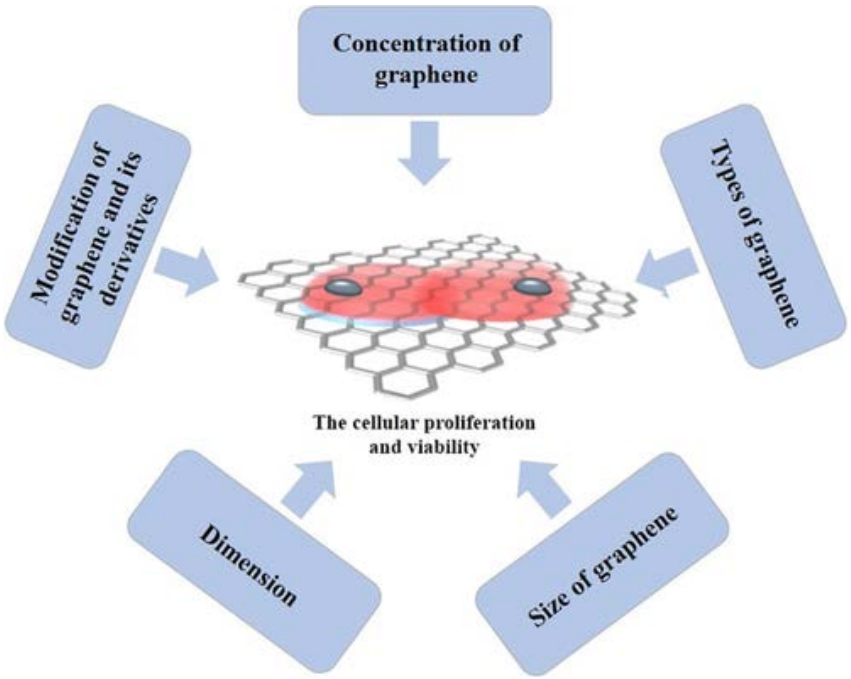

Figure 2 Factors affecting the cellular proliferation and viability.

Concentration of graphene

Despite all the studies regarding the dependence of the toxicity of graphene and its family on concentration, there are no general results about the safe concentration threshold. Many studies[98-101] concluded that concentrations <50 μg/mL of graphene nanoparticles (NPs) are relatively safe for most cell types, and levels higher than this concentration cause intracellular accumulation and high levels of oxidative stress, which is one of the mechanisms playing role in toxicity of carbon nanomaterials (CNMs).[75] Schinwald et al.[102] studied layered graphene platelets with 1–10 layers at concentrations ≥ 5 μg/mL and found that it notably induced the release of LDH in immortalized human acute monocytic leukemia cells, THP-1, which is representative of loss of membrane integrity. Pristine graphene also induces cytotoxicity in cells by ROS generation through a decrease in potential of mitochondrial membrane and activation of mitochondrial pathway, leading to apoptosis.[103]

Zhang et al.[104] investigated the toxicity of GQDs provided by single reduced graphene sheets (diameter: 5–10 nm) on three progenitor cell types: neurosphere cells (NSCs), pancreatic progenitor cells (PPCs), and cardiac progenitor cells (CPCs). They showed that in the presence of GQDs at 100 μg/mL for 3 days, NSC and CPC cell viability was above 80%, however, the cell viability for PPC was about 65%. All the cell groups were alive after incubation with GQDs at 25 μg/mL, which indicates that GQDs can be used as a beneficial biological platform with low cytotoxicity. Similarly, in a study by Qiu et al.,[94] a threshold for toxicity of GQDs to MSC cells was established at 50 μg/mL.

GO causes apoptosis of mitochondrial respiration by generating ROS and has a dose-dependent toxic effects on cells.[105] It was shown that GO with concentration of ≤1 μg/mL in culture medium reached 60% of viability of hMSCs, while at concentrations above 10 μg/mL, viability decreased to <20%.[64] Concentration of 20 and 85 μg/mL were observed to reduce cell viability by 20 and 50%, respectively.[106] In a study by Zancanela et al.,[13] it was established that after 5 days incubation, osteoblasts with various concentrations of GO (10 to 350 μg/mL), samples with 25 and 50 μg/mL GO yielded greatest cell viability. Mazaheri et al.[107] revealed that 1.5 wt % GO in GO-Ct composites showed a proliferation rate of hMSCs similar to that of pure Ct, while in 3 and 6 wt %, GO cytotoxicity significantly increased. Some studies achieved little toxicity, even at higher concentrations. Based on one study, GO concentration <0.1 mg/mL demonstrated no cytotoxicity to hADSCs.[17] Also, in a study by Chang et al.,[108] even high concentrations of 200 μg/mL GO exhibited about 67% viability of A549 cell after 24 h, and similar results could be achieved even after exposure for 48 and 72 h.

The study done by Talukdar et al.[109] investigating graphene NPs with three different morphologies illustrated that graphene nano-onions (GNOs), graphene oxide nanoribbons (GONRs) and graphene oxide nanoplatelets (GONPs) showed a dose-dependent toxicity. Viability of hBMSCs and hADSCs treated with GNOs, GONRs, and GONPs declined with increasing concentration in the range of 0–300 μg/mL, and concentrations of ≤50 μg/mL were observed to be potentially appropriate. In the similar study, 100 μg/mL of the GONR were reported to present no cytotoxic effect on osteoblasts.[85] RGO NPs also showed a dose-dependent decrease in cell viability, as concentrations >60 μg/mL seemed to reduce viability.[58, 110] In a study by Mehrali M et al.,[86] 1.5 wt % RGO-containing composite displayed the most viable cells compared to CS with 1.0, 0.75, 0.5, 0.25, 0 wt % RGO.

To sum up, different concentrations of graphene and its derivatives have shown different toxicity toward various cell lines, indicating the dependency of the toxic effect of graphene on the type of cells. However, based on the literatures, it can be concluded that, up to 50 μg/mL for Graphene and GO, 60

μg/mL for RGO, and 1.5 wt % for all[56, 86, 107] seems to be safest to most of the cells lines. For future studies, we suggest a systematic research on evaluating the safe concentration threshold of graphene derivatives on different cell lines, individually.

Types of graphene

Type of graphene is another important parameter affecting cellular behavior. It was demonstrated that graphene has shown more toxicity compared to GO, as the aggregation of graphene sheet on the membrane of cells can inhibit nutrition transportation.[100] GO is more hydrophilic and biocompatible because of the oxygen-containing groups on its surface. However, some studies report that excess GO might lead to more ROS generation, causing death of cells.[111] Besides, it was discovered that levels ROS generated by synthesized GO with lower oxygenated degree were much higher than those with more oxygenation.[112] Several studies have shown that RGO is more compatible than GO, suggesting reduction may be a means to enhance the compatibility of GO-based biomaterials.[105, 113] Bengtson et al.[12] revealed that ROS generated by GO was more than the RGO materials. Similarly, it was illustrated that human umbilical vein endothelial cells exposed to 10 μg/mL GO and RGO with similar lateral sizes showed more viability in the RGO-containing group compared to GO group after 48 h, which revealed less toxicity of RGO than that of GO.

In contrast, some studies revealed that RGO exhibited dramatically higher effect on cell viability due to its hydrophobic features. In all studies mentioned above, graphene derivatives used in aqueous solution while the application of graphene derivatives as a substrate can be considered as an efficient way to overcome the cytotoxicity effect of that.[54, 114] Akhavan et al.[38] reported that graphene (G) sheets grown by chemical vapor deposition showed not only excellent biocompatibility but also improve the cellular attachment of hMSCs. Indeed, the possibility of the aggregation of hydrophobic graphene derivatives on the cell membrane can be readily decreased by doping and coating them on the surface of materials such as Ti[42] and polydimethylsiloxane (PDMS).[54] Moreover, the initial attachment between cells and surfaces can be affected by surface chemistry and roughness via ionic forces (directly) and adsorption of proteins (indirectly).[115] Therefore, using different graphene derivatives as a substrate can enhance the surface roughness resulting in higher cell proliferation.[114] Compared different graphene derivatives, oxygen-containing groups on GO[45] cause high capacity of protein adsorption through large surface area, intermolecular interactions[116] and surface defects that could serve as binding sites for proteins100 that contribute to cell attachment and viability.[45]

It is important to note that conflicting results observed in comparing GO and RGO can be attributed to their different physical and chemical characteristics or different cell varieties. Conflicting results observed in comparing GO and RGO can be attributed to their different physical and chemical characteristics or different cell varieties.

Size of graphene

Smaller particles are more cytotoxic than larger particles, causing apoptosis through damaging the cellular membrane.[117] Akhavan et al.[101] treated umbilical cord-derived MSCs with graphene nanoplatelets of four different sizes (11 ± 4 nm, 90 ± 37 nm, 418 ± 56 nm, and 3.8 ± 0.4 μm) each at concentrations in the range of 0.01 to 100 μg/mL. The results showed that after 24 h at treatment with the smallest size, 11 ± 4 nm, and concentration of 100 μg/mL, >50% of the cells declined. In another study, it was demonstrated that microsheets of graphene with lateral dimensions <5 μm can penetrate the plasma membrane of mammalian cells and damage the lipid bilayer.[118] Also, a nanosheet of

graphene with lateral dimensions of 100 nm-5 µm has been shown to be easily taken up and accumulate in cells.[119] However, a higher uptake of a graphene NPs cannot be the major reason for the observed cytotoxicity.[108] A study by Talukdar et al.[109] demonstrated that in hADSCs treated with different graphene nanoparticles (GONRs, GNOs and GONPs), GONRs have more cytotoxicity than GONPs, while they did not indicate similar cellular uptake trend.

Bengtson et al.[12] discovered that ROS generated by few layered GO and RGO with lateral size above 1 µm were not toxic in FE1 murine lung epithelial cells at concentrations of > 200 µg/mL.

Reviewed studies indicated that graphene with lateral size of <5 µm and GO and RGO with lateral dimension <1 µm show decline in cell viability. In addition, higher uptake of a graphene is not the main reason for the observed cytotoxicity. More studies are underway to better comprehend the differences in cellular uptake of various size of graphene nanoparticles, including their uptake mechanism and the reasons for the observed variation in death of cells.

Dimension

Three-dimensional (3D) structure is known as a promising structure that better mimics the microenvironment and important features of the native extracellular matrix for cells. Kumar et al.[14] investigated the effect incorporation of two-dimensional (2D) and 3D structures has on GO and RGO in PCL. They found that cells in the 3D scaffold had more cell-cell interaction due to their multicellular organization. The macroporous structure of the 3D foams ensured efficient nutrition substance transportation for cells' metabolic demands, which might facilitate cell proliferation.[14] Researchers have demonstrated that 3D structured graphene, compared to 2D, provides larger accessible specific surface areas, interconnected conductive structure and unique surface microstructure,[120, 121] which might improve cell growth and differentiation.[122, 123] To further compare the compatibility of 3D and 2D structured graphene, Jiang et al.[124] synthesized 2D films and 3D foams of graphene and reported that 3D structured foams are more beneficial for migration of neural stem cells. Indeed, the 3D graphene foam could enhance cell migration through stromal-cell derived factor-1α/CXCR4 signaling pathway, which is essential for the cell migration.[125, 126] In a study performed by Liu et al.,[127] the incorporation of GO changes the 3D topography of scaffold by decreasing the fibrous diameter and porosity, which increases cell proliferation. So far, it is indicated that 3D structure of graphene can promote cell-cell interaction, migration and proliferation, however, few studies focused on the influence 3D architecture has on the cell proliferation, which deserves more consideration.

Modification of graphene and its derivatives

Graphene can be functionalized and combined with other biomaterials, which has the potential to influence cell viability and proliferation.[128] In this review, the effect combination of graphene with these kinds of materials (i.e., metals, polymers and minerals) on cellular behaviors is investigated.

Graphene and metals

Metals are widely utilized in several biomedical applications in pure or alloys forms due to their properties, including toughness, strength, and durability. Graphene has unique physiochemical features, especially its potential for osteogenic induction of stem cells, that make it a promising material for promoting surface modification and bioactive character of metal-based composites.[48] Several studies[13, 26, 28, 45, 47, 50, 65, 69, 71, 76, 86, 89, 92] raised a debate regarding the influential role of metals combined with graphene on cell proliferation and viability.

The chemical functionalization of graphene is an efficient way to enhance its dispersibility and viability to generate various functional groups such as amino, hydroxyl, and carboxyl groups on the basal plane and over the edges.[129] These abundant groups could serve as nucleation sites for metals to anchor and grow through electrostatic and coordinate methods.[130] Thus, many metals and graphene derivatives composites have been fabricated for biomedical applications, demonstrating synergistic effects over the two individual components.[131, 132] For example, Kumar et al.[71] prepared RGO decorated with Sr NPs (RGO/Sr), promoting proliferation owing to the release of Sr^{2+} and hydrophilic nature of hybrid nanoparticles. Additionally, it was proven that cell proliferation was improved by RGO coated multipass caliber-rolled Ti alloy of $Ti_{13}Nb_{13}Zr$ (MPCR-TNZ)[69] compared to MPCR-TNZ and GO-coated Ti compared to Ti-Na[26] and Ti.[76] Graphene sheets can act as substrates for metallic particles and as the storage sites for dissolved metal ions; therefore, preventing the aggregation of metallic particles, decreasing the toxic effects of metallic particles and resulting in the sustained release of metal ions.[133] For instance, In studies by Chen S et al.[65] and Chen J et al.,[89] the controlled release of ions, including Si (Iv) and Zn, from GO compositions stimulated cell proliferation. Release of >3 µg/mL Zn has been shown to be cytotoxic to cells.[134] However, GO-COOH, by providing ZnO NPs with anchor sites, prevents the rapid release of Zn and shows a sustained pattern of release without toxicity to the cells.[89] Likewise, Cu has been shown to improve osteogenic potential, however, since additional Cu in a composite causes oxidative damage,[135] the amount of Cu used in biomaterials is limited. In a study by Zhang et al.,[49] in order to release Cu ions moderately and to prevent the cytotoxicity and related adverse effects, GO-Cu nanocomposite was fabricated and deposited on the surface of porous calcium phosphate cement (Cpc) scaffolds. The good initial attachment and growth of rBMSCs on CPC/GO-Cu scaffolds show the successful results of nanocomposite of GO and Cu.

Various nanocomposites of AgNPs anchored onto GO have been successfully prepared. AgNPs can promote the formation of the callus and the reconstruction of bone defects through enhancing osteogenesis of bone cells via induction/activation of TGF-β/bone morphogenetic protein signaling.[136] However, they are shown the sustained release of a high dose of Ag ions during the degradation process of scaffolds, increasing cytotoxicity. In the study by Zhang et al.,[50] GNSs with a large number of functional groups, such as $–COO^-$ and –OH, combined with AgNPs to form Ag-GO nanocomposites. Release of Ag^+ from the scaffolds was shown to be well controlled below the concentration range, and scaffolds modified by Ag-GO nanocomposites maintained a high cell proliferation level.[50]

Recently, a surface modification of Ti-based materials and promotion of their biological activities has gained attention of researchers in the field of biomaterial engineering.[28] A study performed by Dong et al.[92] represented that by grafting GO on Ti by functional terminal groups, including -COOH, $-NH_2$, and -OH, the GO/Titanate OH-grafted composite was found to significantly improve cell viability. This increase in viability is likely due to the fact that -OH groups play a crucial role in modifying the surface to allow attachment of growth factors, proteins, or other biological molecules.[92] Also, cell proliferation and viability were dramatically greater with Ti-GO than others. In a study by Subbiah et al.,[76] Fibronectin (Fn)-Ti-GO (i.e., Fn bound onto GO) showed the highest proliferation rate. They observed that the extensive filopodia formation improved cell migration and cell–cell interactions around preosteoblasts on Ti-GO and Fn-Ti-GO. These filopodia connections were dramatically found on the Fn-Ti-GO because of arginine-glycine-aspartic acid (RGD) binding moieties of Fn, which is in charge of cell attachment and proliferation. Similarly, graphene coating on the Ti alloy scaffolds also enhanced cell proliferation due to promoted adsorption of the growth factor of the seeding cells;[28] however, in some studies different

observations were reported. In a study by Qiu et al.,[47] increased layers of graphene coated on Ti showed less cell proliferation, and cells grown on Ti exhibited the greatest proliferation among all GO modified groups after 4 days. Indeed, increasing layer-number of GO resulted in decreased cell proliferation. In addition, Zancanela et al.[13] showed that presence of GO decreased the osteoblasts' viability on Ti discs, while the viability of cells cultured on the plastic surface in the presence of 25 µg/mL GO increased up to 170% after 21 days.

Based on the most literatures a number of metallic particles and graphene derivatives composites have been prepared for biomedical applications, exhibiting synergistic effects over the two individual components. In addition, GO is one of the important derivatives of graphene used more than other derivatives with metals to result in positive effects on cell viability and proliferation.

Graphene and polymers

Polymer-based materials are widely used for biomedical applications since they are easily shaped and have adjustable chemical properties.[137-140] However, some of the polymeric materials used in tissue regeneration have to simulate inflammatory reactions, and their degradation might simulate an autocatalytic ester breakdown than can decrease the pH in the microenvironment, causing problems for cell viability and differentiation.[141] In order to overcome these limitations, graphene and its derivatives can be incorporated into polymers through different methods to produce composites exhibiting synergistic effects over the two individual components with improved properties.[34, 36, 37, 46, 52, 61, 63, 66, 68, 70, 73, 75, 78, 91] Recently, graphene-polymer composites have been used for orthopedic applications.[142, 143] For example, GO in Ct matrix was shown to affect interactions between cells and scaffold leading to improved cell proliferation.[142] Interestingly, a few studies represented that biomaterial surface with multifunctional chemical groups can cause remarkable hemocompatibility and cytocompatibilty[144] and affect the physical, chemical and biological features because of the synergetic effect of different chemical functional groups. Thus, the aim of this part is to investigate the effect of functionalized graphene nanoparticles in polymer composites on cell proliferation and viability.

Kumar et al.[37, 71] investigated the influence of adding different graphene derivatives to polymer on cell behavior. They presented that addition of 3 and 5 wt % of GO, 5 wt % of RGO, and just 1 wt % of AGO in PCL led to a dramatic increase in proliferation compared to PCL only. AGO exhibited higher cell proliferation compared to GO and RGO, respectively, due to its higher chemical functionalization.[36] According to recent studies, among various graphene-based substrates, those with greater chemical functional groups generally present enhanced safety profiles.[145-147] It was also reported that adding PEI conjugated GO in PCL was more effective in proliferation than only addition of GO.[37] The promoted proliferation on PCL-GO-PEI might be due to the hydrophilic and polycationic properties of PEI conjugated GO.[148]

Additionally, in recent studies, incorporation of CNTs and GNSs to promote the mechanical properties of polymer has attracted attention of researchers.[149-152] Feng et al.[34] displayed the synergetic effect of CNTs and GNSs on enhancement of mechanical properties, as well as cellular behavior. They showed that a scaffold constructed by combination of HAP-PEEK with GNSs at 0.2 wt % and CNTs at 0.8 wt % had positive influence on cell proliferation with significantly more optical density than other treatment groups. Kaur et al.[71] also investigated the effect of reinforcing PLGA with CNT, graphene nanoplates (GN) and active carbon (AC). They found that cells treated with GN-PLGA showed the highest viability due to its surface functional groups and high protein adsorption that enhanced the cell adhesion and growth.[71]

Furthermore, it was observed that GO incorporated in other polymers, including PLGA[76] and PLGA-tussah silk[61] and also functionalizing Car with GO[73] increased the rate of cell proliferation and viability noticeably. This outcome can be attributed to the unique nanotopography of the graphene-reinforced polymer composites with considerable hydrophilicity of surface, which caused expression of various integrins and connexins.[143, 153]

For biomaterials that have physical interaction with cell membranes, toxicity will probably be generated initially due to the disruption of the membrane integrity, followed by the production of intracellular enzymes (e.g., LDH), and, ultimately, apoptosis or cell death.[154] However, functionalizing RGO with PDA decrease this cytotoxicity, especially during the first days.[68] While bulk GO stimulated the strongest leakage of LDH, indicative of serious membrane damage, rGO-PDA only mildly affected the cell membrane. All These studies confirm the synergetic effects of graphene derivatives and polymers and enhanced cell proliferation on graphene-polymer composites.

Despite all the reviewed articles indicating positive effect of graphene on cell proliferation, in one study performed by Kanayama et al.,[70] early cell proliferation was shown to be dramatically inhibited on GO and RGO films coated COL compared to control culture plate, which is attributed to oxidative stress[155, 156] that stimulates the inhibition of cell viability.

Based on the most reviewed literatures, graphene and its derivatives can be incorporated into polymers to produce composites with multifunctional chemical groups that represent synergistic influences over the two individual components exhibiting improved mechanical properties as well as better cell proliferation and viability. Moreover, it is noteworthy to mention that among various graphene-based substrates in graphene-polymer composites, those with greater chemical functional groups generally demonstrate more safety profiles. There are several opportunities for further development and optimization of graphene-modified polymer composites.

Graphene and minerals

Typically, minerals induce the differentiation of stem cells into osteoblastic lineage.[157-159] However, they are innately brittle, hard to form and exhibit slow resorption rates.[157, 160] Therefore, the development of strategies that can overcome some of these limitations is of interest for biomaterial studies. Notably, graphene and its derivatives can be incorporated into minerals, resulting in composites with both modified mechanical properties and modified osteogenic potential.

Among various graphene derivatives, GO was utilized in several studies to enhance the mechanical properties of mineral-graphene composites and behaviors of cells, including proliferation, viability and differentiation. For instance, GO–CaP nanocomposite with 0.5 μg/mL GO and 10 μg/mL CaP showed cell viability above 80%,[64] due to the hydrophilic surface of GO.[106] In a study by Xie et al.,[29] cells proliferated higher in the adsorbed Bone Morphogenetic Protein-2 (BMP2)-encapsulated bovine serum albumin (BSA) on GO than in other groups, including GO-tissue culture plates (TCP), BMP2-GO-TCP and pure TCP. Indeed GO modification increased the BMP2-encapsulated BSA adsorption capacity of HAP and TCP scaffolds,[29] which can be attributed to the carboxyl groups of GO interacted with the amino groups of the BMP2-encapsulated BSA via electrostatic attraction.[48] Bioactive glass nanoparticles (BGs) have a great potential to form a bioactive HAP layer and provide powerful surface bonding between bone tissue and implant.[161, 162] Hence, Fan et al.[67] produced a novel BGs/GNSs composite scaffold. These scaffolds showed enhanced physical properties of BGs and cell viability of GO by mixing these materials.

They reported that by setting the mass ratio of BGs to GO as 10, cell viability was significantly improved.[67] Similarly, Xie et al.,[56] studying graphene reinforced into CS coatings, concluded that compared to pure CS, CS with 1.5 wt % of graphene were more favorable to cell proliferation after 6 days.[56] Regarding the effect of GO on CS bioactivity, Xie et al.[48] observed biomineralized octacalcuim phosphate (OCP), known as a beneficial agent for cell proliferation,[163] on the surface of GO-CS scaffold, significantly enhancing cell proliferation. Oyefusi et al.[84] and Nair et al.[23] reported that the HAP grafting onto the graphene sheets and incorporating GO nanoflakes into a Gn– HAP matrix enhanced total protein adsorption, as well as cell viability, respectively.

Besides GO, RGO have also been used in some studies to improve the cell viability and mechanical properties of minerals, but there is a controversy in the result of adding RGO on cell viability. CS is a novel biomaterial that causes effective osteoblast-like cell adhesion and proliferation, along with enhancing apatite formation, leading it to become an interesting substrate for hard tissue repair; however, the insufficient strength and toughness of this material is its limitation, which was promoted by RGO. However, adding RGO to CS had no significance influence on cell proliferation,[86] while in CS/graphene, it was shown that greater contents of graphene caused higher cell proliferation. Among 0, 0.25, 0.5, and 1.0 wt % graphene-containing composites, 1.0 wt % showed the highest cell viability.[60] In addition to CS, HAP is widely used in BTE because of its similar chemical composition to natural bones.[164, 165] Nie et al.,[4] showed that nanohydroxyapatite (nHAP)-incorporated in 3D RGO scaffold dramatically enhances cell behavior as well as mechanical strength, which suggests positive influence of RGO on HAP and vice versa. Among 0, 20, 40, and 80% nHAP-incorporated RGO, 20% nHAP-RGO showed the highest proliferation.[4] This was confirmed, as Fan et al.[166] illustrated that the growth inhibition and proliferation of cells would be stimulated by over-dosed nHAP, due to its toxicity in terms of surface morphology, porosity, alkalinity feature and nutrient permeation. Finally, as it has been illustrated in most of the cases, the presence of sufficient oxygen functional groups on the surface of GO can make it more favorable to incorporate with different minerals so as to not only promote the mechanical strength but also modified proliferation and viability, which leads to effectively promoted differentiation.

Factors affecting the cellular attachment

Cell adhesion and spread within the scaffold are usually the first steps following seeding of cells onto the biomaterials, and therefore, have a significant effect on modulating the forthcoming cell responses, including cell proliferation and differentiation.[47] In most reviewed studies, presence of graphene and its derivatives resulted in accelerated cell adhesion and spreading,[19, 21, 52] yet, there are few studies showing no difference between cell density on GO-coated substrates and noncoated substrate.[62, 79] Besides, in a study by Kanayama et al.,[70] GO and RGO films were found to show less DNA content compared to controls.

Various factors seem to be effective in cell adhesion and subsequent cell proliferation and differentiation, such as CA, hydrophilicity, functionalization, morphology, size, porosity, layers and roughness (Fig. 3),[98] as discussed below.

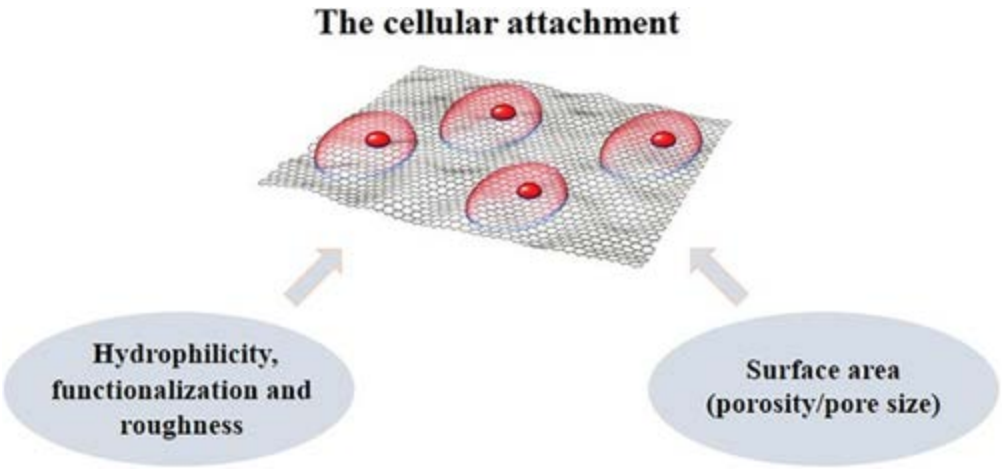

Figure 3 Factors affecting the cellular attachment.

Hydrophilicity, functionalization and roughness

A high CA value indicates the hydrophobicity of the scaffold surface, while a low CA describes the hydrophilicity.[68] Hydrophilic substrate can provide a surface that allow cells to adhere, spread and grow better on them.[69] Usually, hydrophilic surfaces lead to the attachment of adhesive proteins, such as Fn and vitronectin, which can facilitate cell adhesion and growth.[167] It was illustrated that the structure of the adsorbed proteins on surfaces with amine and hydroxyl groups helps more integrin bind in osteoblasts, enhancing formation of focal adhesions (FAs) and eventually activating the osteogenic pathways.[36] FAs, key factors for adjusting cells adhesion and migration, are a type of adhesive contact between cells and extra cellular matrix (ECM).[168, 169] Cells cultivated on the GO film were found to have greater FAs compared to that on the uncoated GO materials.[17]

Kumar et al.[36, 37, 71] investigated the effect of graphene derivatives on cell adhesion in three different studies. They indicated that the incorporation of GO and AGO nanoparticles in PCL increased the hydrophilic features of the composite, which can be result of hydrophilic functional groups on GO and AGO surface.[170] In contrast, adding RGO nanoparticles with no oxygen-containing functional groups decreased the hydrophilicity of PCL and did not dramatically influence cell adhesion. However, they reported in another study[71] that decorating RGO with Sr resulted in increased wettability. It was observed that the amine nanoparticles of AGO in PCL tend to better adsorbed cell-adhesive proteins; therefore, AGO-PCL exhibited higher cell attachment compared to GO-PCL and RGO-PCL.[36] They also indicated that presence of GO-PEI in the PCL composite improved surface wettability more than addition of GO, and GO functionalized with PEI suggested a synergetic effect of chemical, as well as topographical, improvement for reinforcing cell adhesion and proliferation, particularly on PCL-GO-PEI with the highest content of GO (50 mg).[37]

In a study by Kaur et al.,[91] the hydrophobicity nature of PLGA is reformed by reinforcing it with carbon materials such as CNT, GN, and AC. Indeed, the oxygen-containing functional groups of these materials have hydrogen bond interactions with the water molecules, which causes the CA value of PLGA to decrease. Furthermore, GN-PLGA and CNT-PLGA were observed to have more hydrophilicity due to the existence of more carboxyl acid groups on their surface. Also, they found that surface roughness of carbon-based materials, as well as van der Waals and electrostatic forces between surface hydrophilic

groups of them, particularly GN, resulted in high protein adsorption playing a remarkable role in improving cell attachment.[91]

In a study by Lee et al.,[59] high adsorption capacity of graphene (up to 8%) and GO (up to 25%) for serum proteins was observed, whereas PDMS-adsorbed serum was just <1% after one day. Serum proteins are known to consist of several extracellular matrix globular proteins and glycoproteins, including albumin and fibronectin.[171] Therefore, graphene and GO sheets showed better cell attachment compared to PDMS. For graphene, despite its hydrophobic feature, its π-electron cloud is able to interact with the hydrophobic core of proteins. For hydrophilic GO, the polar groups on the surface can bind to serum proteins through electrostatic connection.[59] It also has been reported in studies that G and GO have significant loading capacities for DNA and cytochrome C through intermolecular interactions.[172] Li et al.[28] also discovered that GO coating promoted cell attachment and early extension of BMSCs on the Ti alloy scaffolds. The mean integrated optical density for vinculin is an important component for cell FAs,[173] was notably greater for scaffolds coated with GO than groups without GO. This might be due to the higher surface wettability and roughness of the scaffold with graphene coating.

In a recent study by Ren et al.,[45] BSA was chosen for further investigating the interaction of protein adsorption and cell adhesion. GO-Ti absorbed the highest amount of BSA compared to RGO-Ti. In fact, hydrazine reduction caused elimination of many functional groups, which weakened the electrostatic interaction between BSA and RGO-Ti. In a study by Jia et al.,[68] the number of MC3T3-E1 cells cultured on RGO-PDA was observed to be more than that on bulk GO due to the presence of PDA on the RGO, leading to decreasing the hydrophobicity of RGO. RGO-PDA showed high potential in adsorbing BSA that grafted to PDA through o-benzoquinone – amine coupling;[154] however, GO had a rougher surface and might have a greater capacity for holding protein. The better cell attachment on RGO-PDA may be due to the special role of PDA in mediating biological activity anchorage and stretching during cell attachment, leading to forming a beneficial matrix for stable adherence.[174-176] In an another study, utilizing RGO after incubation of synthesized RGO-MPCR-TNZ in serum protein for 2 hours, which had high CA value due to hydrophobic property of RGO, hydrophobic RGO surface became hydrophilic, and the CA value was dramatically decreased, inducing cell adhesion.[69]

Although several studies have reported improved cell attachment and proliferation on hydrophilic scaffold surfaces, graphene with hydrophobic features can improve the cell adhesion. Similarly, in a study by Duan et al.,[46] it was illustrated that incorporation of multiwalled carbon nanotubes multiwall carbon nanotube (MWCNT) and graphene in PLLA resulted in more mBMSCs adhesion, while hydrophobicity was increased compared to pure PLLA scaffolds. Increased hydrophobicity is due to the interaction between hydrophilic groups, including hydroxyl and carboxyl of CNMs, and the hydroxyl or carboxyl end-groups of PLLA through hydrogen bonds, leading to reduction in hydrophilic groups existing on the surface of scaffolds.[46] It was found that the effect of hydrophilicity of scaffold on cell behavior may depend on cell nature.[2]

Coating the metal surfaces with carboxyl, hydroxyl and amine functional groups was reported to contribute in enhancement of cell adhesion and proliferation.[177] For instance, coating Cu[49] and Ti[26] with GO could remarkably increase the amount of initial adherent cells. In addition, Subbiah et al.[76] improved the efficiency of GO-Ti by bonding Fn on GO and reported the expansive filopodia formation around preosteoblasts on the GO-Ti-Fn because of the cell binding moiety, RGD, of Fn that is accountable for cell attachment. Increased number of FA molecules, FA area per cell, and single FA diameter illustrated

that GO-Ti-Fn can be used as a suitable surface for cell adhesion and, consequently, FA formation. Also, Si-O-Si and Si-OH bonds in RGO–aminosilica hybrid were observed by FTIR.[65] These bonds were found to support the attachment and stimulate the proliferation of cells.[178, 179] Si–O–Si bond was also found in CS/RGO[86] and BGs-GNSs composites.[67] Surface roughness is another important factor playing a significant role in the biological activity of biomaterials. In general, higher roughness provides larger surface areas to interact with protein molecules and cells, which are beneficial for cell adhesion, thereby promoting the biological activity of the biomaterials.[92, 180-182]

It was demonstrated that the rough topology of a cross-linked GO film increases the tension of the cell scaffold and facilitates the growth of hMSCs.[183] Kim et al.[153] discovered that the specific nanomorphology of graphene (i.e., asymmetric nanostructures), as well as its rigidity and roughness, are vital factors for promoting the differentiation of hMSCs. From the studies above, it might be concluded that cell attachment on hydrophilic surfaces, such as GO and AGO, is improved since the hydrophilic surfaces cause much more adsorption of adhesive proteins and formation of FAs. However, moderate hydrophilicity was shown to be better for cell adhesion. Indeed, it was found that the effect of scaffold hydrophilicity on cell behavior is likely to depend on cell nature. Moreover, in most cases, graphene and its derivatives have been found to increase the surface roughness,[28, 37, 59, 92] which can enhance cell adhesion with some limitations.

Surface area (porosity/pore size)

Porosity and pore size have enormous effects on cellular responses, including cell penetration within the scaffold and differentiation. Studies suggest that macroporosity (i.e., pores >50 μm) enhances osteogenesis through cell migration and blood vessel infiltration.[184, 185] Microporosity (i.e., pores < 20 μm) is considered to help bone growth into scaffolds by increasing the surface area for protein adsorption,[186] improving ionic solubility in the microenvironment[187, 188] and providing more adhesion sites for osteoblasts.[184] 3D GFs were seen to be highly porous with individual pore sizes ≥100 μm, providing appropriate surface area for cell attachment.[33]

It was also reported that adding GO to the polymer matrix caused decrease in interconnected pore size and provided a massive porous structure.[61, 189] The optimal pore size in scaffolds to mimic ECM employed in BTE is reported to be in the range of 150–300 μm.[190] In a study by Saravanan et al.,[75] addition of GO decreased the pore size of scaffold from ≥ 220 to ≤ 180 μm. Therefore, the presence of interconnective pores in GO-CS-Gn scaffolds supported cell infiltration, nutrient transfer and metabolic waste elimination. Furthermore, in a study by Nie et al.,[4] it was obvious that number of cells adhered to 20% nHAP-incorporated RGO was much more than that on 40% nHAP-RGO and 80% nHAP-RGO scaffolds. This can be attributed to porous structure of RGO scaffold, which can be changed by incorporating different contents of nHAP. However, in some studies, no significant influence of graphene on porosity was observed. Zhang et al.,[50] showed that the Ag-GO on β-TCP surfaces had no significant influences on the porosity of the scaffolds. Finally, it can be reported that porous structure of graphene and its family provides appropriate surface area for cell attachment and spreading, and therefore enhances osteogenesis through cell migration and blood vessel infiltration.

Factors affecting the cellular osteogenic differentiation

Graphene has been found to not only influence cell attachment, migration, and proliferation, but also promote the differentiation of stem cells to different lineages (Fig. 4).[114, 191, 192]

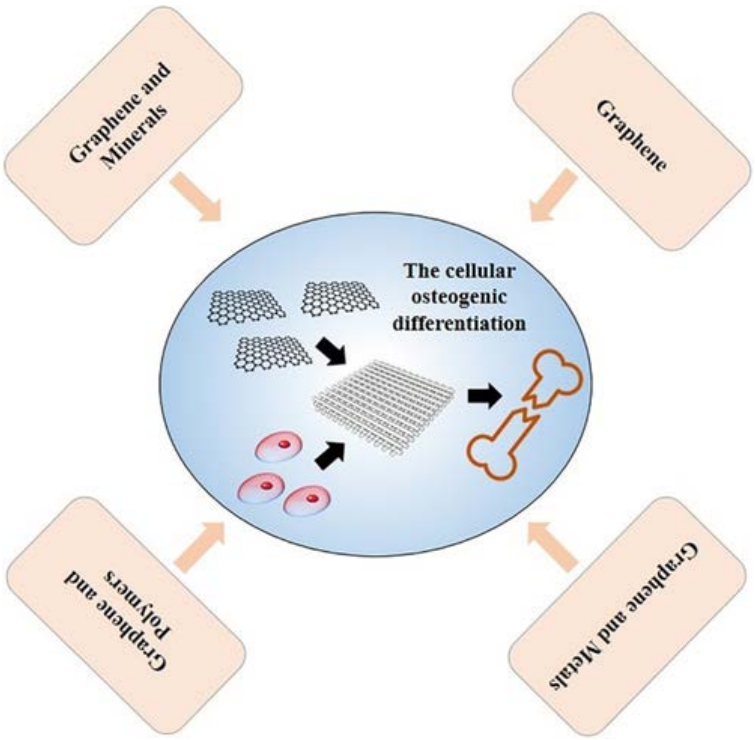

Figure 4 Factors affecting the cellular osteogenic differentiation.

Graphene and its derivatives' properties affecting osteogenesis

Several studies confirm the osteopromotive activity of graphene,[24, 57, 59, 93] GO,[33, 62, 79, 192] RGO[58, 77] and GQDs.[94] It was demonstrated that cells cultured on graphene exhibit higher levels of mineralization and significantly up-regulated osteogenic genes and proteins, including Runt-related transcription factor 2 (Runx2), COL and OCN,[24] even without the use of osteogenic medium (OM).[33, 62] The mechanisms of how graphene affects stem cell behavior remains unknown. It seems cooperation of factors, such as nanoscale structure, high stiffness, roughness, oxygen-contained functional groups, and absorption of biomolecules on graphene and its family, prepare suitable environments for cell behavior regulation such as attachment, proliferation, and differentiation.[17]

In the presence of osteogenic inducers, it was revealed that the mineralization of MSCs cultured on graphene was more enhanced than on GO and the PDMS control. Graphene adsorbed the remarkably higher amount of dexamethasone (Dex) and β-glycerolphosphate compared to GO and PDMS, which can be attributed to the π-π bond between the aromatic structure of Dex and the graphene structure.[59] Dex is a synthetic glucocorticoid changing the expression levels of many proteins and enzymes demanded during osteogenesis.[193, 194] In fact, graphene increasing the local concentration of Dex on its surface increases mineralization and causes fast and influential cell differentiation. In addition, in the study by Ren et al.,[45] GO-Ti samples showed larger adsorption of Dex compared to RGO-Ti samples. The ALP activity, mineralization and osteopontin (OPN) and OCN expression of Dex-GO-Ti was more than Dex-RGO-Ti and Dex-Control. However, GO-Ti and RGO-Ti in the absence of Dex were found to not influence ALP activity effectively.[45] Dex is not the only chemical that is in charge of directing cells to osteogenic differentiation, but it has a synergistic effect with β-glycerolphosphate, binding to graphene by H-bonding and intracellular ALP enzyme for mineralization.[59] Besides, it has been proven that ascorbic acid (AA) influences mainly postdifferentiation,[195] and GO, which has a high density of oxygen functionalities,

showed greater degree of H-binding with AA compared to graphene. ALP, an early and quantitative osteoblastic differentiation marker, is a significant factor in formation of hard tissue. ALP helps in declining the concentration of extracellular pyrophosphate, which inhibits mineralization and increases the inorganic phosphate concentration to enhance mineral formation.[59]

Another factor that may influence osteogenic differentiation is graphene morphology. Talukdar et al.[109] investigated the graphene NPs with three different morphologies: GNOs, GONRs, and GONPs. Greater ALP activity was observed after treatment of hBMSCs with 10 μg/mL GONR. In a similar study by Ricci et al.,[85] up to 100 μg/mL of GONR seemed to not dramatically change gene expression of ALP, OCN, OPN and Runx2, whereas higher concentrations (200 μg/mL) showed reduction in expression of genes, playing a critical role in bone regeneration process.

Several studies reported that RGO can induce osteogenic differentiation individually. For example, in a study by Jin et al.,[58] the amount of ALP synthesized after 14 days and mineralized nodule after 21 days by the cells on RGO NPs was found to be significantly higher than those of the other groups without RGO NPs. Indeed, π-electron cloud of graphene and its derivatives cause interactions with the inner hydrophobic core of proteins.[59] Also, because of the H-bonding and electrostatic interactions, graphene allows the noncovalent binding of proteins and osteogenic inducers on its surface.[195] Interestingly, the 3D-rGO film was observed to offer a faster osteogenic differentiation of MC3T3-E1 compared to RGO, indicating the 3D structure is beneficial for osteogenic differentiation.[14, 77]

Although graphene can enhance osteogenesis, it can be chemically modified or combined with other materials to further induce its osteopromotive activity, such as other carbon-based materials, hydrogels, metals, minerals or polymers. Recently, it has been shown that graphene combined with single-walled carbon nanotube (SWCNT) exhibited better mineralization rather than administration of graphene and SWCNT alone. The G/SWCNT hybrids increased the level of expression genes of OCN, OPN, and Runx2 in a dose-dependent manner. The G-SWCNT hybrids at a concentration of 10 μg/mL after 14 days illustrated the greatest mineralization. It has been reported that graphene and SWCNTs exhibited high surface area in the G-SWCNT hybrids, which led to greater adsorption of osteogenic inducers and proteins from the culture medium. Hydrogel was found to enhance the strength and flexibility of graphene film.[93] Lyu et al.[20] utilized the self-supporting graphene hydrogel (SGH) film for cell seeding and reported the greater levels of the OCN, ALP, BMP2, and Runx2 genes expression, as well as higher ALP activity and mineralization on SGH compared to graphene and carbon films. These findings might attributed to two factors; first, the wrinkled and rippled nanostructure of SGH surface showed significantly higher protein absorption rate, such as BSA molecules compared to other carbonaceous films; second, the SGH film indicated higher hydrophilic surface, which is a vital factor for protein interactions with the surface.

All the results above confirmed the capability of graphene and its different derivatives in improving osteogenesis of stem cells.

Modification of graphene and its derivatives

Incorporation of graphene and its families in the materials utilized for bone reconstructionmetals, polymers and minerals—promotes osteoconductivity via stimulating bio-mineralization as well as cellular osteogenesis, as discussed below.

Graphene and metals

Several studies have utilized metals with graphene.[13, 26, 28, 38, 39, 45, 47-49, 65, 71, 76, 89, 92] GO is widely reported as an efficient adsorbent for metal NPs.[196, 197] In studies by Chen S et al.[65] and Chen J et al.,[89] controlled release of Si (Iv)[65] and Zn[89] ions from GO composition were reported, which can be attributed to the negatively charged surface of GO contributing to the stability of the positively charged metallic ions.[198] Chen J et al.[89] showed that synthesized carboxylated GO (GO-COOH) offers anchor sites for ZnO NPs to prevent ZnO NPs from releasing rapidly. Thus, GO caused sustained release of Zn ions for a relatively long-term, which was shown to enhance ALP activity and OCN secretion. It was reported that a proper dose of zinc ions could promote cell proliferation and differentiation,[89] while a high concentration of Zn ions might cause cytotoxic reactions.[199] This promotion could be due to the mitogen-activated protein kinase (MAPK) pathway.[89] Zn ions induce formation of osteoblastic COL, therefore increase the binding of osteoblasts to matrix integrins, which activate the MAPK pathway. This pathway transduces signals to phosphorylate to ALP and Runx2, which then bind to the promoter region of the OCN gene.

Many studies[26, 38, 39, 47, 76] used titanium incorporated with graphene for enhanced osteogenesis. It is proven that surface roughness and hydrophilicity of Ti can affect differential Wnt pathways and signaling molecules, leading to the osteogenic differentiation.[200] Studies by Zhou et al.[26] and Subbiah et al.[76] suggested that the level of gene expression of collagen type I (COL-I) and OCN were more up-regulated on GO-Ti substrate than on Na-Ti[26] or Ti.[76] In addition, binding Fn onto GO-Ti composition led to the higher levels of osteogenesis than GO-Ti substrate, which was confirmed by ALP activity and ARS staining.[76] Likewise, in a recent study by Li et al.,[28] GO coating on Ti alloy significantly promoted the osteogenesis, which might be attributed to the outstanding surface activity of graphene that increases the capacity of adsorption of the growth factors of the seeding cells to GO-Ti alloy. Zancanela and collaborations[13] reported that in a situation demanding Ti, such as in prostheses and implants, the use of GO might promote mineralized nodule formation, biomineralization, and accelerate bone formation.

La et al.[38, 39] evaluated the bioactivity of BMP2 released from Ti and Ti-GO-substrates. The notable higher level of expression of OCN and ALP was observed in the groups with GO, due to the better conformational stability, greater bioactivity, and increased local concentration of BMP2 on the Ti-GO surface. This increase can be due to the interactions between π-electron clouds in the GO and the inner hydrophobic cores of BMP2, and electrostatic interaction between negatively charged carboxylic groups of GO and the positively charged BMP2. In fact, GO caused sustained release of BMP2, which both play significant role in bone formation.

In another recent study by Qiu et al.,[47] the effect of varying numbers of layers of GO deposited on Ti on osteogenesis was investigated. With increasing the layer-number of GO, wrinkling as well as roughness may promote the cell-material interactions and improve the osteogenic differentiation, though, as stated earlier, increase in thickness or number of layers could reduce cell adhesion and proliferation.

In a study by Dong et al.,[92] the surface chemistry of GO was optimized by constructing -COOH, -OH and -NH_2 terminals through covalent bonding, then grafting these GO sheets on Titanate. This study showed that the scaffold terminated with -OH groups significantly enhanced differentiation compared to those with other terminated groups. The scaffold terminated with -COOH showed less effect on osteogenesis due to the fact that it induced ROS by contributing electrons to oxygen molecules as a result of its high ZP in cell culture medium.

Kumar et al.[71] illustrated that the incorporation of RGO decorated with Sr in PCL was found to have enhanced mineral deposited compared to PCL-RGO composites and neat PCL. These differences were more evident as the amount of the hybrid RGO-Sr particles increased.[71] The Sr ions were found to be beneficial for improving differentiation, even in the absence of osteogenic inducers,[201] since these ions contribute to the activation of calcium sensing receptors and osteoblast markers.[202, 203]

Zhang et al.[49] illustrated that GO and GO-Cu used to coat the Cpc enhanced ALP expression and OCN. GO-Cu was found to be more influential than GO. Moreover, they reported that use of GO, and especially GO-Cu, boosted the activation of Hif-1α through the Erk1/2 signaling pathway causing higher expression of vascular endothelial growth factor (VEGF) and BMP2, two principal regulation factors of osteogenesis. In addition, Ag NPs have exhibited a special property to effectively enhance the osteogenesis of mBMSCs at concentrations of 5–10 μ*M*.[136, 204] Zhang et al.[50] discovered the controlled release of Ag^+ from the Ag-GO-β-TCP, with concentration below the concentration range. GO has showed high adsorptive ability for AgNPs due to the hydrophilic features and high specific surface area of GO. This adsorption could enhance the osteoinductivity properties of biomimetic GO scaffolds.[48] At short term, Ag was seen to inhibit proliferation of bone cells at the defect sites. However, at a long-term, scaffolds can promote BMSC differentiation toward the osteogenic lineage.

Most of the studies included in this section have provided evidence that incorporation of metals and graphene promote the differentiation of stem cells. Also, graphene has been shown to help sustained release of metals.

Graphene and polymers

Several included papers[14, 34, 36 37, 46, 52, 61-63, 66, 68-70, 73, 75, 78, 90, 91] investigated the different polymers improved by graphene and its derivatives or vice versa.

Four included studies have reported a successful use of Gn as a modifying agent. Indeed, Gn improved the HAP nucleation through its negatively charged carboxylate groups existing on its surface.[74] Liu et al.[74] used Gn functionalized GO to mimic charged proteins existing in ECM and observed a higher amount of ALP activity, as well as fibrous organic bundles for GO-Gn compared to GO and Gl. In the study performed by Saravanan et al.,[75] the addition of GO at the concentration of 0.25% in Ct-Gn scaffolds improved apatite deposition, as confirmed by XRD. The $-NH_2$ and C=O functional groups of Ct were reported to contribute to bio-mineralization.[48]

Zou et al.[87] demonstrated that Gn-derived graphene/laponite (GL) powder enhanced osteodifferentiation due to the physical stresses induced on cells, as a result of the surface topographic, stiffness and roughness of graphene sheet.[87] Furthermore, the GL-powder promoted matrix mineralization of the cells by increasing BMP9-induced osteogenesis; BMP9 is one of the most potent to induce MSC osteogenic differentiation.

Two polymers of PET-based artificial ligaments with low known bioactivity[78] and nHAP/PA66[52] were promoted by graphene and showed more osteoability represented by notably up-regulated expression of ALP and OCN compared to polymers alone. This can be attributed to graphene enhancing the adsorption of the growth factors and chemicals containing benzene rings, such as β-glycerophosphate and Dex.[52] Also, the electric characteristics of CNMs may be a significant factor in this improvement.[205]

Nayak et al.[62] compared the effect of common growth factors (BMP2) and graphene on osteogenesis. Without BMP2, graphene coating dramatically increased differentiation of all substrates (glass slide, Si/SiO_2, PET and PDMS), while this increase was more pronounced with the stiffer substrate (glass slide and Si/SiO_2). On the other hand, in the presence of BMP2, it was observed that coating graphene on the stiffer substrates did not further improve the production of calcium deposits, but a clear dramatic increase was seen on the softer materials, PET and PDMS. This again represents that graphene itself has a significant role in the osteogenesis of hMSCs.

A study done by Kumar et al.[37] illustrated that the PCL-GO-PEI exhibited more mineralization and ALP activity compared to the PCL-GO and neat PCL. The greatest graphene and GO-PEI content (5 wt %) in the PCL-GO5 and PCL-GO-PEI5 exhibited highest mineralized deposition. This increase for the PCL-GO-PEI may be rooted in the fact that the GO-PEI is rich in amine and oxygen-containing functional groups, which have been proved to promote FAs[206, 207] and adsorption of the osteogenic inducers (β-glycerol phosphate, Dex and AA), followed by the PCL-GO and, finally, neat PCL. They showed in another study[36] that composition of 5 wt % of AGO (PCL-AGO5) and 5 wt % of GO (PCL-GO5) with PCL exhibited 40 and 25% higher mineralization than neat PCL, respectively. It was observed that mineral deposition increased with increase in content of GO and AGO in PCL. The more mineralized deposits, such as HAP, calcium and phosphorous, on the PCL-AGO5 may be due to the fact that the combination of AGO and PCL proposed both amine and carboxyl functional groups, which led to better mineralization.

In one study by Jia et al.,[68] ALP expression, COL secretion and Ca^{2+} content on PDA-functionalized RGO, and particularly on bulk GO, was improved compared to that on commercial pure titanium (cpTi). For RGO-PDA, it can be stated that the amine groups of PDA cause great interaction with the graphene, as well as provide active sites for mineral ions, therefore improving apatite nucleation and growth.[208] For bulk GO, beside polar groups in its structure, the special topographical ridges known as “graphene patterns” deserve consideration as they provide biophysical cues for greater improvement in osteogenesis. Furthermore, micropatterned geometries of graphene were illustrated to be influential in stem cell differentiation.[18] Another article by Kanayama et al.,[70] comparing GO and RGO films coated COL, displayed that cells adhered to RGO illustrated the highest ALP activity, due to high adsorption of Ca^{2+} on RGO rather than that on GO. This significantly high Ca^{2+} accumulation on RGO can be attributed to AA used as reducing agent that was adsorbed onto the GO surface and interacts well with Ca^{2+}. On the other hand, Kumar et al.[14] demonstrated that functionalized groups on the GO surface and its tendency toward adsorbing osteoinductive factors led to better mineralization compared to nonfunctionalized RGO. As there are distinct results from comparing osteoability of GO and RGO, generalization in this case is not acceptable.

Using Car could enhance the bioactivity of GO, as it was shown that cells cultured on the GO-Car exhibited greater levels of ALP activity, along with increased mineral deposits consisting of COL fibers and some matrix vesicles, loaded with CaP crystals, than those on the GO and glass. Also, the Ca and P contents and calcium deposition of GO-Car film were significantly more than the GO film. This is because of the carrageenan's effect on cell proliferation and differentiation, and the improved nucleation of HAP due to sulfate groups on GO-Car surface, which promote the calcium binding.[73]

In some studies[20, 36, 37, 64, 69, 71, 109] it was represented that cells cultured in osteogenic media, mostly supplemented with osteogenic factors such as Dex, ascorbate, and β-glycerolphosphate,[59] illustrated improved osteogenesis in comparison with cells cultured in nonosteogenic media. For example, cells

cultured on MPCR-TNZ, RGO-MPCR-TNZ, and Dex-RGO-MPCR-TNZ in nonosteogenic media suggested relatively inadequate osteogenic tendency compared to that in osteogenic media.[69] On the other hand, seldom different results have been reported. For instance, in one study by Elkhenany et al.,[53] cells cultivated on GO in growth medium showed notably greater alizarin red content compared to cells grown on GO in the presence of the differentiation medium.

Reviewed studies suggest that graphene and its derivatives, due to their unique features and remarkable osteability, are good choices to not only overcome polymer limitation but also improve their osteoconductive effects.

Graphene and minerals

An alternative strategy for improving the osteogenic potential of stem cells is to utilize mineral materials with graphene family.[4, 20, 21, 29, 40, 41, 48, 56, 60 64, 72, 74, 75, 86, 87]

In three other studies,[56, 60, 86] CS was utilized as a mineral agent. Si is known as a principal component of the CS and has a mitogenic effect on human osteoblast cells,[209] acting via the insulin-like growth factor II.[210] Si ions released from materials have been shown to stimulate differentiation, gene expression and proliferation, which can be considered as evaluation criteria for bioactivity.[210, 211] Mehrali et al.[86] demonstrated that Si concentrations in simulated body fluid, level of ALP activity, and the amount of HAP formed on the surface of composites increase with increase in RGO content. In CS-RGO composites, CS − 1 wt % RGO composite has the best performance among other groups: 0.25, 0.5, 0.75 and 1.5 wt % of RGO. Similarly, it was reported that the expression level of ALP, OCN, and OPN enhanced with increasing graphene content in graphene-CS composites.[56, 60]

In some studies, HAP is utilized with 3D-graphene[35] and RGO.[4, 40, 72] The expression level of OCN, OPN, and COL-I enhanced in both composites, while in the former this expression mainly remained less than that in HAP.[35] It was found that HAP and RGO have an interactive effect on the early and late osteogenic differentiation markers. Therefore, cells exposed to RGO-HAP exhibited higher osteogenesis.[40, 72] For nHAP-RGO, despite up-regulated relative expression of Runx2 with using 20% nHAP-RGO scaffold, its value initially enhanced to the maximum at day 7, after which it dropped down at day 14. This observation might be due to the role of the Runx2 as a key transcription factor to launch early osteogenesis.[4] Oyefusi et al.[84] also grafted HAP onto the surface of graphene sheets and treated cells with various concentrations (200 and 400 ng/mL) of them at different temperatures (34 and 39°C). Interestingly, they found that G-HAP400 at 39°C showed higher OCN expression than G-HAP400 at 34°C, and the opposite occurred for GO-HAP200.

Incorporation of GO in CaP exhibited great levels of ALP activities and OCN expression, as well as high calcification compared to GO and CaP individually, which suggests synergistic contribution of GO and CaP to promoted osteogenesis.[64] This increase can be attributed to not only increased connection between the intracellular FA complexes of the cells and the CaP on GO–CaP composite,[212] but also to higher stiffness of these composites than solely GO or CaP.[213] It is reported that increased stiffness of materials leads to improve a mechano-transduction influence for differentiation regulation.[214]

Recently, Xie et al.[29, 48] utilized GO nanolayer to provide anchor sites for the immobilization of BMP2-encapsulated BSA (Nps) on HAP and TCP. Nps-GO-HAP scaffold showed the highest ALP activity compared to BMP2-GO-TCP, GO-TCP and pure TCP. This scaffold provided a nanostructure with charge-balanced surface, achieved by negative charged GO, positive charged Nps, and long-term sustained

release of BMP2. All of these factors synergistically enhance the BMSCs proliferation and differentiation. Moreover, the results of ALP assay show that the immobilization of BMP2 on the surfaces of GO-modified CaP scaffolds improve their osteoinductivity.

Although the utilization of graphene family and minerals can improve the osteogenic differentiation of stem cells individually, it seems that the combination of these materials may provide better features to induce and enhance cell differentiation.

LIMITATIONS

Several limitations were found in the included articles, which deserve to be considered:

1. Some studies did not investigate cell attachment, even though it has an important role modulating the forthcoming cell responses, like cell differentiation.[47]
2. Since the cytotoxicity of graphene and its derivatives impose serious limitation on biomedical application, evaluation of viability and proliferation of cells exposed to them is very important, however, some studies did not evaluate this kind of cell response. In addition, MTT assay performed in 21 included studies was discovered to be not successful in predicting the toxicity of graphene and its derivatives due to the spontaneous reduction of MTT by them, leading to a false positive signal.[100] Therefore, to evaluate the toxicity of graphene, it is much better to use alternate assays, such as water-soluble tetrazolium salt (WST-8) assay,[58] ROS assay,[41] CCK-8 assay[52, 76, 77, 79] and DNA counting[25, 36, 37, 71]
3. In nine included studies the type of the MSCs, and in one study, type of the preosteoblast cells were not defined.
4. Size (i.e., thickness and lateral dimension), topography of graphene surface (roughness) and hydrophilicity of graphene (CA) are the important factors affecting the graphene bioactivity, were not measured in some studies.
5. In most of the included studies, C/O ratio of graphene, indicative of oxidation state, was not determined as a significant criteria, which made it impossible to make a reasonable comparison between studies.

CONCLUSIONS

The current review is systematic review regarding the effect of graphene and its derivatives on cell osteogenic differentiation. Despite the limitations in the included studies, which made the comparison difficult, some general conclusions can be drawn:

1. Different concentration of graphene and its derivatives have shown different toxicity toward various cell lines, demonstrating the dependency of the toxic effect of graphene on the type of cells. However, based on the literatures, it can be concluded that, up to 50 µg/mL for Graphene and GO, 60 µg/mL for RGO, and 1.5 wt% for all seems to be safest to most of the cells lines.
2. GO seems to be more biocompatible than graphene, while the conflicting results were observed in comparing GO with RGO.
3. Graphene with lateral size less than 5µm and GO or RGO with lateral dimension less than 1 µm showed decline in cell viability.
4. Graphene and its derivatives incorporated with metals, polymers, and minerals showed promoted mechanical properties and bioactivity, in most cases.

5. Graphene and its derivatives have been found to increase the surface roughness, which can highly enhance cell adhesion and differentiation.
6. Graphene exhibits better osteogenic differentiation result compared to GO, but making comparison between osteogenic potential of GO and RGO is not feasible to precisely due to the contradictory reports.

REFERENCES

1Gong T, Xie J, Liao J, Zhang T, Lin S, Lin Y. Nanomaterials and bone regeneration. *Bone Res* 2015;3:15029.

2 Jafari M, Paknejad Z, Rad MR, Motamedian SR, Eghbal MJ, Nadjmi N, Khojasteh A. Polymeric scaffolds in tissue engineering: A literature review. *J Biomed Mater Res—Part B Appl Biomater* 2017;105:431–459.

3 Kang E-S, Kim D-S, Suhito IR, Choo S-S, Kim S-J, Song I, Kim T-H. Guiding osteogenesis of mesenchymal stem cells using carbon-based nanomaterials. *Nano Converg* 2017;4:2.

4 Nie W, Peng C, Zhou X, Chen L, Wang W, Zhang Y, Ma PX, He C. Three-dimensional porous scaffold by self-assembly of reduced graphene oxide and nano-hydroxyapatite composites for bone tissue engineering. *Carbon N Y* 2017;116:325–337.

5 Bunch JS, Verbridge SS, Alden JS, van der Zande AM, Parpia JM, Craighead HG, McEuen PL. Impermeable atomic membranes from graphene sheet. *Nano Lett* 2008;8:2458–2462.

6 Geim AK, Novoselov KS. The rise of graphene. *Nat Mater* 2007;6:183–191.

7 Neto AHC, Guinea F, Peres NMR, Novoselov KS, Geim AK. The electronic properties of graphene. *Rev Mod Phys* 2009;81:109.

8 Omidi M, Fathinia A, Farahani M, Niknam Z, Yadegari A, Hashemi M, et al. Bio-applications of graphene composites: from bench to clinic. In: Tiwari A, Syväjärvi M, editors. Advanced 2D Materials; New York: John Wiley & Sons; 2016. p. 433–471.

9 Holt BD, Wright ZM, Arnold AM, Sydlik SA. Graphene oxide as a scaffold for bone regeneration. *WIREs Nanomed Nanobiotechnol* 2016 2017;9:e1437–e1418.

10 Dubey N, Bentini R, Islam I, Cao T, Castro Neto AH, Rosa V. Graphene: A versatile carbon-based material for bone tissue engineering. *Stem Cells Int* 2015;2015:1–23.

11 Rosa V, Xie H, Dubey N, Madanagopal TT, Rajan SS, Morin JLP, Islam I, Castro Neto AH. Graphene oxide-based substrate: Physical and surface characterization, cytocompatibility and differentiation potential of dental pulp stem cells. *Dent Mater* 2016;32:1019–1025.

12 Bengtson S, Kling K, Xie S-H, Liu A-L, Chen Y-Y, Zhang L. No cytotoxicity or genotoxicity of graphene and graphene oxide in murine lung epithelial FE1 cells in vitro. *Environ Mol Mutagen* 2010;51:229–235.

13 Zancanela DC, Simão AMS, Francisco CG, de Faria AN, Ramos AP, Gonçalves RR, Matsubara EY, Rosolen JM, Ciancaglini P. Graphene oxide and titanium: Synergistic effects on the biomineralization ability of osteoblast cultures. *J Mater Sci Mater Med* 2016;27:1–9.

14 Kumar S, Azam D, Raj S, Kolanthai E, Vasu KS, Sood AK, Chatterjee K. 3D scaffold alters cellular response to graphene in a polymer composite for orthopedic applications. *J Biomed Mater Res—Part B Appl Biomater* 2016;104:732–749.

15 Compton OC, Nguyen ST. Graphene oxide, highly reduced graphene oxide, and graphene: Versatile building blocks for carbon-based materials. *Small* 2010;6:711–723.

16 Akhavan O, Ghaderi E, Abouei E, Hatamie S, Ghasemi E. Accelerated differentiation of neural stem cells into neurons on ginseng-reduced graphene oxide sheets. *Carbon N Y* 2014;66:395–406.

17 Kim J, Choi KS, Kim Y, Lim K-T, Seonwoo H, Park Y, Kim D-H, Choung P-H, Cho C-S, Kim SY, Choung Y-H, Chung JH. Bioactive effects of graphene oxide cell culture substratum on structure and function of human adipose-derived stem cells. *J Biomed Mater Res Part A* 2013;101:3520–3530.
18 Kim T-H, Shah S, Yang L, Yin PT, Hossain MK, Conley B, Choi J-W, Lee K-B. Controlling differentiation of adipose-derived stem cells using combinatorial graphene hybrid-pattern arrays. *ACS Nano* 2015; 9:3780–3790.
19 Liu Y, Chen T, Du F, Gu M, Zhang P, Zhang X, Liu J, Longwei Lv Xiong C, Zhou Y. Single-layer graphene enhances the osteogenic differentiation of human mesenchymal stem cells in vitro and in vivo. *J Biomed Nanotechnol* 2016;12:1270–1284.
20 Lyu C-Q, Lu J-Y, Cao C-H, Luo D, Fu Y-X, He Y-S, Zou D-R. Induction of osteogenic differentiation of human adipose-derived stem cells by a novel self-supporting graphene hydrogel film and the possible underlying mechanism. *ACS Appl Mater Interfaces* 2015;7:20245–20254.
21 Nair M, Nancy D, Krishnan AG, Anjusree GS, Vadukumpully S, Nair SV. Graphene oxide nanoflakes incorporated gelatin–hydroxyapatite scaffolds enhance osteogenic differentiation of human mesenchymal stem cells. *Nanotechnology* 2015;26:161001.
22 Patel SC, Owais Alam BS. Osteogenic differentiation of human adipose derived stem cells on chemically crosslinked carbon nanomaterial coatings. *J Biomed Mater Res Part A* 2017;
23 Elkhenany H, Bourdo S, Hecht S, Donnell R, Gerard D, Abdelwahed R, Lafont A, Alghazali K, Watanabe F, Biris AS, Anderson D, Dhar M. Graphene nanoparticles as osteoinductive and osteoconductive platform for stem cell and bone regeneration. *Nanomed Nanotechnol Biol Med* 2017;13:2117–2126.
24 Xie H, Chua M, Islam I, Bentini R, Cao T, Viana-Gomes JC, Castro Neto AH, Rosa V. CVD-grown monolayer graphene induces osteogenic but not odontoblastic differentiation of dental pulp stem cells. *Dent Mater* 2017;33:e13–e21.
25 Lim K-T, Seonwoo H, Choi KS, Jin H, Jang K-J, Kim J, Kim J-W, Kim SY, Choung P-H, Chung JH. Pulsed-electromagnetic-field-assisted reduced graphene oxide substrates for multidifferentiation of human mesenchymal stem cells. *Adv Healthc Mater* 2016;5:2069–2079.
26 Zhou Q, Yang P, Li X, Liu H, Ge S. Bioactivity of periodontal ligament stem cells on sodium titanate coated with graphene oxide. *Sci Rep* 2016;6:19343.
27 Xie H, Cao T, Gomes JV, Castro Neto AH, Rosa V. Two and three-dimensional graphene substrates to magnify osteogenic differentiation of periodontal ligament stem cells. *Carbon N Y* 2015;93:266–275.
28 Li K, Yan J, Wang C, Bi L, Zhang Q, Han Y. Graphene modified titanium alloy promote the adhesion, proliferation and osteogenic differentiation of bone marrow stromal cells. *Biochem Biophys Res Commun* 2017;489:187–192.
29 Xie C, Wen W-S, Yuan Z-M, Ma S-J, Xu J, Yuan D-T. Graphene oxide nanolayers as nanoparticle anchors on biomaterial surfaces with nanostructures and charge balance for bone regeneration chaoming. *J Biomed Mater Res Part A* 2013;1–23.
30 Han L, Sun H, Tang P, Li P, Xie C, Wang M. Mussel-inspired graphene oxide nanosheet-enwrapped Ti scaffolds with drug-encapsulated gelatin microspheres for bone regeneration. *Biomater Sci* 2018;3:39–48.
31 Wei C, Liu Z, Jiang F, Zeng B, Huang M, Yu D. Cellular behaviours of bone marrow-derived mesenchymal stem cells towards pristine graphene oxide nanosheets. *Cell Prolif* 2017;50:e12367.
32 Balikov DA, Fang B, Chun YW, Crowder SW, Prasai D, Lee JB, Bolotin KI, Sung H-J. Directing lineage specification of human mesenchymal stem cells by decoupling electrical stimulation and physical patterning on unmodified graphene. *Nanoscale* 2016;8:13730–13739.

33 Crowder SW, Prasai D, Rath R, Balikov DA, Bae H, Bolotin KI, Sung H-J. Three-dimensional graphene foams promote osteogenic differentiation of human mesenchymal stem cells. *Nanoscale* 2013;5:4171–7176.
34 Shuai C, Peng S, Wu P, Gao C, Huang W, Deng Y, Xiao T, Feng P. A nano-sandwich construct built with graphene nanosheets and carbon nanotubes enhances mechanical properties of hydroxyapatite-polyetheretherketone scaffolds. *Int J Nanomed* 2016;Volume 11:3487–3500.
35 Jakus AE, Shah RN, Jakus AE, St ES, St ES, Printing K. Multi- and mixed 3D-printing of graphene-hydroxyapatite hybrid materials for complex tissue engineering. *J Biomed Mater Res Part A* 2016;1–20.
36 Kumar S, Raj S, Kolanthai E, Sood AK, Sampath S, Chatterjee K. Chemical functionalization of graphene to augment stem cell osteogenesis and inhibit biofilm formation on polymer composites for orthopedic applications. *ACS Appl Mater Interfaces* 2015;7:3237–3252.
37 Kumar S, Raj S, Sarkar K, Chatterjee K. Engineering a multi-biofunctional composite using poly(ethylenimine) decorated graphene oxide for bone tissue regeneration. *Nanoscale* 2016;8:6820–6836.
38 La W-G, Park S, Yoon H-H, Jeong G-J, Lee T-J, Bhang SH, Han JY, Char K, Kim B-S. Delivery of a therapeutic protein for bone regeneration from a substrate coated with graphene oxide. *Small* 2013;9:4051–4060.
39 La W-G, Kim B-S, Jin M, Park S, Yoon H-H, Jeong G-J. Delivery of bone morphogenetic protein-2 and substance P using graphene oxide for bone regeneration. *Int J Nanomed* 2014;107:
40 Lee JH, Shin YC, Jin OS, Kang SH, Hwang Y-S, Park J-C, Hong SW, Han D-W. Reduced graphene oxide-coated hydroxyapatite composites stimulate spontaneous osteogenic differentiation of human mesenchymal stem cells. *Nanoscale* 2015;7:11642–11651.
41 Zhou Z, Xu Z, Wang F, Lu Y, Yin P, Jiang C, Liu Y, Li H, Yu X, Sun Y. New strategy to rescue the inhibition of osteogenesis of human bone marrow-derived mesenchymal stem cells under oxidative stress: Combination of vitamin C and graphene foams. *Oncotarget* 2016;7:
42 Qiu J, Guo J, Geng H, Qian W, Liu X. Three-dimensional porous graphene nanosheets synthesized on the titanium surface for osteogenic differentiation of rat bone mesenchymal stem cells. *Carbon N Y* 2017;125:227–235.
43 Wang Q, Chu Y, He J, Shao W, Zhou Y, Qi K, Wang L, Cui S. A graded graphene oxide-hydroxyapatite/silk fibroin biomimetic scaffold for bone tissue engineering. *Mater Sci Eng C* 2017;80:232–242.
44 Xiong K, Wu T, Fan Q, Chen L, Yan M. Novel reduced graphene oxide/zinc silicate/calcium silicate electroconductive biocomposite for stimulating osteoporotic bone regeneration. *ACS Appl Mater Interfaces* 2017;9:44356–44368.
45 Ren N, Li J, Qiu J, Yan M, Liu H, Ji D, Huang J, Yu J, Liu H. Growth and accelerated differentiation of mesenchymal stem cells on graphene-oxide-coated titanate with dexamethasone on surface of titanium implants. *Dent Mater* 2017;33:525–535.
46 Duan S, Yang X, Mei F, Tang Y, Li X, Shi Y, Mao J, Zhang H, Cai Q. Enhanced osteogenic differentiation of mesenchymal stem cells on poly(L-lactide) nanofibrous scaffolds containing carbon nanomaterials. *J Biomed Mater Res—Part A* 2015;103:1424–1435.
47 Qiu J, Geng H, Wang D, Qian S, Zhu H, Qiao Y, Qian W, Liu X. Layer-number dependent antibacterial and osteogenic behaviors of graphene oxide electrophoretic deposited on titanium. *ACS Appl Mater Interfaces* 2017;9:12253–12263.
48 Xie C, Lu X, Han L, Xu J, Wang Z, Jiang L, Wang K, Zhang H, Ren F, Tang Y. Biomimetic mineralized hierarchical graphene oxide/chitosan scaffolds with adsorbability for immobilization of nanoparticles for biomedical applications. *ACS Appl Mater Interfaces* 2016;8:1707–1717.

49 Zhang W, Chang Q, Xu L, Li G, Yang G, Ding X, Wang X, Cui D, Jiang X. Graphene oxide-copper nanocomposite-coated porous CaP scaffold for vascularized bone regeneration via activation of hif-1α. *Adv Healthc Mater* 2016;5:1299–1309.
50 Zhang Y, Zhai D, Xu M, Yao Q, Zhu H, Chang J, Wu C. 3D-printed bioceramic scaffolds with antibacterial and osteogenic activity. *Biofabrication* 2017;9:025037.
51 Kim J, Kim HD, Park J, Lee E-s, Kim E, Lee SS, Yang J-K, Lee Y-S, Hwang NS. Enhanced osteogenic commitment of murine mesenchymal stem cells on graphene oxide substrate. *Biomater Res* 2018;22:9.
52 Zhang S, Yang Q, Zhao W, Qiao B, Cui H, Fan J, Li H, Tu X, Jiang D. In vitro and in vivo biocompatibility and osteogenesis of graphene-reinforced nanohydroxyapatite polyamide66 ternary biocomposite as orthopedic implant material. *Int J Nanomed* 2016; 11:3179–3189.
53 Elkhenany H, Amelse L, Lafont A, Bourdo S, Caldwell M, Neilsen N, Dervishi E, Derek O, Biris AS, Anderson D, Dhar M. Graphene supports in vitro proliferation and osteogenic differentiation of goat adult mesenchymal stem cells: Potential for bone tissue engineering. *J Appl Toxicol* 2015;35:367–374.
54 Akhavan O, Ghaderi E, Shahsavar M. Graphene nanogrids for selective and fast osteogenic differentiation of human mesenchymal stem cells. *Carbon N Y* 2013;59:200–211.
55 Yao Q, Jing J, Zeng Q, Lu TL, Liu Y, Zheng X, Chen Q. Bilayered BMP2 eluting coatings on graphene foam by electrophoretic deposition: Electroresponsive BMP2 release and enhancement of osteogenic differentiation. *ACS Appl Mater Interfaces* 2017;9:39962–39970.
56 Xie Y, Li H, Zhang C, Gu X, Zheng X, Huang L. Graphene-reinforced calcium silicate coatings for load-bearing implants. *Biomed Mater* 2014;9:025009.
57 Li J, Wang G, Geng H, Zhu H, Zhang M, Di Z, Liu X, Chu PK, Wang X. CVD growth of graphene on NiTi alloy for enhanced biological activity. *ACS Appl Mater Interfaces* 2015;7:19876–19881.
58 Jin L, Lee JH, Jin OS, Shin YC, Kim MJ, Hong SW, Lee MH, Park J-C, Han D-W. Stimulated osteogenic differentiation of human mesenchymal stem cells by reduced graphene oxide. *J Nanosci Nanotechnol* 2015;15:7966–7970.
59 Lee WC, Lim CHYX, Shi H, Tang LAL, Wang Y, Lim CT, Loh KP. Origin of enhanced stem cell growth and differentiation on graphene and graphene oxide. *ACS Nano* 2011;5:7334–7341.
60 Shie MY, Chiang WH, Chen IWP, Liu WY, Chen YW. Synergistic acceleration in the osteogenic and angiogenic differentiation of human mesenchymal stem cells by calcium silicate–graphene composites. *Mater Sci Eng C* 2017;73:726–735.
61 Shao W, He J, Sang F, Wang Q, Chen L, Cui S, Ding B. Enhanced bone formation in electrospun poly(l-lactic-co-glycolic acid)-tussah silk fibroin ultrafine nanofiber scaffolds incorporated with graphene oxide. *Mater Sci Eng C* 2016;62:823–834.
62 Nayak TR, Andersen H, Makam VS, Khaw C, Bae S, Xu X, Ee P-LR, Ahn J-H, Hong BH, Pastorin G, Özyilmaz B. Graphene for controlled and accelerated osteogenic differentiation of human mesenchymal stem cells. *ACS Nano* 2011;5:4670–4678.
63 Luo Y, Shen H, Fang Y, Cao Y, Huang J, Zhang M, Dai J, Shi X, Zhang Z. Enhanced proliferation and osteogenic differentiation of mesenchymal stem cells on graphene oxide-incorporated electrospun poly(lactic-co-glycolic acid) nanofibrous mats. *ACS Appl Mater Interfaces* 2015;7:6331–6339.
64 Tatavarty R, Ding H, Lu G, Taylor RJ, Bi X. Synergistic acceleration in the osteogenesis of human mesenchymal stem cells by graphene oxide-calcium phosphate nanocomposites. *Chem Commun* 2014;50:8484–8487.
65 Chen S, Du X, Jia L, Chang H, Ikoma T, Hanagata N. Synthesis and osteo-compatibility of novel reduced graphene oxide-aminosilica hybrid nanosheets. *Mater Sci Eng C* 2016;61:251–256.

66 Cicuéndez M, Silva VS, Hortigüela MJ, Matesanz MC, Vila M, Portolés MT. MC3T3-E1 pre-osteoblast response and differentiation after graphene oxide nanosheet uptake. *Colloids Surfaces B Biointerfaces* 2017;158:33–40.
67 Fan Z, Wang J, Liu F, Nie Y, Ren L, Liu B. A new composite scaffold of bioactive glass nanoparticles/graphene: Synchronous improvements of cytocompatibility and mechanical property. *Colloids Surfaces B Biointerfaces* 2016;145:438–446.
68 Jia Z, Shi Y, Xiong P, Zhou W, Cheng Y, Zheng Y, Xi T, Wei S. From solution to biointerface: graphene self-assemblies of varying lateral sizes and surface properties for biofilm control and osteodifferentiation. *ACS Appl Mater Interfaces* 2016;8:17151–17165.
69 Jung HS, Lee T, Kwon IK, Kim HS, Hahn SK, Lee CS. Surface modification of multipass caliber-rolled ti alloy with dexamethasone-loaded graphene for dental applications. *ACS Appl Mater Interfaces* 2015;7:9598–9607.
70 Kanayama I, Miyaji H, Takita H, Nishida E, Tsuji M, Fugetsu B. Comparative study of bioactivity of collagen scaffolds coated with graphene oxide and reduced graphene oxide. *Int J Nanomedicine* 2014;9:3363–3373.
71 Kumar S, Chatterjee K. Strontium eluting graphene hybrid nanoparticles augment osteogenesis in a 3D tissue scaffold. *Nanoscale* 2015;7:2023–2033.
72 Lee JH, Shin YC, Lee S-M, Jin OS, Kang SH, Hong SW, Jeong C-M, Huh JB, Han D-W. Enhanced osteogenesis by reduced graphene oxide/hydroxyapatite nanocomposites. *Sci Rep* 2016;5:18833.
73 Liu H, Cheng J, Chen F, Hou F, Bai D, Xi P, Zeng Z. Biomimetic and cell-mediated mineralization of hydroxyapatite by carrageenan functionalized graphene oxide. *ACS Appl Mater Interfaces* 2014;6:3132–3140.
74 Liu H, Cheng J, Chen F, Bai D, Shao C, Wang J, Xi P, Zeng Z. Gelatin functionalized graphene oxide for mineralization of hydroxyapatite: Biomimetic and in vitro evaluation. *Nanoscale* 2014;6:5315–5322.
75 Saravanan S, Anjali C, Vairamani M, Sastry TP, Subramanian KS, Selvamurugan N. Scaffolds containing chitosan, gelatin and graphene oxide for bone tissue regeneration in vitro and in vivo. *Int J Biol Macromol* 2017;104:1975–1985.
76 Subbiah R, Du P, Van SY, Suhaeri M, Hwang MP, Lee K, Park K. Fibronectin-tethered graphene oxide as an artificial matrix for osteogenesis. *Biomed Mater* 2014;9:065003.
77 Tian Z, Huang L, Pei X, Chen J, Wang T, Yang T, Qin H, Sui L, Wang J. Electrochemical synthesis of three-dimensional porous reduced graphene oxide film: Preparation and in vitro osteogenic activity evaluation. *Colloids Surfaces B Biointerfaces* 2017;155:150–158.
78 Wang C-H, Guo Z-S, Pang F, Zhang L-Y, Yan M, Yan J-H, Li K-W, Li X-J, Li Y, Bi L, Han Y-S. Effects of graphene modification on the bioactivation of polyethylene-terephthalate-based artificial ligaments. *ACS Appl Mater Interfaces* 2015;7:15263–15276.
79 Zhao C, Lu X, Zanden C, Liu J. The promising application of graphene oxide as coating materials in orthopedic implants: Preparation, characterization and cell behavior. *Biomed Mater* 2015;10:015019.
80 Jaidev LR, Kumar S, Chatterjee K. Multi-biofunctional polymer graphene composite for bone tissue regeneration that elutes copper ions to impart angiogenic, osteogenic and bactericidal properties. *Colloids Surfaces B Biointerfaces* 2017;159:293–302.
81 Fu C, Bai H, Zhu J, Niu Z, Wang Y, Li J, Yang X, Bai Y. Enhanced cell proliferation and osteogenic differentiation in electrospun PLGA/hydroxyapatite nanofibre scaffolds incorporated with graphene oxide. *PLoS One* 2017;12:e0188352.

82 Zhang L, Zhou Q, Song W, Wu K, Zhang Y, Zhao Y. Dual-functionalized graphene oxide based siRNA delivery system for implant surface biomodification with enhanced osteogenesis. *ACS Appl Mater Interfaces* 2017;9:34722–34735.
83 Liu M, Hao L, Huang Q, Zhao D, Li Q, Cai X. Tea polyphenol-reduced graphene oxide deposition on titanium surface enhances osteoblast bioactivity. *J Nanosci Nanotechnol* 2018;18:3134–3140.
84 Oyefusi A, Olanipekun O, Neelgund GM, Peterson D, Stone JM, Williams E, Carson L, Regisford G, Oki A. Hydroxyapatite grafted carbon nanotubes and graphene nanosheets: Promising bone implant materials. *Spectrochim Acta—Part A Mol Biomol Spectrosc* 2014;132:410–416.
85 Ricci R, Leite NCS, da-Silva NS, Pacheco-Soares C, Canevari RA, Marciano FR, Webster TJ, Lobo AO. Graphene oxide nanoribbons as nanomaterial for bone regeneration: Effects on cytotoxicity, gene expression and bactericidal effect. *Mater Sci Eng C* 2017;78:341–348.
86 Mehrali M, Moghaddam E, Shirazi SFS, Baradaran S, Mehrali M, Latibari ST, Metselaar HSC, Kadri NA, Zandi K, Osman NAA. Synthesis, mechanical properties, and in vitro biocompatibility with osteoblasts of calcium silicate-reduced graphene oxide composites. *ACS Appl Mater Interfaces* 2014;6:3947–3962.
87 Zou Y, Qazvini NT, Zane K, Sadati M, Wei Q, Liao J, Fan J, Song D, Liu J, Ma C, Qu X, Chen L, Yu X, Zhang Z, Zhao C, Zeng Z, Zhang R, Yan S, Wu T, Wu X, Shu Y, Li Y, Zhang W, Reid RR, Lee MJ, Wolf JM, Tirrell M, He T-C, de Pablo JJ, Deng Z-L. Gelatin-derived graphene-silicate hybrid materials are biocompatible and synergistically promote BMP9-induced osteogenic differentiation of mesenchymal stem cells. *ACS Appl Mater Interfaces* 2017;9:15922–15932.
88 Dubey N, Ellepola K, Decroix FED, Morin JLP, Castro Neto AH, Seneviratne CJ, Rosa V. Graphene onto medical grade titanium: An atom-thick multimodal coating that promotes osteoblast maturation and inhibits biofilm formation from distinct species. *Nanotoxicology* 2018;0:1–16.
89 Chen J, Zhang X, Cai H, Chen Z, Wang T, Jia L, Wang J, Wan Q, Pei X. Osteogenic activity and antibacterial effect of zinc oxide/carboxylated graphene oxide nanocomposites: Preparation and in vitro evaluation. *Colloids Surfaces B Biointerfaces* 2016;147:397–407.
90 Silva E, Vasconcellos L. M R d, Rodrigues BVM, dos Santos DM, Campana-Filho SP, Marciano FR, Webster TJ, Lobo AO. PDLLA honeycomb-like scaffolds with a high loading of superhydrophilic graphene/multi-walled carbon nanotubes promote osteoblast in vitro functions and guided in vivo bone regeneration. *Mater Sci Eng C* 2017;73:31–39.
91 Kaur T, Kulanthaivel S, Thirugnanam A. Biological and mechanical evaluation of poly(lactic2 co-glycolic acid) based composites reinforced with 3 one, two and three dimensional carbon biomaterials 4 for bone tissue regeneration. *Biomed Mater* 2017;
92 Dong W, Hou L, Li T, Gong Z, Huang H, Wang G, Chen X, Li X. A dual role of graphene oxide sheet deposition on titanate nanowire scaffolds for osteo-implantation: Mechanical hardener and surface activity regulator. *Sci Rep* 2016;5:18266.
93 Yan X, Yang W, Shao Z, Yang S, Liu X. Graphene/single-walled carbon nanotube hybrids promoting osteogenic differentiation of mesenchymal stem cells by activating p38 signaling pathway. *Int J Nanomedicine* 2016;Volume 11:5473–5484.
94 Qiu J, Li D, Mou X, Li J, Guo W, Wang S, Yu X, Ma B, Zhang S, Tang W, Sang Y, Gil PR, Liu H. Effects of graphene quantum dots on the self-renewal and differentiation of mesenchymal stem cells. *Adv Healthc Mater* 2016;5:702–710.
95 Bastami F, Paknejad Z, Jafari M, Salehi M, Rezai Rad M, Khojasteh A. Fabrication of a three-dimensional β-tricalcium-phosphate/gelatin containing chitosan-based nanoparticles for sustained release of bone morphogenetic protein-2: Implication for bone tissue engineering. *Mater Sci Eng C* 2017;72:481–491.

96 Hosseinpour S, Ghazizadeh Ahsaie M, Rezai Rad M, Baghani M. t, Motamedian SR, Khojasteh A. Application of selected scaffolds for bone tissue engineering: a systematic review. *Oral Maxillofac Surg* 2017;21:109–129.
97 Rezwan K, Chen QZ, Blaker JJ, Boccaccini AR. Biodegradable and bioactive porous polymer/inorganic composite scaffolds for bone tissue engineering. *Biomaterials* 2006;27:3413–3431.
98 Mullick Chowdhury S, Lalwani G, Zhang K, Yang JY, Neville K, Sitharaman B. Cell specific cytotoxicity and uptake of graphene nanoribbons. *Biomaterials* 2013;34:283–293.
99 Mao HY, Laurent S, Chen W, Akhavan O, Imani M, Ashkarran AA, Mahmoudi M. Graphene : Promises, facts, opportunities, and challenges in nanomedicine. *Chem Rev* 2013;113:3407–3424.
100 Liao KH, Lin YS, MacOsko CW, Haynes CL. Cytotoxicity of graphene oxide and graphene in human erythrocytes and skin fibroblasts. *ACS Appl Mater Interfaces* 2011;3:2607–2615.
101 Akhavan O, Ghaderi E, Akhavan A. Size-dependent genotoxicity of graphene nanoplatelets in human stem cells. *Biomaterials* 2012;33:8017–8025.
102 Schinwald A, Murphy F. a, Jones A, Macnee W, Donaldson K. Graphene-based nanoplatelets: A new risk to the respiratory system. *ACS Nano* 2012; 6:736–746.
103 Li Y, Liu Y, Fu Y, Wei T, Le Guyader L, Gao G, Liu R-S, Chang Y-Z, Chen C. The triggering of apoptosis in macrophages by pristine graphene through the MAPK and TGF-beta signaling pathways. *Biomaterials* 2012;33:402–411.
104 Zhang M, Bai L, Shang W, Xie W, Ma H, Fu Y, Fang D, Sun H, Fan L, Han M, Liu C, Yang S. Facile synthesis of water-soluble, highly fluorescent graphene quantum dots as a robust biological label for stem cells. *J Mater Chem* 2012;22:7461.
105 Duch MC, Budinger GRS, Liang YT, Soberanes S, Urich D, Chiarella SE, Campochiaro LA, Gonzalez A, Chandel NS, Hersam MC, Mutlu GM. Minimizing oxidation and stable nanoscale dispersion improves the biocompatibility of graphene in the lung. *Nano Lett* 2011;11:5201–5207.
106 Ruiz ON, Fernando KAS, Wang B, Brown NA, Luo PG, McNamara ND, Vangsness M, Sun Y-P, Bunker CE. Graphene oxide: a nonspecific enhancer of cellular growth. *ACS Nano* 2011;5:8100–8107.
107 Mazaheri M, Akhavan O, Simchi A. Flexible bactericidal graphene oxide-chitosan layers for stem cell proliferation. *Appl Surf Sci* 2014;301:456–462.
108 Chang Y, Yang S-T, Liu J-H, Dong E, Wang Y, Cao A, Liu Y, Wang H. In vitro toxicity evaluation of graphene oxide on A549 cells. *Toxicol Lett* 2011;200:201–210.
109 Talukdar Y, Rashkow J, Lalwani G, Kanakia S, Sitharaman B. The effects of graphene nanostructures on mesenchymal stem cells. *Biomaterials* 2014;35:4863.
110 Gurunathan S, Woong Han J, Eppakayala V, Kim J. Green synthesis of graphene and its cytotoxic effects in human breast cancer cells. *Int J Nanomed* 2013;1015:
111 Das S, Singh S, Singh V, Joung D, Dowding JM, Reid D, Anderson J, Zhai L, Khondaker SI, Self WT, Seal S. Oxygenated functional group density on graphene oxide: Its effect on cell toxicity. *Part Part Syst Charact* 2013;30:148–157.
112 Zhang W, Yan L, Li M, Zhao R, Yang X, Ji T, Gu Z, Yin J-J, Gao X, Nie G. Deciphering the underlying mechanisms of oxidation-state dependent cytotoxicity of graphene oxide on mammalian cells. *Toxicol Lett* 2015;237:61–71.
113 Sydlik SA, Jhunjhunwala S, Webber MJ, Anderson DG, Langer R. In vivo compatibility of graphene oxide with di ff ering oxidation states. *ACS Nano* 2015;9:3866–3874.
114 Kalbacova M, Broz A, Kong J, Kalbac M. Graphene substrates promote adherence of human osteoblasts and mesenchymal stromal cells. *Carbon N Y* 2010;48:4323–4329.
115 Akasaka T, Yokoyama A, Matsuoka M, Hashimoto T, Watari F. Thin films of single-walled carbon nanotubes promote human osteoblastic cells (Saos-2) proliferation in low serum concentrations. *Mater Sci Eng C* 2010;30:391–399.

116 Alava T, Mann JA, Théodore C, Benitez JJ, Dichtel WR, Parpia JM, Craighead HG. Control of the graphene-protein interface is required to preserve adsorbed protein function. *Anal Chem* 2013;85:2754–2759.
117 Turk M, Deliormanlı AM. Electrically conductive borate-based bioactive glass scaffolds for bone tissue engineering applications. *J Biomater Appl* 2017;32:28.

118 Zhang Y, Ali SF, Dervishi E, Xu Y, Li Z, Casciano D, Biris AS. Cytotoxicity effects of graphene and single-wall carbon nanotubes in neural phaeochromocytoma-derived pc12 cells. *ACS Nano* 2010;4:3181.
119 Horvath L, Magrez A, Burghard M, Kern K, Forro L, Schwaller B. Evaluation of the toxicity of graphene derivatives on cells of the lung luminal surface. *Carbon N Y* 2013;64:45–60.
120 Loeblein M, Perry G, Tsang SH, Xiao W, Collard D, Coquet P, Sakai Y, Teo EHT. Three-dimensional graphene: A biocompatible and biodegradable scaffold with enhanced oxygenation. *Adv Healthc Mater* 2016;5:1177–1191.
121 Novoselov KS, Geim AK, Morozov SV, Jiang D. Zhang Y, Dubonos SV, Grigorieva IV, Firsov AA. Electric field effect in atomically thin carbon films. *Science* 2004;306(5696):666–669.
122 Li N, Zhang Q, Gao S, Song Q, Huang R, Wang L, Liu L, Dai J, Tang M, Cheng G. Three-dimensional graphene foam as a biocompatible and conductive scaffold for neural stem cells. *Sci Rep* 2013;3:1604.
123 Dasdia T, Bazzaco S, Bottero L, Buffa R, Ferrero S, Campanelli G, Dolfini E. Organ culture in 3-dimensional matrix: In vitro model for evaluating biological compliance of synthetic meshes for abdominal wall repair. *J Biomed Mater Res* 1998;43:204–209.
124 Jiang Z, Song Q, Tang M, Yang L, Cheng Y, Zhang M, Xu D, Cheng G. Enhanced migration of neural stem cells by microglia grown on a three-dimensional graphene scaffold. *ACS Appl Mater Interfaces* 2016;8:25069–25077.
125 Li X, Liang H, Sun J, Zhuang Y, Xu B, Dai J. Electrospun collagen fibers with spatial patterning of sdf1α for the guidance of neural stem cells. *Adv Healthc Mater* 2015;4:1869–1876.
126 Alsayed Y, Ngo H, Runnels J, Leleu X, Singha UK, Pitsillides CM, Spencer JA, Kimlinger T, Ghobrial JM, Jia X, Lu G, Timm M, Kumar A, Côté D, Veilleux I, Hedin KE, Roodman GD, Witzig TE, Kung AL, Hideshima T, Anderson KC, Lin CP, Ghobrial IM. Mechanisms of regulation of CXCR4/SDF-1 (CXCL12) dependent migration and homing in Multiple Myeloma. *Blood* 2007;109:2708–2718.
127 Liu C, Wong HM, Yeung KWK, Tjong SC. Novel electrospun polylactic acid nanocomposite fiber mats with hybrid graphene oxide and nanohydroxyapatite reinforcements having enhanced biocompatibility. *Polymers (Basel)* 2016;8:287.
128 Xie H, Cao T, Rodríguez-Lozano FJ, Luong-Van EK, Rosa V. Graphene for the development of the next-generation of biocomposites for dental and medical applications. *Dent Mater* 2017;33:765–774.
129 Ramanathan T, Abdala AA, Stankovich S, Dikin DA, Herrera-Alonso M, Piner RD, Adamson DH, Schniepp HC, Chen X, Ruoff RS, Nguyen ST, Aksay IA, Prud'Homme RK, Brinson LC. Functionalized graphene sheets for polymer nanocomposites. *Nat Nanotechnol* 2008;3:327–331.
130 Xu C, Wang X, Yang L, Wu Y. Fabrication of a graphene-cuprous oxide composite. *J Solid State Chem* 2009;182:2486–2490.
131 Cao A, Liu Z, Chu S, Wu M, Ye Z, Cai Z, Chang Y, Wang S, Gong Q, Liu Y. A facile one-step method to produce craphene-CdS quantum dot nanocomposites as promising optoelectronic materials. *Adv Mater* 2010;22:103–106.
Wiley Online Library CAS PubMed Web of Science®Google ScholarMarquette University
132 Zou Y, Wang Y. NiO nanosheets grown on graphene nanosheets as superior anode materials for Li-ion batteries. *Nanoscale* 2011;3:2615.

133 Wang Y-W, Cao A, Jiang Y, Zhang X, Liu J-H, Liu Y, Wang H. Superior antibacterial activity of zinc oxide/graphene oxide composites originating from high zinc concentration localized around bacteria. *ACS Appl Mater Interfaces* 2014;6:2791–2798.
134 Ito A, Kawamura H, Otsuka M, Ikeuchi M, Ohgushi H, Ishikawa K, Onuma K, Kanzaki N, Sogo Y, Ichinose N. Zinc-releasing calcium phosphate for stimulating bone formation. *Mater Sci Eng C* 2002;22:21–25.
135 Gaetke LM, Chow CK. Copper toxicity, oxidative stress, and antioxidant nutrients. *Toxicology* 2003;189:147–163.
136 Zhang R, Lee P, Lui VCH, Chen Y, Liu X, Lok CN, To M, Yeung KWK, Wong KKY. Silver nanoparticles promote osteogenesis of mesenchymal stem cells and improve bone fracture healing in osteogenesis mechanism mouse model. *Nanomed Nanotechnol Biol Med* 2015;11:1949–1959.
137 Omidi M, Yadegari A, Tayebi L. Wound dressing application of pH-sensitive carbon dots/chitosan hydrogel. *RSC Adv* 2017;7:10638–10649.
138 Rosa V, Della Bona A, Cavalcanti BN, Nör JE. Tissue engineering : From research to dental clinics. *Dent Mater* 2012;28:341–348.
139 Rosa V, Zhang Z, Grande RHM, Nor JE. Dental pulp tissue engineering in full-length human root canals. *J Dent Res* 2013;92:970–975.
140 Hashemi M, Omidi M, Muralidharan B, Tayebi L, Herpin MJ, Mohagheghi MA, Mohammadi J, Smyth HDC, Milner TE. Layer-by-layer assembly of graphene oxide on thermosensitive liposomes for photo-chemotherapy. *Acta Biomater* 2018;65:376–392.
141 Gunatillake PA, Adhikari R, Gadegaard N. Biodegradable synthetic polymers for tissue engineering. *Eur Cells Mater* 2003;5:1–16.
142 Depan D, Girase B, Shah JS, Misra RDK. Structure-process-property relationship of the polar graphene oxide-mediated cellular response and stimulated growth of osteoblasts on hybrid chitosan network structure nanocomposite scaffolds. *Acta Biomater* 2011;7:3432–3445.
143 Girase B, Shah JS, Misra RDK. Cellular mechanics of modulated osteoblasts functions in graphene oxide reinforced elastomers. *Adv Eng Mater* 2012;14:B101–B111.
144 Miller R, Guo Z, Vogler EA, Siedlecki CA. Plasma coagulation response to surfaces with nanoscale chemical heterogeneity. *Biomaterials* 2006;27:208–215.
145 Hashemi M, Omidi M, Muralidharan B, Smyth H, Mohagheghi MA, Mohammadi J, Milner TE. Evaluation of the photothermal properties of a reduced graphene oxide/arginine nanostructure for near-infrared absorption. *ACS Appl Mater Interfaces* 2017;9:32607–32620.
146 Hashemi M, Yadegari A, Yazdanpanah G, Jabbehdari S, Omidi M, Tayebi L. Functionalized R9–reduced graphene oxide as an efficient nano-carrier for hydrophobic drug delivery. *RSC Adv* 2016;6:74072–74084.
147 Bussy C, Jasim D, Lozano N, Terry D, Kostarelos K. The current graphene safety landscape – a literature mining exercise. *Nanoscale* 2015;7:6432–6435.
148 Kim JH, Choung P-H, Kim IY, Lim KT, Son HM, Choung Y-H, Cho C-S, Chung JH. Electrospun nanofibers composed of poly(ε-caprolactone) and polyethylenimine for tissue engineering applications. *Mater Sci Eng C* 2009;29:1725–1731.
149 Ardjmand M, Omidi M, Choolaei M. The effects of functionalized multi-walled carbon nanotube on mechanical properties of multi-walled carbon nanotube/epoxy composites. *Orient J Chem* 2015;31:2291–2301.
150 Omidi M, Rokni D.T H, Milani AS, Seethaler RJ, Arasteh R. Prediction of the mechanical characteristics of multi-walled carbon nanotube/epoxy composites using a new form of the rule of mixtures. *Carbon N Y* 2010;48:3218–3228.
151 Li W, Dichiara A, Bai J. Carbon nanotube-graphene nanoplatelet hybrids as high-performance multifunctional reinforcements in epoxy composites. *Compos Sci Technol* 2013;74:221–227.

152 Hatui G, Bhattacharya P, Sahoo S, Dhibar S, Das CK. Combined effect of expanded graphite and multiwall carbon nanotubes on the thermo mechanical, morphological as well as electrical conductivity of in situ bulk polymerized polystyrene composites. *Compos Part A Appl Sci Manuf* 2014;56:181–191.
153 Kim J, Kim Y-R, Kim Y, Lim KT, Seonwoo H, Park S, Cho S-P, Hong BH, Choung P-H, Chung TD, Choung Y-H, Chung JH. Graphene-incorporated chitosan substrata for adhesion and differentiation of human mesenchymal stem cells. *J Mater Chem B* 2013;1:933.
154 Jia Z, Xiu P, Li M, Xu X, Shi Y, Cheng Y, Wei S, Zheng Y, Xi T, Cai H, Liu Z. Bioinspired anchoring AgNPs onto micro-nanoporous TiO2 orthopedic coatings: Trap-killing of bacteria, surface-regulated osteoblast functions and host responses. *Biomaterials* 2016;75:203–222.
155 Fatokun AA, Stone TW, Smith RA. Hydrogen peroxide-induced oxidative stress in MC3T3-E1 cells: The effects of glutamate and protection by purines. *Bone* 2006;39:542–551.
156 Kamata H, Honda SI, Maeda S, Chang L, Hirata H, Karin M. Reactive oxygen species promote TNFα-induced death and sustained JNK activation by inhibiting MAP kinase phosphatases. *Cell* 2005;120:649–661.
157 Tonetto A, Lago PW, Borba M, Rosa V. Effects of chrondro-osseous regenerative compound associated with local treatments in the regeneration of bone defects around implants: An in vivo study. *Clin Oral Investig* 2016;20:267–274.
158 Stevens MM. Biomaterials for bone tissue engineering. *Mater Today* 2008;11:18–25.
159 Xie H, Liu H. A novel mixed-type stem cell pellet for cementum/periodontal ligament–like complex. *J Periodontol* 2012;83:805–815.
160 Lin L, Chow KL, Leng Y. Study of hydroxyapatite osteoinductivity with an osteogenic differentiation of mesenchymal stem cells. *J Biomed Mater Res - Part A* 2009;89A:326–335.
161 Rahaman MN, Day DE, Bal BS, Fu Q, Jung SB, Bonewald LF, Tomsia AP. Bioactive glass in tissue engineering. *Acta Biomater* 2011;7:2355–2373.
162 Zeimaran E, Pourshahrestani S, Djordjevic I, Pingguan-Murphy B, Kadri NA, Towler MR. Bioactive glass reinforced elastomer composites for skeletal regeneration: A review. *Mater Sci Eng C* 2015;53:175–188.
163 Suzuki O. Octacalcium phosphate (OCP)-based bone substitute materials. *Jpn Dent Sci Rev* 2013;49:58–71.
164 Xia L, Lin K, Jiang X, Fang B, Xu Y, Liu J, Zeng D, Zhang M, Zhang X, Chang J, Zhang Z. Effect of nano-structured bioceramic surface on osteogenic differentiation of adipose derived stem cells. *Biomaterials* 2014;35:8514–8527.
165 Lin K, Wu C, Chang J. Advances in synthesis of calcium phosphate crystals with controlled size and shape. *Acta Biomater* 2014;10:4071–4102.
166 Wang L, Zhou G, Liu H, Niu X, Han J, Zheng L, Fan Y. Nano-hydroxyapatite particles induce apoptosis on MC3T3-E1 cells and tissue cells in SD rats. *Nanoscale* 2012;4:2894.
167 Wilson CJ, Clegg RE, Leavesley DI, Pearcy MJ. Mediation of biomaterial–cell interactions by adsorbed proteins: A review. *Tissue Eng* 2005;11:1–18.
168 Kim DH, Han K, Gupta K, Kwon KW, Suh KY, Levchenko A. Mechanosensitivity of fibroblast cell shape and movement to anisotropic substratum topography gradients. *Biomaterials* 2009;30:5433–5444.
169 Humphries JD, Wang P, Streuli C, Geiger B, Humphries MJ, Ballestrem C. Vinculin controls focal adhesion formation by direct interactions with talin and actin. *J Cell Biol* 2007;179:1043–1057.
170 Wang S, Zhang Y, Abidi N, Cabrales L. Wettability and surface free energy of graphene films. *Langmuir* 2009;25:11078–11081.
171 von der Mark K, Bauer S, Park J, Schmuki P. Stem cell fate dictated solely by altered nanotube dimension. *Proc Natl Acad Sci USA* 2009;106:E60–E60.

172 Tang LAL, Wang J, Loh KP. Graphene-based SELDI probe with ultrahigh extraction and sensitivity for DNA oligomer. *J Am Chem Soc* 2010;132:10976–10977.
173 Hytönen VP, Wehrle-Haller B. Protein conformation as a regulator of cell-matrix adhesion. *Phys Chem Chem Phys* 2014;16:6342–6357.
174 Ku SH, Ryu J, Hong SK, Lee H, Park CB. General functionalization route for cell adhesion on non-wetting surfaces. *Biomaterials* 2010;31:2535–2541.
175 Dang Y, Xing C-M, Quan M, Wang Y-B, Zhang S-P, Shi S-Q, Gong Y-K. Substrate independent coating formation and anti-biofouling performance improvement of mussel inspired polydopamine. *J Mater Chem B* 2015;3:4181–4190.
176 Madhurakkat Perikamana SK, Lee J, Lee YB, Shin YM, Lee EJ, Mikos AG, Shin H. Materials from mussel-inspired chemistry for cell and tissue engineering applications. *Biomacromolecules* 2015;16:2541–2555.
177 Zhan Z-M, Yang W-X, Li W-B, Li J-H. Efficient scheme for Greenberger-Horne-Zeilinger State and cluster state with trapped ions. *Chinese Phys Lett* 2006;23:1984–1987.

178 Chen S, Chinnathambi S, Shi X, Osaka A, Zhu Y, Hanagata N. Fabrication of novel collagen-silica hybrid membranes with tailored biodegradation and strong cell contact guidance ability. *J Mater Chem* 2012;22:21885.
179 Chen S, Osaka A, Ikoma T, Morita H, Li J, Takeguchi M, Hanagata N. Fabrication, microstructure, and BMP-2 delivery of novel biodegradable and biocompatible silicate–collagen hybrid fibril sheets. *J Mater Chem* 2011;21:10942.
180 Hallab NJ, Bundy KJ, O'Connor K, Moses RL, Jacobs JJ. Evaluation of metallic and polymeric biomaterial surface energy and surface roughness characteristics for directed cell adhesion. *Tissue Eng* 2001;7:55–71.
181 Chung TW, Liu DZ, Wang SY, Wang SS. Enhancement of the growth of human endothelial cells by surface roughness at nanometer scale. *Biomaterials* 2003;24:4655–4661.
182 Lampin M, Warocquier-Clérout R, Legris C, Degrange M, Sigot-Luizard MF. Correlation between substratum roughness and wettability, cell adhesion, and cell migration. *J Biomed Mater Res* 1997;36:99–108.
183 Tang LAL, Lee WC, Shi H, Wong EYL, Sadovoy A, Gorelik S, Hobley J, Lim CT, Loh KP. Highly wrinkled cross-linked graphene oxide membranes for biological and charge-storage applications. *Small* 2012;8:423–431.
184 Bignon A, Chouteau J, Chevalier J, Fantozzi G, Carret J-P, Chavassieux P, Boivin G, Melin M, Hartmann D. Effect of micro- and macroporosity of bone substitutes on their mechanical properties and cellular response. *J Mater Sci Mater Med* 2003;14:1089–1097.
185 Gotoh Y, Fujisawa K, Satomura K, Nagayama M. Osteogenesis by human osteoblastic cells in diffusion chamber In vivo. *Calcif Tissue Int* 1995;56:246–251.
186 Hing K, Annaz B, Saeed S, Revell P, Buckland T. Microporosity enhances bioactivity of synthetic bone graft substitutes microporosity enhances bioactivity of synthetic bone graft substitutes. *J Mater Sci Mater Med* 2005;16:467–475.
187 Lenihouannen D, Daculsi G, Saffarzadeh A, Gauthier O, Delplace S, Pilet P, Layrolle P. Ectopic bone formation by microporous calcium phosphate ceramic particles in sheep muscles. *Bone* 2005;36:1086–1093.
188 Habibovic P, Yuan H, Valk CMVD, Meijer G, Blitterswijk CAV, Groot KD. 3D microenvironment as essential element for osteoinduction by biomaterials. *Biomaterials* 2005;26:3565–3575.
189 Dinescu S, Ionita M, Pandele AM, Galateanu B, Iovu H, Ardelean A. In vitro cytocompatibility evaluation of chitosan/graphene oxide 3D scaffold composites designed for bone tissue engineering. *Biomed Mater Eng* 2014;24:2249–2256.

190 Hollister SJ. Porous scaffold design for tissue engineering. *Nat Mater* 2005;4:518–524.
191 Chen GY, Pang DWP, Hwang SM, Tuan HY, Hu YC. A graphene-based platform for induced pluripotent stem cells culture and differentiation. *Biomaterials* 2012;33:418–427.
192 Wang Y, Lee WC, Manga KK, Ang PK, Lu J, Liu YP, Lim CT, Loh KP. Fluorinated graphene for promoting neuro-induction of stem cells. *Adv Mater* 2012;24:4285–4290.
193 Haynesworth SE, Goshima J, Goldberg VM, Caplan AI. Characterization of cells with osteogenic potential from human marrow. *Bone* 1992;13:81–88.
194 Scutt A, Bertram P, Brautigam M. The Role of Glucocorticoids and Prostaglandin E z in the Recruitment of Bone Marrow Mesenchymal Cells to the Osteoblastic Lineage: Positive and Negative Effects. *Clasif Tissue Int* 1996;59:154–162.
195 Quarles LD, Yohay DA, Lever LW, Caton R, Wenstrup RJ. Distinct proliferation and differentiated stages of murine MC3T3-E1 cells in culture: an in vitro model of osteoblast development. *J Bone Min Res* 2009;7:683–692.
196 Zhang N, Qiu H, Si Y, Wang W, Gao J. Fabrication of highly porous biodegradable monoliths strengthened by graphene oxide and their adsorption of metal ions. *Carbon N Y* 2011;49:827–837.
197 Gui X, Wei J, Wang K, Cao A, Zhu H, Jia Y, Shu Q, Wu D. Carbon nanotube sponges. *Adv Mater* 2010;22:617–621.
198 Goncalves G, Marques PAAP, Granadeiro CM, Nogueira HIS, Singh MK, Grácio J. Surface modification of graphene nanosheets with gold nanoparticles: The role of oxygen moieties at graphene surface on gold nucleation and growth. *Chem Mater* 2009;21:4796–4802.
199 Palmiter RD. Protection against zinc toxicity by metallothionein and zinc transporter 1. *Proc Natl Acad Sci USA* 2004;101:4918–4923.
200 Kim SY, Yoo J-Y, Ohe J-Y, Lee J-W, Moon J-H, Kwon Y-D, Heo JS. Differential expression of osteo-modulatory molecules in periodontal ligament stem cells in response to modified titanium surfaces. *Biomed Res Int* 2014;2014:1.
201 Nardone V, Fabbri S, Marini F, Zonefrati R, Galli G, Carossino A, Tanini A, Brandi ML. Osteodifferentiation of human preadipocytes induced by strontium released from hydrogels. *Int J Biomater* 2012;2012:1.
202 Zhu L-L, Zaidi S, Peng Y, Zhou H, Moonga BS, Blesius A, Dupin-Roger I, Zaidi M, Sun L. Induction of a program gene expression during osteoblast differentiation with strontium ranelate. *Biochem Biophys Res Commun* 2007;355:307–311.
203 Saidak Z, Marie PJ. Strontium signaling: Molecular mechanisms and therapeutic implications in osteoporosis. *Pharmacol Ther* 2012;136:216–226.
204 Li WR, Xie XB, Shi QS, Zeng HY, Ou-Yang YS, Chen YB. Antibacterial activity and mechanism of silver nanoparticles on Escherichia coli. *Appl Microbiol Biotechnol* 2010;85:1115–1122.
205 Zanello L, Zhao B, Hu H, Haddon R. Bone cell proliferation on carbon nanotubes. *Nano Lett* 2006;6:562.
206 Keselowsky BG, Collard DM, García AJ. Surface chemistry modulates focal adhesion composition and signaling through changes in integrin binding. *Biomaterials* 2004;25:5947–5954.
207 Curran JM, Chen R, Hunt JA. The guidance of human mesenchymal stem cell differentiation in vitro by controlled modifications to the cell substrate. *Biomaterials* 2006;27:4783–4793.
208 Liu H, Xi P, Xie G, Shi Y, Hou F, Huang L, Chen F, Zeng Z, Shao C, Wang J. Simultaneous reduction and surface functionalization of graphene oxide for hydroxyapatite mineralization. *J Phys Chem C* 2012;116:3334–3341.
209 Keeting PE, Oursler MO, Wiegand KE, Bonde SK, Spelsberg TC, Riggs BL. Zeolite a increases proliferation, differentiation, and transforming growth factor. *J Bone Miner Res* 2009;7:1281–1289.

210 Xynos ID, Edgar AJ, Buttery LDK, Hench LL, Polak JM. Ionic products of bioactive glass dissolution increase proliferation of human osteoblasts and induce insulin-like growth factor II mRNA expression and protein synthesis. *Biochem Biophys Res Commun* 2000;276:461–465.
211 Gandolfi MG, Ciapetti G, Taddei P, Perut F, Tinti A, Cardoso MV, Van Meerbeek B, Prati C. Apatite formation on bioactive calcium-silicate cements for dentistry affects surface topography and human marrow stromal cells proliferation. *Dent Mater* 2010;26:974–992.
212 Müller P, Bulnheim U, Diener A, Lüthen F, Teller M, Klinkenberg E-D, Neumann H-G, Nebe B, Liebold A, Steinhoff G, Rychly J. Calcium phosphate surfaces promote osteogenic differentiation of mesenchymal stem cells. *J Cell Mol Med* 2007;12:281–291.
213 Li M, Wang Y, Liu Q, Li Q, Cheng Y, Zheng Y, Xi T, Wei S. In situ synthesis and biocompatibility of nano hydroxyapatite on pristine and chitosan functionalized graphene oxide. *J Mater Chem B* 2013;1:475–484.
214 Shin JW, Swift J, Ivanovska I, Spinler KR, Buxboim A, Discher DE. Mechanobiology of bone marrow stem cells: From myosin-II forces to compliance of matrix and nucleus in cell forms and fates. *Differentiation* 2013;86:77–86.